**Distribution Agreement**

In presenting this thesis or dissertation as a partial fulfillment of the requirements for an advanced degree from Emory University, I hereby grant to Emory University and its agents the non-exclusive license to archive, make accessible, and display my thesis or dissertation in whole or in part in all forms of media, now or hereafter known, including display on the world wide web. I understand that I may select some access restrictions as part of the online submission of this thesis or dissertation. I retain all ownership rights to the copyright of the thesis or dissertation. I also retain the right to use in future works (such as articles or books) all or part of this thesis or dissertation.

Signature:

| _____ | _____ |
| --- | --- |
| Sarah Strassler | Date |

# Defining the mechanism of substrate recognition by the tRNA methyltransferase Trm10

By

Sarah Esther Strassler
Doctor of Philosophy

Graduate Division of Biological and Biomedical Sciences
Biochemistry, Cell and Developmental Biology

_____

Graeme L. Conn, Ph.D.
Advisor

_____

Anita H. Corbett, Ph.D.
Committee Member

_____

Christine M. Dunham, Ph.D.
Committee Member

_____

Homa Ghalei, Ph.D.
Committee Member

_____

Eric A. Ortlund, Ph.D.
Committee Member

Accepted:

_____

Kimberly Jacob Arriola, Ph.D.
Dean of the James T. Laney School of Graduate Studies

_____

Date

# Defining the mechanism of substrate recognition by the tRNA methyltransferase Trm10

By

Sarah Esther Strassler
B.S., University of Florida, 2014

Advisor: Graeme L. Conn, Ph.D.

An abstract of
A dissertation submitted to the Faculty of the
James T. Laney School of Graduate Studies of Emory University
in partial fulfillment of the requirements for the degree of
Doctor of Philosophy
In Biochemistry, Cell and Developmental Biology
2023

## ABSTRACT

# Defining the mechanism of substrate recognition by the tRNA methyltransferase Trm10

By Sarah Esther Strassler

RNA modifications are central to proper RNA function and are highly conserved across all kingdoms of life. Of all major RNA classes, transfer RNAs (tRNAs) are the most highly modified with each tRNA molecule containing an average of 14 out of the 94 known modifications. Trm10 (TRMT10A in humans) is a tRNA methyltransferase that is part of the SpoU-TrmD (SPOUT) family of enzymes and is evolutionarily conserved. Trm10 modifies a subset of tRNAs on the base N1 position of guanosine at the ninth nucleotide in the core region. Mutations in the *TRMT10A* gene have been linked to neurological disorders, such as microcephaly and intellectual disability, as well as defects in glucose metabolism. However, despite the clear biomedical importance of TRMT10A and the tRNA methylation it incorporates, there is still a large gap in our understanding of how this enzyme accurately recognizes its specific substrates to generate the pool of correctly modified tRNAs that is essential for normal cell function. Of the 26 tRNAs in yeast with guanosine at position 9, only 13 are substrates for Trm10 and no common sequence or other posttranscriptional modifications have been identified among these substrates. These observations suggest the presence of some other tRNA feature(s) which allow Trm10 to distinguish substrate from nonsubstrate tRNAs. Additionally, little is known about the specific interactions between Trm10 and tRNA that allow for this unique substrate specificity. Here, I show that substrate recognition by *Saccharomyces cerevisiae* Trm10 is dependent on the ability of the enzyme to induce specific conformational changes to the tRNA upon binding which allow Trm10 to gain access to the target nucleotide. I also use cryogenic electron microscopy (cryo-EM) to generate a 3D reconstruction of the Trm10-tRNA complex which is the first structural snapshot of a monomeric SPOUT methyltransferase bound to its substrate in the absence of any additional binding partners. Our results highlight a novel mechanism of substrate recognition by a conserved tRNA-modifying enzyme. Further, these studies reveal a strategy for substrate recognition that may be broadly employed by tRNA-modifying enzymes which must distinguish between structurally similar tRNA species.

# Defining the mechanism of substrate recognition by the tRNA methyltransferase Trm10

By

Sarah Esther Strassler
B.S., University of Florida, 2014

Advisor: Graeme L. Conn, Ph.D.

A dissertation submitted to the Faculty of the
James T. Laney School of Graduate Studies of Emory University
in partial fulfillment of the requirements for the degree of
Doctor of Philosophy
In Biochemistry, Cell and Developmental Biology
2023

**Acknowledgements**

I want to start by thanking my advisor, Dr. Graeme Conn, for acting as a strong mentor before I even joined his lab. You recognized that it would be challenging for me to transition from teaching in rural Ghana to working in a research lab and found an opportunity for me to come early to work in your lab for the summer, which helped me immensely with the transition to graduate school. You have always had my best interests in mind, making me aware of fellowship opportunities and nominating me for awards. It truly makes a difference to have an advisor who believes in your ability to succeed and celebrates your accomplishments. Thank you for making yourself available for even the silliest questions and for giving the most thorough and quick edits I have ever experienced. Your approach to mentoring has helped me tremendously to grow as a scientist and a writer (and has forever changed how I look at figures). Thank you for fostering a positive lab environment that makes all members feel supported and encourages collaboration between members.

Thank you to all the other mentors in my life who have helped me get to this point. Thank you to my committee (Drs. Anita Corbett, Christine Dunham, Homa Ghalei, and Eric Ortlund) for your guidance with my research project and your confidence in me. A special thank you to Anita for treating me like a member of your lab during the RNA Society conference and for constantly connecting me with people who can offer great career advice. Thank you to Dr. Mike Koval for always making me feel welcome in your office and acting as an informal mentor, offering an outsider's perspective. Thank you to Dr. David Wei and Dr. Mark Brantly for exposing me to different areas of research while I was in college and being generous with your time when I had questions. Thank you to Dr.

Anthony DeSantis for supporting me every step of my journey. Thank you to Meisa Salaita for exposing me to the world of science communication and providing me with opportunities to hone my skills. Thank you to Arri Eisen for listening to my interests and generously connecting me with everyone you knew who could be helpful. And last but not least, thank you to Teri Arenstam for getting me excited about Chemistry in high school and showing me how cool scientists can be.

I want to thank all members of the Conn lab, past (Sam Schwartz, Zane Laughlin, Esther Park, Meisam Nosrati, Paige LaMore, and Clio Hancock) and present (Logan Kavanaugh, Natalia Zelinskaya, Alejandro Oviedo, Kurt Miller, Debayan Dey, Suparno Nandi, Mohamed Barmada, Enoch Ayamga, Shraddha Hariharan, Alex Vasilakopoulos, Sada Boyd, and Mina Henes) for cheering me on every step of the way. You've been there to celebrate the big moments of graduate school with me and you've been there to lament with me when things aren't working. You all make the hard moments much more enjoyable and I will never take for granted how supported I felt working with this team of people. Logan, thank you especially for bringing me bagels in my times of need and breaking up my workday with coffee runs. Thank you for being an enabler when I had silly ideas like buying a lab fish (RIP Gill Nye 2022-2023) or joining Orangetheory. I hope we continue to match accidentally even when we're not working in the same space.

Thank you to the members of BCDB who made campus feel like a community. It's humbling to be part of this group of brilliant, motivated individuals who are still kind and giving. I want to give a special shout out to my Day One, Tala Khatib, who never lets me forget how exciting science is. You have been by my side for every scientific breakthrough, every big life event, and for every event with free food. We knew this day

would come and now it's happening! I don't know how I would have gotten here without you.

Thank you to the monks and nuns from the Emory and Tibet Science Initiative who became very dear friends (Pasang, Kalsang, Rabga, Taga, Tenzin, Le Thi, Loga, and Kalden). Working with you challenged me to teach scientific topic in new ways. You expanded how I think about basic science questions and I cherish our sessions where you asked the most thoughtful questions. You helped me to think outside of the box during my time in graduate school and offered a welcome reprieve during long days in lab.

Thank you to my family (Mom, Dad, Andy, and Joe) for supporting me even when the process of getting a PhD was a bit of a mystery to all of you. Thank you for celebrating my scientific achievements with me and for being a support system when experiments weren't working, even when you didn't understand what I was doing exactly. Mom and Dad, thank you for looking up articles and reading books to learn more about my research. Thank you for raising me to value education, to have confidence in my own abilities, to prioritize a work-life balance, and to trust my intuition.

And last but not least, thank you to my husband. Fouad, you have been my sounding board and my biggest cheerleader. I know you basically could have written this dissertation from how many times you have heard my presentation. You made sure I was fed when I came home late and grumpy, and you helped me celebrate during the most exciting times. I appreciate that you understand the experience of doing research, of experiments failing and thesis writing dragging on forever. I will never take for granted how special it is to have a supportive partner.

# TABLE OF CONTENTS

# CHAPTER ONE:

## Introduction

## Gene Expression

Gene expression describes the process of turning the information encoded in our DNA into a functional product. The information contained within DNA is transcribed to make messenger RNA (mRNA), which is used by the ribosome as the blueprints to make a functional protein (**Figure 1.1**). This flow of information from DNA to RNA to protein, also known as the central dogma, is a simplified model which does not address the other roles different types of RNAs can play or the complex ways this process can be regulated. However, understanding the complexities of this process is essential to fully define the molecular underpinnings of gene expression regulation and the human diseases associated with its dysregulation.

### *The Roles of RNA During Translation*

Despite mRNA being the most well-known RNA, it only accounts for 5% of the total RNA in our cells (1). In addition to mRNA, there are several other RNAs that are transcribed from DNA and play essential roles during the process of gene expression. For example, ribosomal RNA (rRNA) is the primary component of ribosomes which are responsible for synthesizing proteins from an mRNA sequence code during translation. The ribosome directs catalysis by stitching together amino acids to make the growing polypeptide chain which eventually becomes a functional protein (**Figure 1.1**) (2, 3). However, ribosomes would be unable to convert the information contained in mRNA to a protein sequence without the help of transfer RNA (tRNA). The anticodon of tRNA interacts specifically with the codon of mRNA to deliver the appropriate amino acid to the ribosome for protein synthesis.

*Regulating Translation through RNA Modifications*

RNA is made up of four nucleotides (guanine, cytosine, adenine, and uracil) which can be modified by RNA-modifying enzymes to expand their chemical and topological properties. These RNA modifications are central to proper RNA function and are highly conserved across all kingdoms of life (4). The correct deposition of these modifications is essential for regulating gene expression and can control both the stability of RNAs and interactions with binding partners.

One way that RNA modifications can regulate gene expression is by controlling the abundance of the key players which are necessary for translation. For example, N6-methyladenosine ($m^6A$) is a methylation that occurs at the adenosine N6-position and is the most prevalent mRNA modification in eukaryotes (5, 6). This modification affects the stability of the mRNA transcript and therefore provides a mechanism to regulate translation of a specific protein encoded by mRNA (5). The formation of functional ribosomes requires rRNA modifications at different stages of ribosome biogenesis and these modifications stabilize the secondary and tertiary structures of the rRNA scaffold. This scaffold is important for proper ribosome assembly and therefore efficient translation (7). Similarly, numerous tRNA modifications fine-tune tRNA structure and stability to alter the pool of available tRNAs. By controlling the pool of available tRNAs, cells are able to control expression levels of specific transcripts (8).

RNA modifications can also affect specific interactions between RNA and RNA-binding proteins or between different RNA molecules. For example, during the process of translation, the codon of mRNA must bind to the anticodon of tRNA to ensure the appropriate amino acid is delivered for the growing polypeptide chain (**Figure 1.1**).

Modifications to tRNA in the anticodon loop serve to open the loop and constrain the dynamics of this region to ensure correct codon-anticodon interactions (9, 10).

**tRNA**

As a group, tRNAs are the most abundant type of RNA transcript, with each cell containing tens of millions of copies (11). Although there are only 20 different amino acids, most cells have between 40 to 60 different tRNAs which each interact with a different codon in mRNA. tRNAs can range in length from 70 to 100 nucleotides, with most of this variability in length occurring in a hairpin region called the variable loop (12) (**Figure 1.2**). The length of the variable loop determines if a tRNA is classified as Type I (shorter variable loop of 4-5 nucleotides) or Type II (longer variable loop of 10 or more nucleotides). Despite differences in sequence and length, all tRNAs have a similar cloverleaf secondary structure with four stems composed of Watson-Crick base pairs (**Figure 1.2**) (12). tRNAs fold into an L-shape tertiary structure which is stabilized by hydrogen bonding and base stacking between nucleotides which are distant from each other in the secondary structure. For example, stacking occurs between the acceptor stem and the T-loop to form one arm of the L-shape, while the other arm is formed from stacking of the D-loop and anticodon loop.

*tRNA-Modifying Enzymes*

Throughout their lifetime, tRNAs can be altered by a variety of enzymes which can ultimately dictate the fate of the tRNA. For example, endo- and exonucleases are responsible for removing leader and trailer sequences in the initial steps of tRNA

maturation (13). In some organisms, sequences may be added to the tRNA prior to aminoacylation such as addition of the sequence CCA sequence by CCA-adding enzymes (14). Other enzymes are solely responsible for catalyzing the modification of nucleotides within tRNA to alter their properties (15). These tRNA-modifying enzymes can be responsible for methylation, acetylationdeamination, isomerization, glycosylation, thiolation reactions, or pseudouridylation (16). Each enzyme acts at a specific location on the tRNA and with varying specificity for the identity of the nucleotide at that site. Aberrant expression or dysfunction of tRNA-modifying enzymes has been linked to a large number of human diseases including neurological disorders, diabetes, cancer, and mitochondrial disorders (17). Many of these diseases are related to defects in protein synthesis and highlight the importance of tRNA modifications in regulating gene expression.

*tRNA Modifications*

tRNA modifications are central to proper tRNA function and are highly conserved across all kingdoms of life (4). While many types of RNAs can undergo modification, tRNAs are the most highly modified, containing an average of 13 modifications per molecule (**Figure 1.3**) (11). The role of these modifications varies depending on where they occur on the tRNA. For example, modifications to the anticodon of tRNA are critical for ensuring correct interactions between the codon of mRNA and the anticodon of tRNA during translation as mentioned previously (15). Position 34, which is also known as the wobble position, is highly modified and these modifications expand base pairing capabilities, confer decoding bias, or enhance codon-anticodon interactions (18-21). Position 37 tends to contain bulky modifications which can help to prevent frameshifting (22).

Other modifications, such as modifications to the core region of tRNA, can impact the tRNA structure and stability. These core modifications can fine-tune the tRNA structure by influencing the hydrophobic character of the base, altering its stacking ability, or even changing the net-charge (23). However, the biological role of modifications in regions of tRNA outside of the anticodon loop can be difficult to define considering that deletion of a single enzyme responsible for these modifications often results in no noticeable phenotype (24).

## The tRNA Methyltransferase Trm10

### *Biological Relevance of Trm10*

The tRNA methyltransferase Trm10 modifies the N1 base position on the 9$^{th}$ nucleotide in the core region of tRNA (25) (**Figure 1.2**). Trm10 is conserved throughout eukarya and archaea and, unlike many other tRNA core-modifying enzymes, is linked to distinct disease phenotypes in humans. In humans, loss of function mutations in the *TRMT10A* gene are linked to microcephaly and intellectual disability, as well as defects in glucose metabolism (26-30).

The importance of Trm10 is further highlighted using the model organism *Saccharomyces cerevisiae,* with *trm10* knockout strains exhibiting hypersensitivity to the antitumor drug 5-fluorouracil (5FU) (31). The drug 5FU is a pyrimidine analog that can be misincorporated into RNA in place of uracil or thymine and is also known to inhibit pseudouridine modification, which is abundant and functionally important for many RNA molecules including tRNA (32). Hypersensitivity to 5FU in the *trm10Δ* strain is due to the depletion of $tRNA^{Trp}$ in the absence of the $m^1G9$ modification, meaning this modification

helps the tRNA to withstand the effects of 5FU toxicity (33). Further, *trm10Δ* hypersensitivity and decreased $tRNA^{Trp}$ levels are rescued by deletion of *met22* which is an enzyme associated with tRNA quality control pathways. Therefore, the $m^1G9$ modification prevents tRNAs from being degraded by nuclease(s) associated with *MET22*-dependent tRNA quality control pathways and is only functionally important for one tRNA, which has been seen for other tRNA-modifying enzymes as well.

*Trm10 Enzymes in Humans*

Humans express three Trm10 enzymes that are distinct in their cellular localization and pool of tRNA substrates: TRMT10A (the direct homolog of *S. cerevisiae* Trm10), TRMT10B, and TRMT10C. While Trm10/TRMT10A and TRMT10B are believed to be nuclear/ cytosolic, TRMT10C is localized to the mitochondria as part of the mitochondrial RNase P complex and is the only member of the Trm10 family which is known to function as part of a larger complex (34). Each human Trm10 enzyme also methylates a unique subset of tRNAs, modifying only G9 (Trm10/TRMT10A), only A9 (TRMT10B), or exhibiting bifunctional activity to modify either G9 or A9 (TMRT10C) (35-37).

*The SPOUT Family of Methyltransferases*

Trm10 is a member of the SPOUT family of methyltransferases, which is a large family of S-adenosyl-L-methionine (SAM)-dependent enzymes characterized by an α/β fold with a deep topological knot (38-40). This knot forces SAM into a bent conformation which is favorable for catalysis by this family of enzymes (41). This family is composed of mainly RNA-modifying enzymes and one protein methyltransferase. Many SPOUT

methyltransferases are involved in posttranscriptional tRNA modifications (40), including the methyltransferase TrmD which catalyzes N1-methylation of the guanosine at position 37 of tRNA in bacteria (42, 43). TrmD is essential for bacterial growth because it suppresses translational frameshift errors at proline codons by methylating the anticodon using a mechanism that has been well-defined (22). However, despite their shared knotted SAM-binding domain, TrmD and other SPOUT methyltransferases display a remarkable degree of mechanistic diversity for substrate recognition. A summary of our current knowledge of mechanisms of substrate recognition by SPOUT methyltransferases is described in detail in **Chapter 2**.

Although Trm10 is structurally similar to TrmD and catalyzes an identical methylation of a guanosine at position 9 of some tRNAs, TrmD and Trm10 employ very different mechanisms of catalysis (25, 36). For example, Trm10 does not require a divalent metal ion for catalysis and does not possess the same catalytic residues as demonstrated for TrmD (44-47). Furthermore, in contrast to TrmD and most other SPOUT enzymes, Trm10 is catalytically active as a monomer (48). These differences suggest that Trm10 uses a mechanism of substrate recognition and catalysis that is distinct from TrmD and all other SPOUT methyltransferases.

*Trm10 Structure*

Our current knowledge about the structures of the human Trm10 proteins come from the structure of a truncated Trm10 from *S. cerevisiae* (Δ1-83) which is the direct homolog of human TRMT10A and from a structure of human TRMT10C as part of the mitochondrial RNAse P complex (**Figure 1.4**). The crystal structure of Trm10 from *S. cerevisiae* shows

a monomeric protein in the absence of substrate tRNA (48). Considering that the active site of other SPOUT methyltransferases occurs at the dimer interface, this structure does not provide information about how the active site of Trm10 would form without the presence of an additional protomer. Additionally, the N-terminal domain (NTD) is essential for catalytic activity (48). Therefore, the currently available structure of Trm10 with an NTD-deletion is missing important structural information.

The structure of the mitochondrial RNase P complex was solved in complex with the pre-tRNA and includes TRMT10C as one of the RNase P subunits responsible for tRNA binding and recognition (49). The structure shows the NTD of TRMT10C wrapping around the tRNA so that the tRNA is encased by the catalytic C-terminal domain (CTD) and the NTD, with the target A9 base flipped into the active site of the CTD. However, multiple domains of the protein-only RNase P (PRORP) subunit of RNase P also contact the pre-tRNA. This is not surprising considering that PRORP has a known role in RNA recognition and contains a nuclease domain which makes direct contact with the RNA for cleavage of the 5’ end. Additionally, TRMT10C has been shown to require SDRC51 to be catalytically active (34). The other Trm10 enzymes, however, do not have any known binding partners and it remains unclear how they are able to recognize the correct substrate without dimerization or the presence of additional proteins.

**Research Goals**

Trm10 modifies only 13 of 26 possible tRNA substrates in yeast that contain a G9 nucleotide (25, 36, 50), but no common sequence or posttranscriptional modification(s) have been identified that can explain this substrate specificity (47, 48). Trm10 has also

been shown to efficiently modify *in vitro* transcribed substrate tRNAs, indicating that prior modifications are not necessary for methylation (36). Therefore, some other inherent tRNA property (or properties) must be exploited by Trm10 to discriminate between substrate and nonsubstrate. Additionally, differences in substrate recognition must exist within the Trm10 family to allow the human Trm10 paralogs (TRMT10A/B/C) to recognize different nucleotides for modification.

Preliminary RNA footprinting data suggested that induced conformational changes in tRNA play an important role in correct substrate recognition by Trm10. Inability of non-substrate tRNA to undergo such conformational changes would also prevent Trm10 from modifying the incorrect tRNA. Therefore, the goal of my research was to uncover the mechanism of substrate recognition by Trm10 by defining the necessary conformational changes and structural features that control the formation of a catalytically productive Trm10-tRNA complex (**Figure 1.5**).

In **Chapter 3**, I used selective 2'OH-acylation analyzed by primer extension (SHAPE) to define tRNA dynamics during substrate recognition. This study was performed using both wild-type Trm10 from *S. cerevisiae* (ScTrm10) and a variant (Trm10-KRR) which is able to bind to substrate tRNA but is catalytically inactive. The comparison of tRNA dynamics in substrate and nonsubstrate tRNAs in the presence of the two enzymes allowed us to identify conformational changes that are necessary for methylation specifically as opposed to binding (51). The changes include increased reactivity in the D-loop of the substrate tRNA and decreased reactivity in the anticodon loop, which are consistent with a model in which local conformational changes position

the target nucleotide in its binding pocket, while distant conformational changes may be related to specific interactions with the N-terminal domain of Trm10.

In **Chapter 4**, I summarize my unpublished work using cryogenic electron microscopy (cryo-EM) to gain structural information about the Trm10-tRNA complex during substrate recognition. There is currently no structure of full-length or tRNA-bound Trm10. Therefore, my current 3D reconstruction provides the first glimpse of the Trm10-tRNA complex during substrate recognition. This model clearly shows Trm10 binding to tRNA in a 1:1 ratio and is the first time a monomeric SPOUT methyltransferase has been seen binding to substrate in the absence of additional proteins. Additionally, a dimeric Trm10 protein can be seen in a small percentage of the 2D classes which may reflect an important intermediate for methylation by Trm10. By processing and refining the dataset further, I will be able to define the role of the NTD and to identify critical interactions with tRNA that allow for recognition of the correct substrate.

Collectively, these studies further our understanding of how Trm10 selects the correct tRNA for modification from the large pool of tRNAs in our cells. Trm10 binds to substrate tRNA in a 1:1 ratio and exploits the differences in inherent flexibilities of tRNA molecules to recognize substrates for modification. Similar flexibilities may result from very different tRNA sequences, which would explain why previous studies were unable to identify similarities among substrates. These results highlight a novel mechanism of substrate recognition by a conserved tRNA modifying enzyme. Further, these studies reveal a strategy for substrate recognition that may be broadly employed by tRNA-modifying enzymes which must distinguish between structurally similar tRNA species.

**Figures**

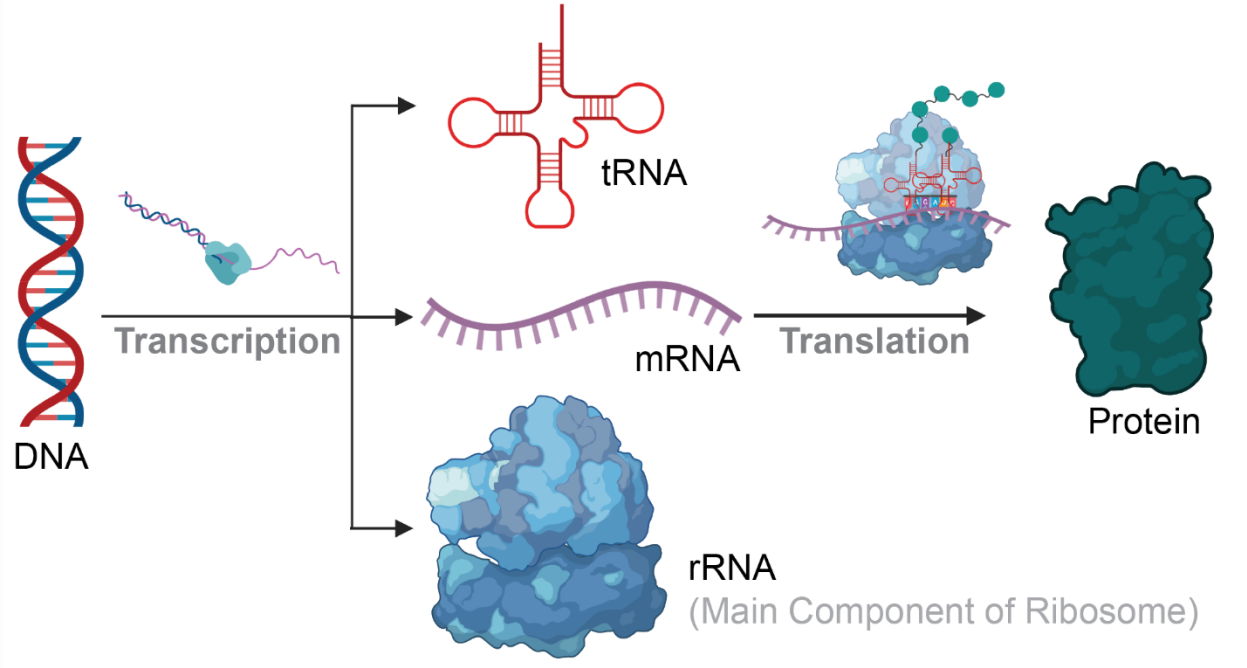


**Figure 1.1 The Central Dogma.** During the process of gene expression, the information encoded in DNA is used to make RNA through the process of transcription. Some of the RNAs which are critical for gene expression include transfer RNA (tRNA), messenger RNA (mRNA), and ribosomal RNA (rRNA). These three types of RNA come together during translation to turn the message encoded in mRNA into a function protein.

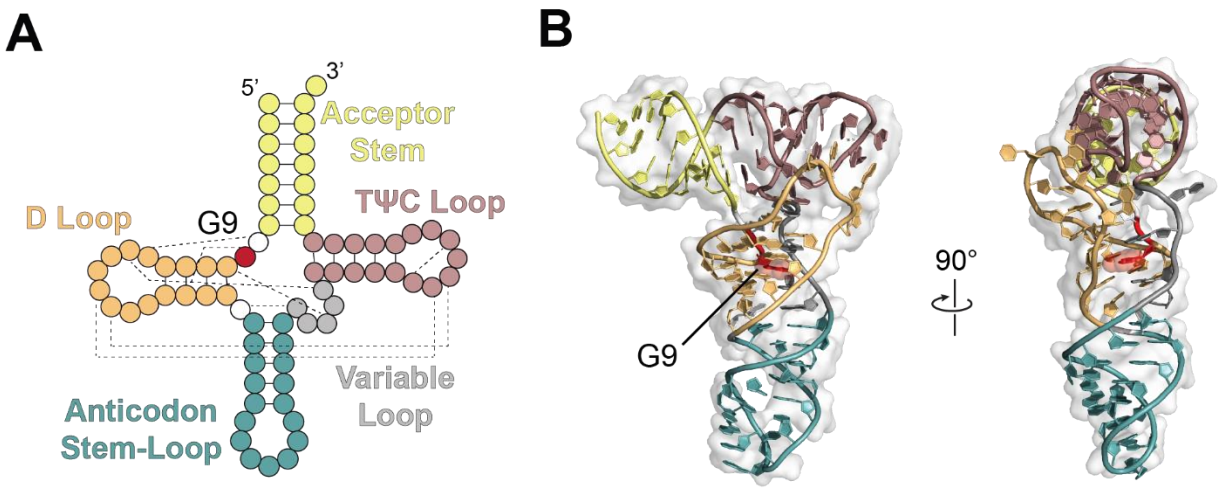


**Figure 1.2 tRNA Secondary and Tertiary Structure.** ***A***, All tRNAs fold into a cloverleaf secondary structure in which base-pairing is designated by lines between nucleotides. Tertiary interactions which form the L-shaped three-dimensional structure are shown as dotted lines on the secondary structure. The 9$^{th}$ nucleotide, shown in red, is the site of modification for the tRNA methyltransferase Trm10. ***B,*** The L-shaped tertiary structure of tRNA is shown.

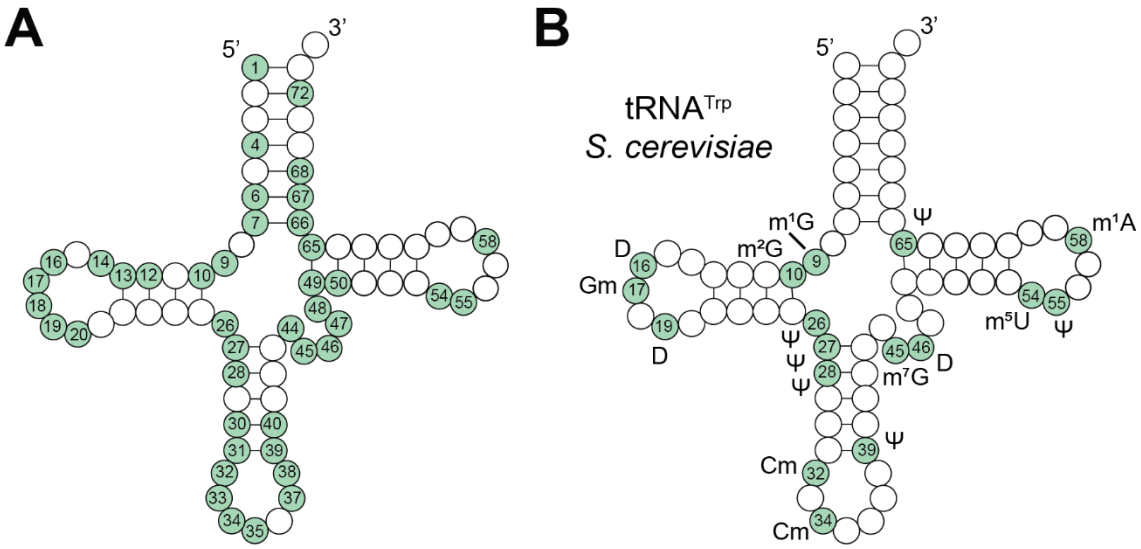

**Figure 1.3 tRNA Modifications. *A*,** Nucleotides which contain a modification in at least one type of tRNA are shown in green with the nucleotide number shown (52). Some tRNAs contain additional nucleotides in the D-loop (between nucleotides 20 and 21) and in the variable loop (between nucleotides 44 and 45), which are not shown. ***B***, The modifications for Trm10 substrate $tRNA^{Trp}$ from *S. cerevisiae* are shown in green. These modifications include 1-methyladenosine ($m^1A$), 2′-*O*-methylcytidine (Cm), dihydrouridine (D), 1-methylguanosine ($m^1G$), $N^2$-methylguanosine ($m^2G$), 7-methylguanosine ($m^7G$), 2′-*O*-methylguanosine (Gm), 5-methyluridine ($m^5U$), and pseudouridine (Ψ) (53).

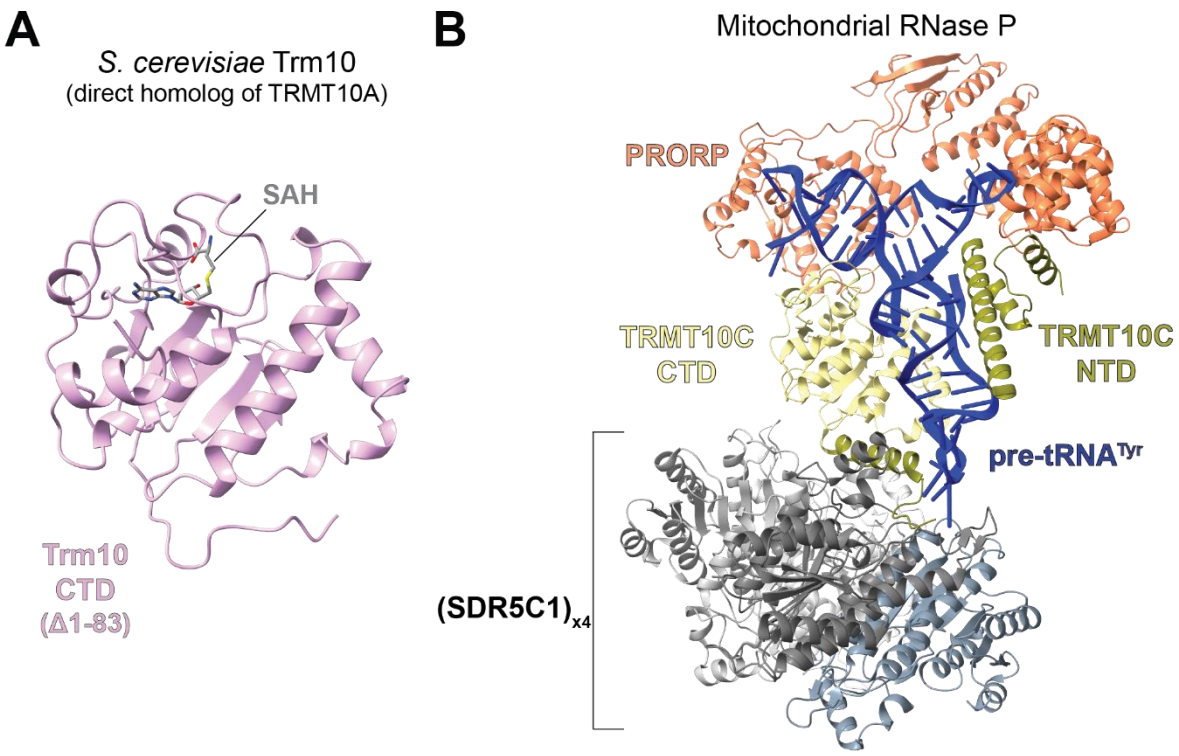


**Figure 1.4 The Structure of Trm10. *A*,** The structure of the CTD of Trm10 from *S. cerevisiae* is shown which is the direct homolog of human TRMT10A. The truncated protein is missing residues 1-83 (PDB: 4JWJ). The cofactor SAH (the methylation

byproduct of SAM) is shown in the SAM-binding pocket. ***B,*** The structure of TRMT10C was solved in complex with pre-tRNA as part of the mitochondrial RNase P complex. The NTD of TRMT10C can be seen wrapping around the pre-tRNA$^{Tyr}$ to make critical contacts with regions distant from the site of modification (PDB: 7ONU).

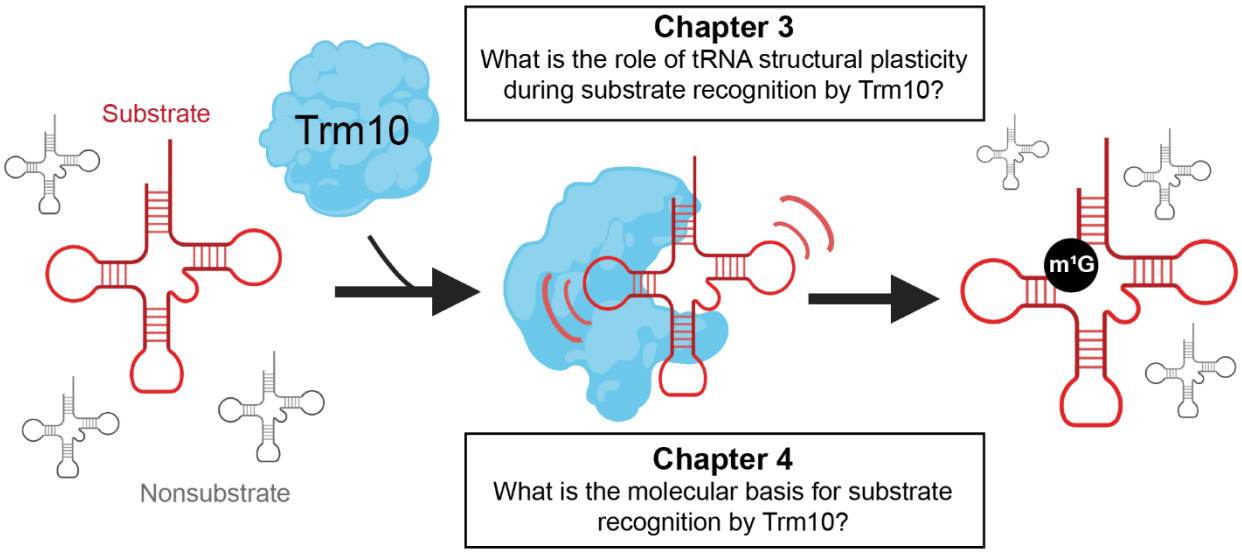


**Figure 1.5 Overview of Research Objectives.** The main research objectives are outlined. These works are described in further detail in **Research goals** as well as their respective chapters.

## References


1. Westermann, A. J., Gorski, S. A., andVogel, J. (2012) Dual RNA-seq of pathogen and host Nat Rev Microbiol **10**, 618-630 10.1038/nrmicro2852

2. Nissen, P., Hansen, J., Ban, N., Moore, P. B., andSteitz, T. A. (2000) The structural basis of ribosome activity in peptide bond synthesis Science **289**, 920-930 10.1126/science.289.5481.920

3. Schmeing, T. M., Seila, A. C., Hansen, J. L., Freeborn, B., Soukup, J. K., Scaringe, S. A. *et al.* (2002) A pre-translocational intermediate in protein synthesis observed in crystals of enzymatically active 50S subunits Nat Struct Biol **9**, 225-230 10.1038/nsb758

4. Nachtergaele, S., andHe, C. (2017) The emerging biology of RNA post-transcriptional modifications RNA Biol **14**, 156-163 10.1080/15476286.2016.1267096

5. Dominissini, D., Moshitch-Moshkovitz, S., Schwartz, S., Salmon-Divon, M., Ungar, L., Osenberg, S. *et al.* (2012) Topology of the human and mouse m6A RNA methylomes revealed by m6A-seq Nature **485**, 201-206 10.1038/nature11112

6. Meyer, K. D., Saletore, Y., Zumbo, P., Elemento, O., Mason, C. E., andJaffrey, S. R. (2012) Comprehensive analysis of mRNA methylation reveals enrichment in 3' UTRs and near stop codons Cell **149**, 1635-1646 10.1016/j.cell.2012.05.003

7. Polikanov, Y. S., Melnikov, S. V., Soll, D., andSteitz, T. A. (2015) Structural insights into the role of rRNA modifications in protein synthesis and ribosome assembly Nat Struct Mol Biol **22**, 342-344 10.1038/nsmb.2992

8. Wilusz, J. E. (2015) Controlling translation via modulation of tRNA levels Wiley Interdiscip Rev RNA **6**, 453-470 10.1002/wrna.1287

9. Olejniczak, M., andUhlenbeck, O. C. (2006) tRNA residues that have coevolved with their anticodon to ensure uniform and accurate codon recognition Biochimie **88**, 943-950 10.1016/j.biochi.2006.06.005

10. Agris, P. F. (2008) Bringing order to translation: the contributions of transfer RNA anticodon-domain modifications EMBO Rep **9**, 629-635 10.1038/embor.2008.104

11. Pan, T. (2018) Modifications and functional genomics of human transfer RNA Cell Res **28**, 395-404 10.1038/s41422-018-0013-y

12. Krahn, N., Fischer, J. T., andSoll, D. (2020) Naturally Occurring tRNAs With Non-canonical Structures Front Microbiol **11**, 596914 10.3389/fmicb.2020.596914

13. Hopper, A. K. (2013) Transfer RNA post-transcriptional processing, turnover, and subcellular dynamics in the yeast Saccharomyces cerevisiae Genetics **194**, 43-67 10.1534/genetics.112.147470

14. Betat, H., Rammelt, C., andMorl, M. (2010) tRNA nucleotidyltransferases: ancient catalysts with an unusual mechanism of polymerization Cell Mol Life Sci **67**, 1447-1463 10.1007/s00018-010-0271-4

15. Cantara, W. A., Crain, P. F., Rozenski, J., McCloskey, J. A., Harris, K. A., Zhang, X. *et al.* (2011) The RNA Modification Database, RNAMDB: 2011 update Nucleic Acids Res **39**, D195-201 10.1093/nar/gkq1028

16. Grosjean, H., Edqvist, J., Straby, K. B., andGiege, R. (1996) Enzymatic formation of modified nucleosides in tRNA: dependence on tRNA architecture J Mol Biol **255**, 67-85 10.1006/jmbi.1996.0007

17. Cui, W., Zhao, D., Jiang, J., Tang, F., Zhang, C., andDuan, C. (2023) tRNA Modifications and Modifying Enzymes in Disease, the Potential Therapeutic Targets Int J Biol Sci **19**, 1146-1162 10.7150/ijbs.80233

18. Novoa, E. M., Pavon-Eternod, M., Pan, T., andRibas de Pouplana, L. (2012) A role for tRNA modifications in genome structure and codon usage Cell **149**, 202-213 10.1016/j.cell.2012.01.050

19. Liu, R. J., Zhou, M., Fang, Z. P., Wang, M., Zhou, X. L., andWang, E. D. (2013) The tRNA recognition mechanism of the minimalist SPOUT methyltransferase, TrmL Nucleic Acids Res **41**, 7828-7842 10.1093/nar/gkt568

20. Bjork, G. R., Huang, B., Persson, O. P., andBystrom, A. S. (2007) A conserved modified wobble nucleoside (mcm5s2U) in lysyl-tRNA is required for viability in yeast RNA **13**, 1245-1255 10.1261/rna.558707

21. Nedialkova, D. D., andLeidel, S. A. (2015) Optimization of Codon Translation Rates via tRNA Modifications Maintains Proteome Integrity Cell **161**, 1606-1618 10.1016/j.cell.2015.05.022

22. Bjork, G. R., Wikstrom, P. M., andBystrom, A. S. (1989) Prevention of translational frameshifting by the modified nucleoside 1-methylguanosine Science **244**, 986-989 10.1126/science.2471265

23. Lorenz, C., Lunse, C. E., andMorl, M. (2017) tRNA Modifications: Impact on Structure and Thermal Adaptation Biomolecules **7**, 10.3390/biom7020035

24. Phizicky, E. M., andHopper, A. K. (2015) tRNA processing, modification, and subcellular dynamics: past, present, and future RNA **21**, 483-485 10.1261/rna.049932.115

25. Jackman, J. E., Montange, R. K., Malik, H. S., andPhizicky, E. M. (2003) Identification of the yeast gene encoding the tRNA m1G methyltransferase responsible for modification at position 9 RNA **9**, 574-585 10.1261/rna.5070303

26. Igoillo-Esteve, M., Genin, A., Lambert, N., Desir, J., Pirson, I., Abdulkarim, B. *et al.* (2013) tRNA methyltransferase homolog gene TRMT10A mutation in young onset diabetes and primary microcephaly in humans PLoS Genet **9**, e1003888 10.1371/journal.pgen.1003888

27. Gillis, D., Krishnamohan, A., Yaacov, B., Shaag, A., Jackman, J. E., andElpeleg, O. (2014) TRMT10A dysfunction is associated with abnormalities in glucose homeostasis, short stature and microcephaly J Med Genet **51**, 581-586 10.1136/jmedgenet-2014-102282

28. Yew, T. W., McCreight, L., Colclough, K., Ellard, S., andPearson, E. R. (2016) tRNA methyltransferase homologue gene TRMT10A mutation in young adult-onset diabetes with intellectual disability, microcephaly and epilepsy Diabet Med **33**, e21-25 10.1111/dme.13024

29. Zung, A., Kori, M., Burundukov, E., Ben-Yosef, T., Tatoor, Y., andGranot, E. (2015) Homozygous deletion of TRMT10A as part of a contiguous gene deletion in a syndrome of failure to thrive, delayed puberty, intellectual disability and diabetes mellitus Am J Med Genet A **167A**, 3167-3173 10.1002/ajmg.a.37341

30. Narayanan, M., Ramsey, K., Grebe, T., Schrauwen, I., Szelinger, S., Huentelman, M. *et al.* (2015) Case Report: Compound heterozygous nonsense mutations in TRMT10A are associated with microcephaly, delayed development, and periventricular white matter hyperintensities F1000Res **4**, 912 10.12688/f1000research.7106.1

31. Gustavsson, M., andRonne, H. (2008) Evidence that tRNA modifying enzymes are important in vivo targets for 5-fluorouracil in yeast RNA **14**, 666-674 10.1261/rna.966208

32. Zhang, N., Yin, Y., Xu, S. J., andChen, W. S. (2008) 5-Fluorouracil: mechanisms of resistance and reversal strategies Molecules **13**, 1551-1569 10.3390/molecules13081551

33. Bowles, I. E., andJackman, J. E. (2023) A tRNA-specific function for tRNA methyltransferase Trm10 is associated with a new tRNA quality control mechanism in Saccharomyces cerevisiae bioRxiv 2023.2010.2006.561306 10.1101/2023.10.06.561306

34. Vilardo, E., Nachbagauer, C., Buzet, A., Taschner, A., Holzmann, J., andRossmanith, W. (2012) A subcomplex of human mitochondrial RNase P is a bifunctional methyltransferase--extensive moonlighting in mitochondrial tRNA biogenesis Nucleic Acids Res **40**, 11583-11593 10.1093/nar/gks910

35. Howell, N. W., Jora, M., Jepson, B. F., Limbach, P. A., andJackman, J. E. (2019) Distinct substrate specificities of the human tRNA methyltransferases TRMT10A and TRMT10B RNA **25**, 1366-1376 10.1261/rna.072090.119

36. Swinehart, W. E., Henderson, J. C., andJackman, J. E. (2013) Unexpected expansion of tRNA substrate recognition by the yeast m1G9 methyltransferase Trm10 RNA **19**, 1137-1146 10.1261/rna.039651.113

37. Vilardo, E., Amman, F., Toth, U., Kotter, A., Helm, M., andRossmanith, W. (2020) Functional characterization of the human tRNA methyltransferases TRMT10A and TRMT10B Nucleic Acids Res **48**, 6157-6169 10.1093/nar/gkaa353

38. Anantharaman, V., Koonin, E. V., andAravind, L. (2002) SPOUT: a class of methyltransferases that includes spoU and trmD RNA methylase superfamilies, and novel superfamilies of predicted prokaryotic RNA methylases J Mol Microbiol Biotechnol **4**, 71-75, https://www.ncbi.nlm.nih.gov/pubmed/11763972

39. Kurowski, M. A., Sasin, J. M., Feder, M., Debski, J., andBujnicki, J. M. (2003) Characterization of the cofactor-binding site in the SPOUT-fold methyltransferases by computational docking of S-adenosylmethionine to three crystal structures BMC Bioinformatics **4**, 9 10.1186/1471-2105-4-9

40. Tkaczuk, K. L., Dunin-Horkawicz, S., Purta, E., andBujnicki, J. M. (2007) Structural and evolutionary bioinformatics of the SPOUT superfamily of methyltransferases BMC Bioinformatics **8**, 73 10.1186/1471-2105-8-73

41. Sulkowska, J. I., Sulkowski, P., Szymczak, P., andCieplak, M. (2008) Stabilizing effect of knots on proteins Proc Natl Acad Sci U S A **105**, 19714-19719 10.1073/pnas.0805468105

42. Bystrom, A. S., andBjork, G. R. (1982) The structural gene (trmD) for the tRNA(m1G)methyltransferase is part of a four polypeptide operon in Escherichia coli K-12 Mol Gen Genet **188**, 447-454 10.1007/bf00330047

43. Bystrom, A. S., Hjalmarsson, K. J., Wikstrom, P. M., andBjork, G. R. (1983) The nucleotide sequence of an Escherichia coli operon containing genes for the tRNA(m1G)methyltransferase, the ribosomal proteins S16 and L19 and a 21-K polypeptide EMBO J **2**, 899-905, https://www.ncbi.nlm.nih.gov/pubmed/6357787

44. Sakaguchi, R., Lahoud, G., Christian, T., Gamper, H., andHou, Y. M. (2014) A divalent metal ion-dependent N(1)-methyl transfer to G37-tRNA Chem Biol **21**, 1351-1360 10.1016/j.chembiol.2014.07.023

45. Krishnamohan, A., andJackman, J. E. (2017) Mechanistic features of the atypical tRNA m1G9 SPOUT methyltransferase, Trm10 Nucleic Acids Res **45**, 9019-9029 10.1093/nar/gkx620

46. Perlinska, A. P., Kalek, M., Christian, T., Hou, Y. M., andSulkowska, J. I. (2020) Mg(2+)-Dependent Methyl Transfer by a Knotted Protein: A Molecular Dynamics Simulation and Quantum Mechanics Study ACS Catal **10**, 8058-8068 10.1021/acscatal.0c00059

47. Van Laer, B., Roovers, M., Wauters, L., Kasprzak, J. M., Dyzma, M., Deyaert, E. *et al.* (2016) Structural and functional insights into tRNA binding and adenosine N1-methylation by an archaeal Trm10 homologue Nucleic Acids Res **44**, 940-953 10.1093/nar/gkv1369

48. Shao, Z., Yan, W., Peng, J., Zuo, X., Zou, Y., Li, F. *et al.* (2014) Crystal structure of tRNA m1G9 methyltransferase Trm10: insight into the catalytic mechanism and recognition of tRNA substrate Nucleic Acids Res **42**, 509-525 10.1093/nar/gkt869

49. Bhatta, A., Dienemann, C., Cramer, P., andHillen, H. S. (2021) Structural basis of RNA processing by human mitochondrial RNase P Nat Struct Mol Biol **28**, 713-723 10.1038/s41594-021-00637-y

50. Juhling, F., Morl, M., Hartmann, R. K., Sprinzl, M., Stadler, P. F., andPutz, J. (2009) tRNAdb 2009: compilation of tRNA sequences and tRNA genes Nucleic Acids Res **37**, D159-162 10.1093/nar/gkn772

51. Strassler, S. E., Bowles, I. E., Krishnamohan, A., Kim, H., Kuiper, E. G., Comstock, L. R. *et al.* (2023) tRNA m (1) G9 modification depends on substrate-specific RNA conformational changes induced by the methyltransferase Trm10 bioRxiv 10.1101/2023.02.01.526536

52. Suzuki, T. (2021) The expanding world of tRNA modifications and their disease relevance Nat Rev Mol Cell Biol **22**, 375-392 10.1038/s41580-021-00342-0

53. Boccaletto, P., Stefaniak, F., Ray, A., Cappannini, A., Mukherjee, S., Purta, E. *et al.* (2022) MODOMICS: a database of RNA modification pathways. 2021 update Nucleic Acids Res **50**, D231-D235 10.1093/nar/gkab1083

# CHAPTER TWO:

## Tied up in knots: Untangling substrate recognition by the SPOUT methyltransferases

The following chapter has been published:

Strassler SE‡, Bowles IE‡, Dey D, Jackman JE, Conn GL. (2022) Tied up in knots: Untangling substrate recognition by the SPOUT methyltransferases. *J Biol Chem* **298** 102393. (PMID: 35988649)

‡These authors contributed equally to this work and should be considered co-first authors.

**Abstract**

The SpoU-TrmD (SPOUT) methyltransferase superfamily was designated when structural similarity was identified between the transfer RNA (tRNA)-modifying enzymes TrmH (SpoU) and TrmD. SPOUT methyltransferases are found in all domains of life and predominantly modify tRNA or ribosomal RNA (rRNA) substrates, though one instance of an enzyme with a protein substrate has been reported. Modifications placed by SPOUT methyltransferases play diverse roles in regulating cellular processes such as ensuring translational fidelity, altering RNA stability, and conferring bacterial resistance to antibiotics. This large collection of S-adenosyl-L-methionine (SAM)-dependent methyltransferases is defined by a unique α/β fold with a deep trefoil knot in their catalytic (SPOUT) domain. Herein, we describe current knowledge of SPOUT enzyme structure, domain architecture, and key elements of catalytic function, including SAM co-substrate binding, beginning with a new sequence alignment that divides the SPOUT methyltransferase superfamily into four major clades. Finally, a major focus of this review will be on our growing understanding of how these diverse enzymes accomplish the molecular feat of specific substrate recognition and modification, as highlighted by recent advances in our knowledge of protein-RNA complex structures and the discovery of the dependence of one SPOUT methyltransferase on metal ion binding for catalysis. Considering the broad biological roles of RNA modifications, developing a deeper understanding of the process of substrate recognition by the SPOUT enzymes will be critical for defining many facets of fundamental RNA biology with implications for human disease.

**Introduction**

Methyltransferases are a large group of enzymes that catalyze methyl transfer on diverse substrates to perform one of the most common cellular modifications (1). Methylation is

important to gene expression, integrity of macromolecular structure and function, and many facets of small molecule metabolism (2-5). Over 95% of known methyltransferases use S-adenosyl-L-methionine (SAM) as their co-substrate, generating S-adenosyl-homocysteine (SAH) as a product of the methylation reaction. These SAM-dependent enzymes are categorized into five main classes (I-V) based on their catalytic domain structure, although several additional subgroups have recently been identified, including the radical SAM methyltransferases (1,6,7).

The largest group, Class I methyltransferases, are characterized by a structurally conserved Rossmann-like fold with a central topological switch point in the seven β-strand core and a GxG(xG) motif that forms the SAM binding pocket (1). Class II methyltransferases are structurally characterized by a long antiparallel β-sheet surrounded by groups of helices. The active site of these enzymes includes a conserved RxxxGY sequence that binds SAM in an extended conformation at a shallow solvent-exposed groove on the surface of the reaction domain (1,7,8). In Class III methyltransferases, SAM binds in a folded conformation at the active site located between two αβα domains consisting of five β- strands and four helices (1,7,9). The Class IV SAM-dependent methyltransferase family contains the SpoU-TrmD (SPOUT) enzymes, characterized by a unique α/β fold and a deep trefoil knot in the C-terminal half of the SPOUT methyltransferase catalytic domain (10-13). Finally, Class V methyltransferases, or the SET-domain proteins, are composed mainly of β-strands and form a knot at their C-terminus distinct from that of Class IV, and bind SAM in a kinked conformation on the enzyme surface (1,7).

The SPOUT superfamily was first designated when crystal structures confirmed the structural similarity of several methyltransferases, supporting the previously identified sequence homology between two enzymes, SpoU and TrmD, which catalyze different

modifications on transfer RNA (tRNA) substrates (10,14-18). SpoU was later renamed TrmH to denote its biochemical function as the eighth tRNA methylation gene identified in Bacteria (19). SPOUT methyltransferases predominantly methylate tRNA and ribosomal RNA (rRNA) substrates, though one instance of an enzyme that methylates a protein substrate has been reported (20-22). RNA-modifying SPOUT methyltransferases perform methylation at two different general locations on RNA nucleotides: some, like TrmH, methylate the ribose 2'-OH, while others, including TrmD, perform nucleobase methylation (17,21). A list of SPOUT methyltransferases, the modifications they incorporate, and other molecular features discussed throughout this review is shown in **Table 1**. The locations of selected example modifications are also shown on their respective RNA structures in **Fig. 1**, highlighting the diversity of RNA methylations, including $m^1R$ (R = purine, A or G), $m^1\Psi$ ($\Psi$ = pseudouridine), $m^3\Psi$/U, and 2'-O-methylation (Nm; N = any nucleotide, A, U, C, G) (23-27).

Modifications by SPOUT methyltransferases are important for all three domains of life and play key roles in RNA function by impacting RNA stability, ribosomal fidelity, and bacterial antibiotic resistance. For example, tRNA methylation by SPOUT methyltransferases provides stability to tRNA through effects on structure (e.g. Gm18, TrmH) and can be essential for fidelity of decoding, such as by preventing ribosomal frameshifting (e.g. TrmD, $m^1G37$) (4,5,28-32). More recent developments have revealed that tRNAs and their modifications play global roles in biological systems beyond simply ensuring tRNA stability or optimal structure for translation. During cellular stress, tRNA modifications can be altered to regulate translation and gene expression, and tRNA fragments are increasingly implicated in diverse processes, such as cell signaling and stress response (33,34). New links have also been described between tRNA modifications and disease, particularly metabolic and neurological disorders, and cancer (35-37). Many tRNA modifications are performed at the same position by non-homologous

enzymes in bacteria and eukaryotes, making them potentially interesting targets for anti-bacterial drugs. A better understanding of bacterial SPOUT methyltransferases could therefore prove important in the age of increasing antibiotic resistance. Other tRNA modifications and modification enzymes could prove useful in drug design, as evident from the immunostimulatory role of Gm18 modification (performed by TrmH) (38).

rRNA modifications placed by SPOUT methyltransferases hold essential functions in ribosome maturation, such as ribosome assembly and biogenesis, and modifications to the peptidyl transferase center and the decoding site aid in accurate translation (39). In some bacteria, lack of modifications to 16S rRNA disrupts formation of the 30S ribosomal subunit and binding of initiator tRNA (40,41). SPOUT methyltransferase Nep1, for example, is required for assembly of the small ribosomal subunit and mutation of the enzyme is linked to Bowen–Conradi Syndrome in humans (42,43). The bacterial ribosome is also a major target for antibiotics and rRNA methylation is a tool exploited by many bacteria to gain antibiotic resistance by sterically blocking antibiotic binding (44). Methylations incorporated by intrinsic or acquired methyltransferases, including some members of the SPOUT superfamily, can confer exceptionally high-level antibiotic resistance. For example, the thiostrepton-resistance (TsnR) and avilamycin-resistance (AviRb) SPOUT 2'O-methyltransferases modify distinct functional regions of the 23S rRNA to sterically block antibiotic binding and eliminate anti-bacterial activity (45,46).

With these important roles in biology–and likely many more that remain to be elucidated–characterization of SPOUT methyltransferases and their mechanisms of action is critical. Interestingly, despite extensive structural and biochemical characterization of several SPOUT family members, there are few common themes that have emerged to date, beyond the active site trefoil knot that serves as a conserved and defining feature. Although Class I

methyltransferases are more diverse with the ability to modify a wide array of DNA, RNA, or protein substrate, the SPOUT methyltransferase family is much smaller and yet has an incredible amount of mechanistic diversity considering that almost all enzymes within the family act on an RNA substrate. SPOUT methyltransferases have relatively little conservation between different family members in terms of primary sequence, overall domain structure, catalytic mechanism, or mode of RNA binding and recognition. For example, some SPOUT methyltransferases only discriminate substrate at a post binding step, allowing methyl transfer to occur for substrate only (e.g. Trm10), while others (e.g. TrmH) only bind and methylate their specific substrates (28,47). These distinct features illustrate the fascinating biochemical and mechanistic diversity of this enzyme superfamily. In this review, we provide a new maximum likelihood (ML)-based phylogenetic analysis of the SPOUT superfamily as a basis to compare similarities and differences in enzyme structure, domain organization and key elements of catalytic function, including SAM binding and substrate recognition.

**Phylogenetic Analysis of the SPOUT Methyltransferase Superfamily**

The SPOUT methyltransferases adopt a characteristic $\alpha/\beta$ knotted fold but show a high level of sequence diversity, making accurate phylogenetic analyses a challenge. A previous study used 15 representative SPOUT enzymes from the Clusters of Orthologous Groups (COGs) database as seeds to generate a homologous sequence set for phylogenetic tree construction (17). However, the common tree reconstruction techniques of neighbor-joining, maximum parsimony, and ML either did not generate a tree with well resolved branches and high support values, or were computationally impractical at that time (for ML). We re-addressed this challenge using the much larger sequence dataset (276,000 sequences) now available in the InterPro database (ID: IPR029028). Specifically, our goal was to infer the phylogenetic

relationship of the evolutionarily conserved SPOUT domain across the entire family of SPOUT methyltransferases, omitting the NTD and CTD extensions which are likely to have been acquired by these enzymes through independent evolutionary events.

Most of the currently available 276,000 SPOUT domain-containing sequences are found in Bacteria (248,000), with Eukarya and Archaea having 15,000 and 9,000 sequences, respectively. Using the UniRef50 dataset (i.e. representative sequences with less than 50% sequence identity) these diverse protein sequences were aligned based on their SPOUT domain only and used to create a phylogenetic tree by the ML method (**Fig. 2A**). For the phylogenetic reconstruction, only the SPOUT domain sequences were considered, as these homologous sequences should contain essential residue signatures, while inclusion of NTD or CTD sequence would result in poor alignment and unrealistic phylogenetic inferences. ProtTest (48) was used to determine the best fit model of amino acid substitution based on Akaike Information Criterion (AIC) and the phylogenetic tree was bootstrapped 100 times. This new data set includes a greater number of COGs compared to the previous analysis, including multiple superfamily members for which functional information is available (enzymes indicated on the tree in **Fig. 2A**). As observed previously (17), our ML tree has low bootstrap values in most deep nodes, while the terminal nodes have high values giving strong support to the composition of individual subclades. Further, we also used a BLOSUM45 similarity matrix of representative SPOUT methyltransferases (indicated in **Fig. 2A**) to corroborate clustering in the ML phylogenetic tree with members of the same clade typically showing higher similarity values compared to those outside (**Fig. 2B**). Two exceptions to this are TrmH and Sfm1 which have broader similarity or dissimilarity scores with members of multiple clades, respectively, and thus are not confidently assigned to one of the major groups. In our multiple sequence

alignment dataset, the lowest amount of pairwise identity is ~4% while the overall average identity as calculated by the ALISTAT server is 16%.

Our new ML phylogenetic tree reveals four major groupings (Clades 1-4; **Fig. 2A**) of SPOUT-domain methyltransferases, with numerous subclades mostly containing at least one functionally characterized enzyme. Most of the enzymes within Clade 1 modify tRNAs in their anticodon stem-loop. These enzymes include the tRNA methyltransferases TrmJ and TrmL, which modify ribose 2'-OH, and TrmD, which methylates a guanosine base. From the phylogenetic tree, TrmD appears to have evolved later than the ribose 2'-OH methyltransferases of the same clade. We also observe a distinct branch that is most closely associated with Clade 1, and which includes another tRNA modifying SPOUT enzyme, TrmH. In contrast to the Clade 1 enzymes noted above, however, TrmH methylates tRNA outside the anticodon stem-loop. This distinct branch also includes the protein methyltransferase Sfm1, indicating it may have a most recent common ancestor with SPOUT superfamily enzymes of Clade 1. Characterized SPOUT methyltransferases in Clade 2 include Nep1, Trm56 and RsmE, with the RsmE methyltransferases more distant phylogenetically from Nep1 and Trm56. Nep1 and RmsE are both rRNA methyltransferases and modify a pseudouridine base in 18S rRNA and uridine base in 16S rRNA, respectively. However, these enzymes are mechanistically distinct in their action, acting on free rRNA (Nep1) and assembled 30S subunit rRNA (RsmE), perhaps reflecting their evolutionary distance within Clade 2. In contrast to both other examples in Clade 2, Trm56 methylates the ribose 2'-OH on a tRNA substrate. Clade 3 represents a large group of diverse methyltransferases, including Trm3, MRM1, MRM3, TsnR, AviRb, and RlmB, all of which methylate the ribose 2'-OH at different locations within tRNA or rRNA. Given this common modification type for all clade members, these enzymes likely evolved from an ancestral SPOUT 2'-OH methyltransferase. Finally, Clade 4 consists of

methyltransferases which diverged from a common ancestor much earlier, and includes all Trm10 enzymes, TrmY and RlmH, which all methylate RNA on the nucleobase.

In summary, this phylogenetic analysis gives a glimpse into the possible phylogenetic relationships between diverse SPOUT superfamily members that have been difficult to rationalize due to the diverse functional features associated with these enzymes, as described in more detail in this review. However, detailed insight into the overall evolution of the SPOUT superfamily remains limited by high sequence divergence, low support in the deep tree branches, and potential influence of the NTD/ CTD sequences which were excluded from the alignment due to their even greater sequence and structural divergence. For example, as all sequences in the phylogenetic tree possess less than 50% sequence identity, predictions for enzymes of unknown function within each clade should be made with caution. While details such as the specific site of base modification would be highly speculative based on the phylogeny alone, new inferences on likely substrate or target (e.g. rRNA vs. tRNA, or 2'-OH vs base modification) might reasonably be made based on phylogenetic closeness to a known representative.

**SPOUT Methyltransferase Structure, SAM Binding, and Domain Organization**

The SPOUT domain consists of a protein backbone (~160 amino acids) which is passed three times in and out of a loop to form a topological trefoil knot in its C-terminal region (16,18,21) (shown using TrmD and TrmH as examples in **Fig. 3**). This characteristic feature of SPOUT methyltransferases has less sequence variation (is more conserved) as compared to other regions of the SPOUT domain, especially within each clade of our phylogenetic tree. The average sequence identity for the full alignment is 16%, while the region corresponding to the trefoil knot exhibits 28% identity. Further, there is 94-99% conservation of glycine residues

within the knot region among highly diverse methyltransferases, showing the role of specific sequence as well as structural conservation in this defining feature of the SPOUT domain.

Knots are known to provide stability to protein structure and resistance to degradation (49,50), and in the case of SPOUT methyltransferases the trefoil knot also provides the binding site for the essential SAM co-substrate (51) (**Fig. 4A,B**). Co-substrate binding at this unique structural feature promotes methyl transfer by orienting groups within the active site in an optimal conformation (49,50). The bound SAM adopts a unique bent conformation in SPOUT methyltransferases with its methionine moiety rotated 80˚ to face the adenosine component (**Fig. 4C**). In contrast, when bound to other SAM-dependent enzymes these groups are extended ~180˚ away from one another (Class I) or the methionine group is rotated ~90˚ in the opposite direction (Classes II, III and V) (1,12,50). Analysis of TrmD structures along with molecular modeling revealed that when the trefoil knot is missing, SAM cannot adopt the bent conformation in the enzyme active site (50). SAM is consequently positioned in a non-optimal extended conformation in which the methyl group is further from the target atom, and there is a steric clash between SAM and the tRNA substrate. The presence of the trefoil knot thus enforces the bent SAM conformation, prevents steric clashes, and optimally positions the methyl group relative to substrate for transfer.

Almost all SPOUT methyltransferases function as homodimers with the active site forming upon dimerization to bind two SAM molecules, but only one RNA substrate. Along with the SAM-bound trefoil knot of the SPOUT domain, a four-helix bundle forms at the dimer interface with two $\alpha$-helices from each protomer assembling in a perpendicular (rotated ~90˚ from one another) or an antiparallel fashion (rotated ~180˚; **Fig. 3D**). Each dimerization mode tends to align with a specific type of RNA methylation, with the perpendicular and anti-parallel dimerization modes corresponding most often to ribose sugar or base modification,

respectively (**Table 1**) (17). Finally, Trm10 and Sfm1 are distinct from other SPOUT methyltransferases as they function as monomers, reminiscent of Class I (Rossmann-like fold) methyltransferases, despite having the SPOUT-defining trefoil knot in their active sites (20,52,53). Our phylogenetic analysis indicates that these enzymes may have evolved from ancestral dimeric proteins by loss of the dimeric interface (**Fig. 2**).

SPOUT methyltransferases can be composed of the SPOUT domain alone or have extended N- and/ or C-terminal domains (NTD/ CTD) surrounding the SPOUT domain (10,21). Extended sequences vary drastically among SPOUT methyltransferases, ranging from very short (<20 amino acids) to over 1000 amino acids in length. Examples of SPOUT methyltransferases with each possible configuration of domain structure have been identified and characterized: SPOUT domain only (e.g. TrmL and RlmH), N-terminal extension only (e.g. RsmE and TsnR), C-terminal extension only (e.g. TrmJ, TrmD and Smf1), and both N- and C-terminal extended (e.g. Trm10 and TrmH) (**Table 1**). Interestingly, each domain structure subgroup contains at least one enzyme that modifies RNA at the ribose 2'-OH, and one that modifies at the base. Though the SPOUT domain binds co-substrate SAM and, in some instances, can discriminate between different modification targets (28), SPOUT methyltransferases with extended domains have been proposed to use these extra sequences to aid in protein dimerization, RNA binding, and/ or methylation of their substrate pool (21). As the SPOUT methyltransferase superfamily evolved, diversification of the SPOUT methyltransferases, presumably driven by expansion of target substrates, resulted in loss or gain of these N- and/or C-terminal appendages.

The minimalist SPOUT methyltransferases, which lack any appended domains, must contain all residues and structural features necessary for specific substrate recognition and methylation within the SPOUT domain itself. The most well-characterized minimalist SPOUT

enzymes are TrmL (YibK) and RlmH (YbeA), which methylate the ribose 2'-OH and nucleobase, respectively (54,55). Although both contain the SPOUT domain and use dimerization to form their active sites, they act at unique positions on their respective tRNA and rRNA substrates providing the clearest example that SPOUT domain sequence variation and dimerization mode alone are sufficient to drive unique methylation abilities (23,56).

Two well-characterized SPOUT methyltransferases with only NTD extensions are TsnR (2'-OH methylation) and RsmE (base methylation). The NTD extensions of TsnR and RsmE are structurally similar to ribosomal protein eL30 and PUA (pseudouridine synthase and archaeosine-specific transglycosylase) RNA-binding domains, respectively, highlighting their likely importance in RNA binding (46,57). In both instances the extended domain is also essential for substrate methylation to occur efficiently, as discussed further in the following sections. SPOUT methyltransferases with CTD extensions again include both a ribose 2'-OH (TrmJ) and a base (TrmD) modifying RNA methyltransferase, as well as Sfm1 which acts on a protein substrate (20,27,29). TrmJ is inactive without its CTD extension, while mutation of critical residues in the TrmD or Sfm1 CTD abolishes methylation in these enzymes (20,24). Despite sharing a common domain organization, these three enzymes show that the presence alone of a domain extension does not enforce a particular quaternary structure or the identity of the substrate to be methylated. Finally, SPOUT methyltransferases with both an extended N- and C-terminal domain around the SPOUT domain include Trm10 and TrmH (19,25). The 2'-OH methyltransferase TrmH is evolutionarily distinct from base methyltransferase Trm10 despite their shared domain architecture (**Fig.2**). TrmH and Trm10 also have far more diversity in their extended domain structures among the homologs of each enzyme than other SPOUT methyltransferases (21,28,52).

A central question to consider when characterizing SPOUT methyltransferases is how this superfamily of enzymes with a common SPOUT domain structure acts on diverse substrates in unique mechanistic ways, while also taking advantage of all the differences that have been identified in external domains, dimerization mode, and/or sequence. Furthermore, some close relatives of the same SPOUT methyltransferase have similar domain structure and yet have distinct mechanisms, attesting to a combination of currently ill-defined factors that define overall methyltransferase activity. Nonetheless, recent advances in structural and biochemical characterization of many SPOUT enzymes have revealed many functional and mechanistic intricacies for each type of SPOUT methyltransferase, and these features are described in more detail below.

**Substrate Recognition and Modification by SPOUT Methyltransferases**

Correct substrate recognition is an essential step for enzyme specificity that involves accurate discrimination between the correct target molecule at its modification site and other structurally similar molecules. SPOUT methyltransferases have strict substrate specificity with each enzyme acting only on a specific subset of RNAs or protein, and at a single or very limited number of modification sites. Despite their shared catalytic SPOUT domain, there is considerable variation in the mechanism of substrate recognition between members of the SPOUT superfamily and, complicating a deep understanding of these processes, even between direct homologs of the same enzyme from different organisms.

As noted already, RNA-modifying SPOUT methyltransferases act on either the ribose 2’-OH or various sites on the nucleobase. Through apparent parallel evolution of various structural and domain organization features within each subgroup of SPOUT methyltransferase, significant variation in the mechanism of substrate recognition has arisen,

including differences in target nucleotide specificity and recognition of distinct RNA structural elements. In the following sections, we discuss features of substrate recognition by SPOUT methyltransferases and highlight our current understanding of both similarities and differences within this diverse pool of enzymes. Enzymes are organized by modification type (ribose 2'-O-methylation, base methylation, and protein methylation) with each subsection ordered by clade (Clade 1-4).

*Ribose 2'-O-methylating SPOUT RNA methyltransferases*

Multiple SPOUT methyltransferases catalyze ribose 2'-O-methylation of target nucleotides in either tRNA or rRNA. Although these enzymes modify the ribose common to the four nucleotide bases, the base identity of the target nucleotide can differentially impact methylation activity of individual SPOUT enzymes, highlighted by experiments where target nucleotides were mutated without affecting overall substrate structure. From our phylogenetic analysis, this nucleotide specificity does not seem to be a monophyletic trait, indicating that this family of enzymes did not evolve uniformly over time to become more or less specific with respect to target nucleotide recognition. Ribose 2'-O-methylating SPOUT methyltransferases are spread out across three different clades with Clade 1 containing two enzymes (TrmJ and TrmL) and being most closely associated with a third (TrmH), Clade 2 containing one (Trm56), and Clade 3 containing the majority (Trm3, MRM1, RlmB, TsnR, MRM3, and AviRB) (**Fig. 2**). As discussed below for the best characterized enzymes, ribose 2'-O-methylating enzymes have been observed to recognize distinct features in their substrate, including, to varying extents, contacts with more distant structural elements.

***TrmJ***–TrmJ methylates tRNA at position 32, within the anticodon stem-loop (24,27). This SPOUT methyltransferase has a CTD extension connected to the SPOUT domain via a

16 amino acid linker sequence (23). The domain lengths of TrmJ homologs across organisms are fairly consistent, with the SPOUT domain and CTD extension consisting of ~180 and ~70 amino acids, respectively (**Table 1**) (58). The CTD contains positively charged residues which aid in RNA binding, although the CTD alone cannot efficiently bind substrate tRNA (58). Deletions of different regions of the protein–CTD, SPOUT domain, or part of the linker–uncovered that each is essential for methylation activity (24,58). Additionally, swapping the CTDs of TrmJ enzymes from different species resulted in loss of methylation activity, despite their similar sizes. Therefore, although these methyltransferases perform the same modification in their respective organisms, each has its own specific CTD dependency to maintain methyltransferase activity. These differences between family members clearly play vital roles in diversifying the substrate pool despite similar domain architecture.

*Escherichia coli* TrmJ is the only SPOUT methyltransferase identified to date that can modify the ribose of tRNA position 32 regardless of the identity of the nucleotide. Although Cm32 and Um32 appear to be the only physiologically relevant modifications introduced (24), this implies that *E. coli* TrmJ does not recognize the nucleotide base at the site of modification. This differs from *Sulfolobus acidocaldarius* TrmJ which is only able to modify a cytidine at the same position. One clear distinction identified between these homologs that might explain these distinct specificities appears to be the differing conformations of the bound co-substrate in each TrmJ enzyme (discussed in more detail later). Another distinction between the two TrmJ orthologs involves overall recognition of the tRNA substrate: *S. acidocaldarius* TrmJ can effectively modify a truncated tRNA structure corresponding to the anticodon stem-loop fused to an acceptor stem (24,58), whereas *E.* coli TrmJ also requires the D- and T- arms within the full tertiary tRNA structure. The different requirements for tRNA substrate recognition may be due to different sizes of the positively charged area in the cleft of the dimer interface. However,

the current lack of a structure of the tRNA-bound enzyme precludes detailed understanding of these or other differences that may contribute to the distinct TrmJ nucleotide specificities.

***TrmL***–TrmL is a minimalist SPOUT methyltransferase that modifies the first anticodon nucleotide (position 34) of tRNA (54). TrmL functions as a homodimer, with dimerization being essential to form a stable complex with substrate tRNA: a Tyr142 to alanine substitution that disrupts dimer formation eliminates the ability of TrmL to bind tRNA (23).

TrmL exhibits some flexibility in target nucleotide selection with the ability to methylate modified 5-carboxymethylaminomethyluridine ($cmnm^5U$), unmodified U, or unmodified C at position 34 (54). Additionally, A35 is a key residue for substrate recognition by TrmL and A36-A37-A38 are important either via direct interaction with TrmL or due to the necessity for prior isopentenylation (i6) on A37 (59). As such, TrmL is one of the few SPOUT enzymes that requires a prior modification to the substrate base before methylation can occur. The i6 modification on A37 has been hypothesized to guide TrmL methylation by increasing the chance of nucleotide 34 having direct interaction with the enzyme (23,59). TrmL is also one of relatively few SPOUT methyltransferases that can efficiently modify a truncated tRNA structure (59), requiring only an anticodon stem-loop minihelix with an extension of two base pairs. A high-resolution structure of TrmL bound to tRNA will be an important future step to help elucidate the determinants of specific substrate recognition.

***TrmH/Trm3***–TrmH and Trm3 catalyze the Gm18 modification in the D-loop of tRNA, in Bacteria and Eukarya, respectively (19,60,61). Among TrmH enzymes, there is considerable variation in the size and configuration of appended domains. *Thermus thermophilus* and *Aquifex aeolicus* TrmH have similar sized NTDs and CTDs (~20 amino acids) with extended $\alpha$-helices surrounding the SPOUT domain (28), while the CTD of *E. coli* TrmH is >30 amino acids longer and forms a structure comprising one $\alpha$-helix and three $\beta$-strands (28). In even

starker contrast, eukaryotic Gm18 modifying enzymes such as *Saccharomyces cerevisiae* Trm3 and human TARBP1 have extremely long NTDs (1280 and 1400 amino acids, respectively) but no CTD extensions (62,63). Although these eukaryotic homologs are fully active without CTD extensions, deletion of the *T. thermophilus* TrmH CTD renders the enzyme unable to bind and methylate tRNA (28). Additionally, the NTD of TrmH in *T. thermophilus* plays an important role in stabilizing the homodimer structure and was found to be important for protein stability, thus making the NTD necessary for both methylation activity and tRNA-binding (16,28,64). The apparent distinct evolutionary origin of TrmH and Trm3 enzymes (**Fig. 2**) may have contributed to the diverse array of domain structures and functions observed within enzymes that catalyze the Gm18 modification, and underscores the complexity present even within SPOUT enzymes that catalyze identical modifications.

Diverse TrmH homologs also exhibit distinct RNA substrate specificities. For example, *T. thermophilus* TrmH can methylate all tRNA species while other TrmH homologs, for example from *A. aeolicus* and *E. coli*, can only modify a subset of tRNA with a G nucleotide at the target position 18 (65). Superposition of the SAM-binding domains of TrmH from *T. thermophilus* and *A. aeolicus* reveals a difference in the orientation of the α1/α8 extensions and *A. aeolicus* TrmH contains a stretch of basic residues on this extension that is not found in the *T. thermophilus* enzyme (66). This region may therefore be responsible for the restricted specificity exhibited by *A. aeolicus* TrmH. Further, TrmH chimeras created by swapping CTD, SPOUT, and NTD domains between *T. Thermophilus* and *E. coli* family members produced enzymes with altered substrate specificities (28). These studies revealed that although the CTD and NTD play important roles in RNA binding, the SPOUT domain is primarily responsible for substrate recognition among studied enzymes in the TrmH family.

In the process of specific tRNA recognition by TrmH, the G18-G19 dinucleotide at the target site appears to be the only essential sequence determinant among the 18 conserved or semi-conserved nucleotides identified among tRNA substrates; mutation of either guanosine nucleotide results in loss of methylation (67). The strict recognition of guanosine by TrmH also means that when G18 is mutated, TrmH can methylate the adjacent G19 instead. More specifically, the $O^6$ atom of the guanine nucleobase is a positive determinant for target site recognition, considering that TrmH can methylate a tRNA with an $O^6$-containing inosine at position 18 (65). TrmH from both *T. thermophilus* and *A. aeolicus* can modify a tRNA 5' fragment with only the intact D-loop structure, although the reaction is considerably less efficient than for full-length tRNA (68,69). Mutations that disrupt the tertiary base pairs between the D- and T-loops decrease binding of TrmH to tRNA significantly (67). This suggests that while the D-loop contains critical positive determinants for substrate recognition, ultimately the full tRNA tertiary structure including intact D- and T-loop interactions is required for optimal methylation activity. These findings also suggest that, apart from the essential dinucleotide sequence at the target site, TrmH recognizes RNA backbone geometry as opposed to specific nucleotide sequences in the full-length tRNA structure (67).

***Trm56***–Trm56 modifies cytosine at nucleotide 56 in the T-loop of tRNA (70-72). Methylation activity is abolished when C56 is mutated to G, indicating that the identity of the nucleotide at the modification site is essential for recognition by Trm56 (71). Characterized Trm56 enzymes typically have CTD extensions of similar lengths appended to the SPOUT domain (**Table I**), though the *Thermoplasma acidophilum* Trm56 CTD is much greater in length with a HD (His-Asp) phosphodiesterase-like domain of almost 200 amino acids (73). Studies of Trm56 from *Pyrococcus abyssi* revealed this enzyme to be another example of a SPOUT methyltransferase which can act on a truncated tRNA, albeit with suboptimal methylation

activity (70). Specifically, Trm56 can methylate the ribose of C56 in a stem-loop RNA corresponding to the isolated T-arm, but methylation is four- to five-fold less efficient than with the full-length substrate.

***TsnR***–The thiostrepton-resistance methyltransferase TsnR is a ribose 2'-OH modifying enzyme that methylates nucleotide A1067 located in a loop at the end of Helix 43 of the bacterial 23S rRNA (74). TsnR has an N-terminal extended domain that resembles the yeast RNA binding ribosomal protein eL30 and, like most SPOUT methyltransferases, TsnR functions as a homodimer (**Table 1**). The full-length enzyme has specific RNA binding that is of higher affinity than the SPOUT domain alone, while the NTD alone has no apparent binding affinity for RNA (46). The two domains thus appear to function in concert; the SPOUT domain initiates RNA binding which positions the NTDs for high affinity binding, substrate discrimination, and formation of a catalytically active complex. Notably, the substrate rRNA must undergo a conformational change led by the NTD that is required for catalysis; the isolated SPOUT domain cannot induce this conformational change and therefore cannot methylate substrate RNA despite having some intrinsic RNA affinity and containing the bound SAM co-substrate. In this instance, the extended domain is essential not only for binding but also catalytic activity.

TsnR specifically recognizes a U1066-A1067-G1068-A1070 loop sequence at the target site which caps 23S rRNA Helix 43 (75). Studies to elucidate the minimal substrate necessary for substrate recognition by TsnR determined that an isolated 29-nucleotide rRNA hairpin containing the target nucleotide acts as a more efficient substrate than the 58-nucleotide domain or full-length 23S rRNA (76). This enhanced substrate preference for the 29-nucleotide hairpin is most likely due to increased accessibility of the target nucleotide in the hairpin which lacks the complex tertiary structure of the full 58-nt rRNA domain. The nosiheptide-resistance

methyltransferase (NshR), a close relative of TsnR, methylates the same site on the 23S rRNA and also displays similar specificities for a 29-nucleotide fragment (77). Interestingly, both TsnR and NshR make a critical contact with nucleotide U1061, located in an internal loop within Helix 43 more distant from the target site, that allows for efficient substrate binding (76). This nucleotide makes interactions that stabilize the RNA tertiary structure of the 58-nt rRNA domain and, as a result, the protein-RNA contact may be required for RNA unfolding to fully expose the target nucleotide for recognition and modification.

*Base-modifying SPOUT RNA methyltransferases*

SPOUT methyltransferases have been identified that modify both purine and pyrimidine nucleotide bases, generating $m^1\Psi$, $m^3U/\Psi$, or $m^1G/A$ modifications. Base-modifying SPOUT methyltransferases are found in Clade 1 (TrmD), Clade 2 (Nep1 and RsmE), and Clade 4 (Trm10 and RlmH); additionally, TrmY appears to have evolved independently from these other enzymes (**Fig. 2**). While most of these enzymes require dimerization for methylation activity, this subcategory contains Trm10 which is the only SPOUT RNA methyltransferase believed to be catalytically active as a monomer. The mechanisms of substrate recognition for base-modifying enzymes are known in some cases, but questions remain about the molecular details of substrate selection for others. The structures of TRMT10C, TrmD, and Nep1 in complex with their target RNAs have provided insight into some of the molecular contacts and structural features of the substrate that are exploited for specific recognition. However, these insights have also highlighted the need for additional structure-function studies to fully define how different members of this diverse enzyme family select and specifically modify their RNA substrate(s).

***TrmD***–Of all SPOUT methyltransferases, the mechanism of substrate recognition by TrmD has been investigated the most extensively. TrmD produces the $m^1G37$ modification in the anticodon loop of tRNA in Bacteria (29,78). TrmD has a CTD extension following the SPOUT domain with a flexible linker connecting the two (**Table 1**) (18). The CTD is similarly sized (~74-95 amino acids) across species where it has been characterized, to date (13). In the TrmD dimer, the SPOUT domain of one protomer and the CTD extension of the second jointly bind one tRNA at its anticodon branch. Additionally, the flexible interdomain linker becomes ordered and forms an α-helix when bound to tRNA (15). Both protomers in the TrmD dimer bind SAM, resulting in an enzyme-substrate complex comprising two SAM molecules but only a single tRNA per dimer, leaving the second active site non-functional. Residue Asp169 from the CTD extension is important for methyl transfer, as its mutation abolished TrmD methylation activity (15,18,51). Therefore, the SPOUT domain of TrmD alone is likely to be insufficient for binding and methyl transfer.

TrmD is highly dependent on nucleotide sequence at its target site, requiring the sequence G36-G37 for optimal tRNA methylation (79). Intriguingly, the dinucleotide GpG alone was found to be a minimal, albeit inefficient, substrate for TrmD. However, in *E. coli*, only a subset of tRNA with the G36-G37 sequence possess the $m^1G37$ modification (80), indicating that GpG is a positive but not sufficient determinant for substrate recognition. Additional structural elements in tRNA are recognized by TrmD that can either make methylation more efficient or hinder the process. Subsequent studies revealed that TrmD from both *E. coli* and *A. aeolicus* can also methylate tRNA with the sequence A36G37, suggesting a more relaxed requirement of a purine nucleotide at position 36 (81). Notably, however, the A36-G37 sequence does not occur naturally in Bacteria (15). In the engineered G36A tRNA variant, the 6-$NH_2$ group of adenine most likely interacts with TrmD carboxyl oxygen atoms of Asp50.

However, the catalytic efficiency of methylation of transcripts with A36-G37 is lower, reflecting an overall $K_M$ value that is slightly higher than that of wild-type tRNA (81,82).

Although G36 and G37 are the only essential nucleotides for substrate recognition, TrmD recognizes additional structural elements throughout the tRNA anticodon loop. TrmD from *A. aeolicus and E. coli* can both modify stem-loop structures corresponding to 17-nucleotide isolated anticodon stem-loop, although *E. coli* TrmD requires the addition of at least four additional base pairs for detectable methylation activity on the truncated substrate (79,81,83). Further, studies on *E. coli* TrmD reveal that although this homolog can modify a truncated tRNA transcript, the full-length tRNA is required for optimal catalytic efficiency (83).

While deletions of different tRNA regions resulted in reduced methylation activity, significant changes in tRNA sequence outside of the anticodon stem-loop had only modest effects on enzyme activity (81,83). As noted for TrmH, this suggests that the primary RNA contacts may be with the phospho-sugar backbone of tRNA and that backbone geometry plays an important role in tRNA substrate recognition. Consistent with the previous biochemical data, the structure of the TrmD-tRNA substrate complex revealed essential contacts with the tRNA anticodon branch, comprising the D and anticodon arms and the variable loop (**Fig. 5A**) (15). However, TrmD does not directly contact the tRNA acceptor branch (acceptor and T arms), at apparent odds with the results of the previous methylation activity assays. These findings can be reconciled based on the essential nature of the overall tRNA structure for TrmD recognition. Specifically, while not directly contacted by the enzyme, the acceptor and T arms must be present for correct tRNA folding and thus presentation of key determinants in the anticodon branch that are necessary for efficient methylation activity.

Uniquely, the methyl transfer reaction by TrmD only occurs when a $Mg^{2+}$ is bound in the active site (84,85). A recent study demonstrated through combined molecular dynamics

simulations, quantum mechanical studies, and mutagenesis/ enzyme activity assays that the essential $Mg^{2+}$ ion binds to a negatively charged pocket in the TrmD active site, causing structural changes that force SAM to adopt its bent conformation and align with active site residues in an optimal orientation for catalysis (84). A previous metal rescue experiment suggested that the essential $Mg^{2+}$ might interact with G37 $O^6$ (85), but the detailed computational studies suggest an alternative mechanism whereby the active site residue Arg154 stabilizes the $O^6$ during the course of the methyl transfer reaction (84).

***Nep1***–Nep1 is a base modifying methyltransferase found in Archaea and Eukarya. Based on the RNA recognition sequence in yeast, Nep1 is predicted to act on Ψ1189 of 18S rRNA (43,86,87). Nep1 is highly dependent on recognition of the specific consensus sequence C/UUCAAC at the rRNA target site. This recognition is accomplished through base-specific interactions with protein residue side chains and peptide backbone in its binding pocket which have been characterized in detail through high-resolution crystallographic structural studies (88). As discussed later, Nep1 undergoes a structural rearrangement to accommodate the rRNA substrate, while also causing a conformational change in the RNA to flip out the target base for methylation.

***RsmE***–SPOUT methyltransferase RsmE methylates U1498 to form $m^3U$ in a conserved region of helix 44 of bacterial 16S rRNA (89). RsmE includes an NTD extension, preceding its SPOUT domain, that is of similar length in most homologs (~69-81 amino acids; **Table 1**). The NTD of *E. coli* RsmE is composed of five β-sheets and an α-helix and resembles the RNA-binding protein PUA (57). RsmE functions as a dimer with the PUA-like NTD of one protomer acting in RNA recognition and binding, and the SPOUT domain of the other presenting a bound SAM for methyl transfer. With its essential role in substrate binding, the NTD extension is thus required for methylation to occur (57). Studies to elucidate the minimal RsmE substrate

uncovered that neither 16S rRNA nor 30S depleted of proteins serves as an efficient substrate. In contrast, mature 30S subunit is efficiently modified suggesting that a highly structured ribonucleoprotein particle late in the subunit assembly pathway is required (90). This substrate preference appears to be a general preference for methyltransferases that modify 16S rRNA near the ribosomal decoding center (91).

***TrmY***–TrmY modifies Ψ54 in the T-loop of tRNA and is another example of a SPOUT methyltransferase which is only able to act on a previously modified tRNA substrate, in which U54/U55 have been converted to pseudouridine by Pus10 (92). The necessity for modification prior to TrmY methylation hindered early efforts to characterize substrate recognition using unmodified tRNA substrates but was resolved by incubation of substrate tRNAs with Pus10 before *in vitro* methylation studies.

The location of the modification site at the end of the T-loop suggests that TrmY may make contacts with both the D-loop and T-loop to disrupt the interactions between the two tRNA arms to access the target nucleotide. However, TrmY was found to readily modify an isolated T-loop RNA transcript indicating that all structural elements necessary for recognition by TrmY are contained within this region (92). Despite the proximity of the D-loop to the modification site and the extensive interactions between the D- and T-loop, the D-loop does not seem to be essential for substrate recognition by TrmY. However, further kinetic and binding studies are necessary to confirm that the efficiency of methylation of this tRNA fragment is comparable to full-length tRNA.

***Trm10***–Trm10 modifies purines (G and/or A) at position 9 of tRNA and is the only SPOUT methyltransferase that modifies a junction nucleotide found in the core of the tRNA (25,93). Trm10 exhibits a remarkable diversity of target nucleotide specificity between orthologs and paralogs. For example, three paralogs of Trm10 are found in humans: TRMT10A,

TRMT10B, and TRMT10C. Each enzyme methylates a unique subset of tRNAs with TRMT10A modifying certain tRNAs containing G9, TRMT10B identified as modifying only one A9-containing tRNA species, and TRMT10C exhibiting bifunctional activity, methylating certain tRNAs containing either G9 or A9 (47,94-96). Trm10 from *S. cerevisiae* is the direct homolog of TRMT10A and only modifies certain G9-containing substrates (47,95). Among archaeal Trm10 orthologs, substrate specificities analogous to those of TRMT10B and TRMT10C have been identified, with Trm10 from *S. acidocaldarius* modifying A9-containing tRNAs and Trm10 from *Thermococcus kodakarensis* modifying G9- and A9-containg tRNAs (22,26,47,95,96). The molecular basis for these differences in target nucleotide specificity remains poorly understood despite extensive biochemical characterization and availability of multiple structures of different members of the Trm10 family (52,53,97,98).

Trm10 enzymes typically contain both NTD and CTD extensions, and function as monomers rather than dimers. However, the length and sequence of the N- and C-terminal extensions can vary drastically even among Trm10 homologs that perform similar modifications (**Table 1**). Yeast Trm10 enzymes (*S. cerevisiae* and *Schizosaccharomyces pombe*) have similarly sized extended domains with NTD and CTD lengths of around 80 and 20 amino acids, respectively. In contrast, the three human Trm10 paralogs exhibit significant differences in size and sequence of the extended domains, with NTDs of 90, 100, and 140 amino acids for TRMT10A, B, and C, respectively, and the CTD extensions having around 60, 8, and 20 amino acids for the same enzymes. Archaeal Trm10 from *S. acidocaldarius* has 79 and 46 amino acid extensions on its NTD and CTD, respectively (26). Overall, Trm10 homologs exhibit more diversity in domain length than other SPOUT family members which is likely related to the distinct catalytic activities identified for different Trm10 enzymes. The fact that Trm10 is active as a monomer, unlike other SPOUT methyltransferases, may also be a reason for the greater

diversity in domain structure since residues from a second protomer are not available to enable flexible RNA substrate recognition. Structures of multiple Trm10 homologs have revealed that dimerization is likely impeded by the placement of the CTD and the α6 helix which block the typical dimer interface (52,53). A computational docking model of tRNA to *S. acidocaldarius* Trm10 predicts that the NTD, SPOUT domain, and CTD of Trm10 interact with the entire L-shape structure of the tRNA (53).

A recently solved single-particle cryo-electron microscopy structure of TRMT10C in complex with substrate pre-tRNA reveals more intricate details of how Trm10 interacts with its substrate (98). The structure shows key interactions between TRMT10C and all arms of the tRNA and explains why TRMT10C requires the full tRNA for substrate recognition by identifying both base-specific and non-specific interactions. In this structure, residues Phe177 and Arg185 in the adapter loops that connect the NTD and SPOUT domain of TRMT10C stack against U35 and C32, respectively, in the tRNA anticodon loop. Arg181 also protrudes into the anticodon loop to interact with the $C^2$ carbonyl of U33 in an interaction specific to pyrimidines. The N-terminal domain of TRMT10C, which wraps around the tRNA and is lined with positively charged residues, encases the anticodon arm with a connector helix that runs along a groove between the D-loop, anticodon loop, and T-loop. Residue Tyr135 stacks against A47 in the variable region, causing a distortion in the tRNA structure wherein the groove is widened between the D arm and anticodon arm of the tRNA, while the anticodon loop placement is shifted. These insights allow rationalization of the role of the NTD in aiding methyl transfer by TRMT10C.

In the SPOUT domain of TRMT10C, the target nucleotide G9 is flipped out of the tRNA core and stacks with Val313. Interactions between Gln226 and the $N^3$ of the primary amine of G9 most likely ensure selectivity of purines at this position. Additionally, Asn350 and Asn348

reach towards the substrate and appear to interact with the carbonyl oxygen of the guanine base (98). TRMT10C also requires dehydrogenase SDR5C1 for activity in the RNase P complex. Further studies and structures will be needed to determine how much relevance this TRMT10C structure, as part of mitochondrial RNase P, has to the specific enzyme-substrate interactions of other Trm10 species that are not part of this complex and act upon different tRNA substrates.

***RlmH***–RlmH is a minimalist SPOUT enzyme which methylates 23S rRNA at Ψ1915 (55,99) and is thus one of the few SPOUT methyltransferases that requires a prior modification–conversion of uridine to pseudouridine–at its target site to perform methylation (56). Dimerization of RlmH is required to form the active site for rRNA methylation and, as revealed by the structure of *E. coli* RlmH, each protomer appears to be capable of binding to a SAM cofactor. However, the asymmetrical dimerization and proposed positioning of one substrate tRNA per dimer suggest that only one cofactor binding site participates in catalysis. In this arrangement, the SAM binding site of one protomer is oriented to face the proposed RNA binding site of the second protomer where several residues essential for methyl transfer are located (56). Docking models with the bacterial ribosome predict that RlmH makes extensive contacts with both ribosomal subunits, despite its activity targeting only a nucleotide of the large subunit. In these models, RlmH interacts with 16S rRNA nucleotides and ribosomal protein uS12 around the decoding center in the 30S subunit, while contacts between 50S and RlmH are limited to domain IV of the 23S rRNA (56). Although awaiting experimental verification, this model nicely explains the requirement for the full 70S ribosome for RlmH methylation activity, as opposed to an isolated 50S subunit (99,100).

*Sfm1: A protein-modifying SPOUT methyltransferase*

Sfm1 is currently the only known SPOUT methyltransferase that modifies a protein substrate and, along with Trm10, is one of only two SPOUT methyltransferases which are catalytically as a monomer. Sfm1 catalyzes ω-monomethylation at Arg146 in 40S ribosomal protein uS3 in yeast (20). Arg146 methylation by Sfm1 is predicted to aid import of uS3 to the nucleolus for assembly of the ribosomal small subunit (20). Sfm1 has no detectable methylation activity against isolated uS3 peptides (20), suggesting that the enzyme exploits the full protein tertiary structure of uS3 for specific substrate recognition, similar to the requirement for highly structured targets observed with many RNA-modifying SPOUT superfamily members. Sfm1 contains a SPOUT domain and a CTD extension comprising four β-strands and an α-helix (**Table 1**) (20). A major difference between Sfm1 and RNA-modifying SPOUT methyltransferases is the negatively charged surface surrounding its active site, including two acidic residues (Glu9 and Glu19) involved in substrate binding, as opposed to the positively charged surfaces implicated in RNA binding for many SPOUT RNA methyltransferases (20). Interestingly, despite overall structural similarity to the SPOUT family, the active site of Sfm1 shares several common elements with the structurally unrelated protein arginine methyltransferases PRMT3, PRMT5, and PRMT7 which belong to PRMT classes I, II, and III, respectively. In particular, three catalytically critical Sfm1 residues (Glu9, Trp15 and Glu19) adopt a similar spatial arrangement to analogous essential residues in PRMT3, PRMT5 and PRMT7, but with their organization reversed relative to the target substrates, generating a "mirror image" active site structure between the two types of enzyme (20).

A fourth essential Sfm1 residue (Phe180) that is part of the CTD appears to be involved in positioning the target Arg residue, similar to the role of the extended domains in target RNA recognition for other SPOUT enzymes (20). A Phe180 to alanine mutation renders Sfm1

inactive, while mutation of several negatively charged residues of the CTD also decreases methylation. Thus, Sfm1 activity is dependent upon residues in both its extended domain and the SPOUT domain. The SAM-binding pocket of Sfm1 resembles that of other SPOUT methyltransferases, promoting bound SAM or SAH to assume the signature bent conformation. Based on its crystal structure, and complementary solution gel filtration chromatography and light scattering analyses, Sfm1 is the second known SPOUT methyltransferase that functions as a monomer rather than a dimer. Two α-helices that typically interact to mediate SPOUT dimer formation are unable to do so in Sfm1 due to the steric hindrance between the two protomers, when compared to the dimerization patterns of TrmL and TrmD (20).

Together, these studies reveal that other than possessing the characteristic SPOUT domain in which SAM is bound in its bent conformation, substrate recognition and modification by Sfm1 is quite distinct from other SPOUT methyltransferases with its reversal of typical surface charges, atypical active site organization, and action as a monomeric enzyme. These mechanistic features undoubtably evolved in Sfm1 due to the distinct demands of modifying a protein substrate. Additional studies are needed to determine if other protein-methylating SPOUT methyltransferases exist, which could expand the mechanistic strategies employed by this already diverse collection of enzymes.

**Role of Molecular Conformational Dynamics in Substrate Recognition and Modification**

The importance of conformational dynamics is an emerging theme in SPOUT methyltransferase substrate recognition. In addition to the unusual bent SAM conformation enforced by binding the SPOUT domain knot structure, substrate recognition by many SPOUT methyltransferases is a dynamic process that requires specific coordinated conformational

changes in the enzyme and/ or substrate. This may be the case particularly for enzymes that modify otherwise inaccessible sites in their target RNA substrate.

*Bent SAM conformation*

The unique trefoil knot in the SPOUT domain allows SPOUT methyltransferases to enforce a bent conformation in the bound SAM co-substrate in which its methionine moiety is folded toward the adenine base (101). As noted earlier, this bent conformation is necessary for methyl transfer activity and is common among SPOUT methyltransferases regardless of substrate (102). However, there are significant variations in the residues in the active sites of SPOUT methyltransferases that affect how the enzyme binds SAM and the degree to which SAM is bent. Based on observations discussed earlier of the distinct substrate specificities of TrmJ homologs from *E. coli* and *S. acidocaldarius*, there is speculation that the differing bent conformations of SAM may play a role in narrowing or broadening substrate specificity at the target nucleotide for some SPOUT methyltransferases (24). For example, *E. coli* TrmJ binds SAH in a “super-bent” conformation (**Fig. 4C**) stabilized by residue Ser142, and can modify any nucleotide at tRNA position 32. In contrast, *S. acidocaldarius* TrmJ, which has a narrower substrate specificity, has a valine residue (Val139) at the equivalent location which cannot form the same stabilizing interactions. In a Ser142Val variant of *E.coli* TrmJ, the enzyme shifts towards a narrower target site specificity, such that methylation efficiency of U32 is significantly decreased. This finding implies that the super-bent SAH conformation creates space to accommodate a larger variety of nucleotides in the active site and that reducing that space by interrupting bonds which stabilize the SAH conformation would narrow specificity. However, additional structural studies on the TrmJ enzymes in complex with substrate RNA are needed

to fully clarify the role of the super-bent co-substrate in controlling substrate nucleotide specificity.

For other SPOUT enzymes, there are variations in the degree to which SAM (or SAH) is bent, even within the same crystal structure. For example, the structure of the TrmL-SAH complex shows the dimeric enzyme bound to two SAH molecules, as would be expected for a homodimeric SPOUT methyltransferase. However, while one SAH adopts the signature bent conformation, the other is found in an elongated conformation (**Fig. 4C**) in which it forms an expanded network of interactions with TrmL residues (23). The authors of this study proposed that the altered conformation is due to the presence of a HEPES buffer molecule which resembles the ribose and phosphate of a nucleotide and mimics the bound substrate nucleotide. However, this same conformation is not seen in structures of Nep1 and TrmD bound to substrate RNA (15,103), and other dimeric SPOUT methyltransferases, such as TsnR, bind both SAM molecules in similar conformations, indicating that this is not necessarily a mechanism shared by all SPOUT methyltransferases (76).

The presence of divalent metal ions may also play a role in ensuring SAM adopts the appropriate bent conformation for some SPOUT enzymes as discussed previously for TrmD. The $Mg^{2+}$ ion causes structural changes that force SAM to adopt its bent conformation and align with active site residues in an optimal orientation for catalysis (84). Why TrmD needs a metal ion to stabilize the bent SAM conformation and for overall enzymatic activity is unclear given that other SPOUT methyltransferase superfamily members apparently do not have this requirement. However, considering that the role of $Mg^{2+}$ in TrmD methyl transfer activity is a relatively recent discovery, future studies may reveal that metal ions play significant mechanistic roles for other SPOUT methyltransferases as well.

*Protein dynamics*

Studies to elucidate enzyme conformational changes during substrate recognition demonstrate that for many SPOUT methyltransferases, a certain degree of protein plasticity is necessary for efficient methylation. TrmH is an example of a SPOUT methyltransferase that undergoes an induced-fit process to bind and modify tRNA (28). Substrate recognition for TrmH has been broken down into a two-step process: initial tRNA binding followed by a subsequent induced-fit conformational change in TrmH to accommodate the target nucleotide of the substrate. Kinetic studies show that TrmH binds to nonsubstrate tRNA, including already methylated tRNA, but does not undergo the subsequent conformational changes necessary for methylation. Similarly, other SPOUT methyltransferases, such as Trm10, can bind nonsubstrate tRNA that they are unable to methylate, although the mechanism of substrate discrimination for these enzymes has yet to be elucidated in detail (47). However, recognition mechanisms involving an initial enzyme-substrate docking step and subsequent changes in protein and/ or RNA have been demonstrated and proposed for Class I methyltransferases (104,105) and may be a common feature of RNA modifying enzymes, including the SPOUT family.

The structure of the TrmD-tRNA-sinefungin complex offers a detailed view of conformational changes that take place upon substrate binding for this enzyme (15). Upon tRNA binding, the CTD of one TrmD protomer changes its conformation to snugly contact the tRNA. Additionally, the disordered interdomain linker from the same TrmD protomer forms an $\alpha$-helix upon tRNA binding. The structure of Nep1 in complex with a model rRNA substrate reveals a similar structural rearrangement at the dimer interface which opens to accommodate the substrate RNA, with the largest conformational changes being observed in the loop regions between the two protomers (88). Other SPOUT methyltransferases that accommodate

substrate RNA at the dimer interface are predicted to undergo similar conformational changes that may be revealed through future structural studies.

Trm10 is the only RNA-modifying SPOUT methyltransferase that is active as a monomer and the recent structure of TRMT10C in complex with substrate pre-tRNA (as part of the mitochondrial RNase P complex) provides some insight into structural changes that may occur upon substrate binding (98). The previous Trm10 crystal structure determined without substrate tRNA lacks its N-terminal domain, likely due to disorder in this region when not bound to substrate. However, when bound to tRNA, the NTD is α-helical and must exhibit some degree of plasticity to wrap around and bind the tRNA. Superposition of TRMT10C from its complex with pre-tRNA (98) and from the structure of the SPOUT domain bound to SAM (106) show that the catalytic domain remains largely unchanged, aside from local reorganization of a conserved loop (residues 314-319). However, a comparison with the structure of the RNase P complex without SAM suggests that this conformational change occurs upon SAM binding as opposed to with RNA substrate (98). While these findings may help predict the conformational dynamics of other Trm10 enzymes, TRMT10C is unique in that it is part of a larger multi-subunit complex which has multiple functions. Other Trm10 enzymes, such as TRMT10A and TRMT10B, may utilize distinct mechanisms of substrate recognition to compensate for the absence of binding partners.

*Protein-induced RNA conformational changes*

***Base flipping and target site reorganization***–For DNA and RNA methyltransferases to act on nucleotides that are part of a base pair or take part in stacking, it is often necessary for the target nucleotide base to be rotated ~180° around its phosphodiester bond so that the base enters the catalytic pocket. Such “base-flipping” is commonly used by methyltransferases, as

first observed in the Class I methyltransferase *M.HaI* DNA C5-methyltransferase complexed with a synthetic DNA complex (1,107). Structures of TrmD, Nep1, and Trm10 in complex with their substrate RNAs support the idea that protein binding induces specific conformational changes in the RNA surrounding the target nucleotide (**Fig. 5**) (15,88,98). The crystal structure of the TrmD-tRNA-sinefungin complex reveals that prior to methylation, the G37 base is flipped out from the anticodon loop and protrudes into the catalytic pocket located in the SPOUT domain of one TrmD protomer in the homodimer (15). This flipped conformation is stabilized by Leu160 which stacks on the guanine base and Ser165 which forms a hydrogen bond via its side chain OH group with the 2'-OH of G37 (**Fig. 5B**). The $N^1$ atom of G37 forms a hydrogen bond with Asp169 which acts as a proton acceptor, with Arg154 also located near the G37 base to stabilize the increased negative charge on the base $O^6$ after proton transfer. After G37 is flipped from its original position, nucleotide G36 is stabilized in a *syn* conformation by Asp50 of the second protomer of the TrmD homodimer and is stacked between nearby nucleotides A38 and U35. Additionally, the structure around adjacent nucleotides G36 and A38 opens to make space to allow a TrmD interdomain loop to fold into an $\alpha$-helix just above the target nucleotide G37. Following these structural reorganization events involving G37 and G36, methylation can occur.

Nep1 uses a similar base-flipping mechanism in the Nep1-rRNA structure in which the target pseudouridine is flipped out from its loop and bound in a pocket in the active site of the Nep1 homodimer (88). The flipped base is stabilized by aspartate and arginine residues in a catalytic pocket at the interface of the two Nep1 protomers (**Fig. 5C**). Finally, in the structure of TRMT10C in the mitochondrial RNase P complex, the G9 target nucleotide in the tRNA core is flipped out of the tRNA fold and buried in the active site to stack against Val313 (98). The

base is also stabilized in this flipped conformation by additional neighboring asparagine and glutamine residues (**Fig. 5D**).

Many docking models of other SPOUT methyltransferases, such as RlmH, predict a similar base flipping mechanism to place the target nucleotide in the active site of the enzyme (55). Thus far, however, base flipping has only been demonstrated for base-modifying SPOUT methyltransferases as there are currently no corresponding structural insights for 2'-O-modifying SPOUT RNA methyltransferases. However, a recently determined structure of the mycobacterial Class I 2'-O-modifying rRNA methyltransferase TlyA shows that this enzyme employs base flipping as part of its ribose methylation mechanism, indicating that these specific local conformational changes and base-flipping are not exclusive to base-modifying RNA methyltransferases (108). Additional SPOUT methyltransferase-RNA substrate complex structures promise to reveal both common and enzyme-specific mechanistic features of these local conformational changes for both base-modifying SPOUT methyltransferases and 2'-O-modifying methyltransferases.

***Global changes in RNA structure*–**Although local rearrangements of RNA structure discussed above appear to be a relatively common feature of modification enzyme mechanisms, conformational changes to the overall substrate RNA structure are comparatively rare. However, TsnR provides one such example of a SPOUT methyltransferase that is proposed to induce this type of large-scale, global conformational change in its 23S rRNA substrate upon binding. Hydroxyl radical probing studies revealed that the backbone of a 58-nucleotide model rRNA substrate is distorted upon TsnR binding due to structural rearrangements in the target loop that are necessary to orient the target nucleotide A1067 at the apex of 23S rRNA Helix 43 into the enzyme's catalytic site (46). Notably, many of the RNA

structural changes observed are distant from the TsnR target site and indicate a more global structural alteration due to TsnR-induced unfolding of the RNA domain's complex tertiary structure (109). This interpretation was corroborated by ribonuclease RNA structure probing and the NTD extension appended to the SPOUT domain was identified as the primary driver of RNA structural rearrangements (46). Further, mutation in an internal bulge loop >20 Å away (U1061 to A), which increases the stability of the rRNA tertiary structure, results in a drastic reduction in methyl transfer activity, further supporting the idea that partial unfolding of the global RNA tertiary structure is a key element of specific substrate recognition.

Similar studies using ribonuclease structure probing indicated that, upon substrate binding, TrmH induces a conformational change in the tRNA that disrupts tertiary interactions involving the target nucleotide loop. Specifically, for TrmH to gain access to its target nucleotide, enzyme binding may loosen or break D-loop and T-loop interactions resulting in conformational changes to the whole tRNA structure (68). This observation was confirmed using a cross-linking experiment that reduced the flexibility of substrate tRNA and thus hindered binding of TrmH to the D-loop containing the target nucleotide (110). Similar to the stabilization of TsnR's substrate rRNA through mutation of a distant loop, the stabilization of TrmH's substrate tRNA through cross-linking resulted in a significant decrease in methylation activity.

Melting assays revealed that Trm56 requires a similar disruption of the interactions between its substrate tRNA D- and T-loops for efficient methylation (70). These studies suggest that Trm56 induces an overall shape transition in substrate tRNA through disruption of key tertiary interactions. These changes shift the tRNA structure from the typical L-shape to an alternative "lambda form" that was first associated with archaeosine modification (111). Critically, this transition is the rate-limiting step for the modification reaction and plays an important role in substrate recognition (70).

Characterization of substrate recognition by other SPOUT methyltransferases hints at similar molecular strategies. For example, TrmJ's ability to bind to its target nucleotide despite insertion or deletion of nucleotides in the target loop suggests that this enzyme unfolds the target structure upon binding as opposed to binding to a rigid tRNA molecule (24). As more structures become available of SPOUT methyltransferases in complex with their RNA substrate, the precise details of these conformational changes will likely be revealed. For example, Trm10 was predicted to require conformational changes to its substrate tRNA based on the inaccessibility of the target nucleotide in the tRNA core. The structure of the RNase P complex containing TRMT10C revealed a distorted tRNA structure with a 17 Å displacement of the anticodon loop and a considerably larger distance between D-loop and the anticodon loop (98). Significant changes in tRNA conformation are also predicted for other Trm10 enzymes and these may be distinct from those induced by TRM10C given that they do not employ the additional protein factors of the RNase P complex. We anticipate that the important role of substrate and enzyme conformational plasticity for other SPOUT methyltransferases will continue to be demonstrated as more superfamily members are characterized in molecular detail.

**Conclusions**

Despite their shared knotted SAM-binding domain, SPOUT methyltransferases display a remarkable degree of mechanistic diversity, as revealed by many recent advances made through high-resolution structural and biochemical investigations. The new alignment of the SPOUT methyltransferases by their SPOUT domain presented here provides insights into the evolution of the superfamily and could support some inferences for currently uncharacterized members. SPOUT methyltransferases evolved to methylate tRNA and rRNA at the base or

ribose, and further to modify at least one protein. Throughout evolution of the SPOUT superfamily, NTD/ CTD extension domains surrounding the SPOUT core have expanded to include enzymes with or without one or both of these appendages, and with significant variation in their lengths and sequences. These distinct domains and their organization confer vastly greater catalytic diversity upon SPOUT enzymes than would likely be achieved with the conserved catalytic SPOUT domain alone. The discovery of the protein-modifying SPOUT methyltransferase Sfm1 suggests that other SPOUT enzymes may exist which act on protein substrates and future studies may further expand the pool of RNA or protein substrates for enzymes of this superfamily.

Structures of a limited number of SPOUT methyltransferase in complex with their substrates have been critical to begin teasing apart the answers to many questions related to enzyme-substrate interactions, including the basis for substrate selectivity and catalytic mechanism. However, the distinct molecular strategies revealed by these first structures underscore the diversity in structure and mechanism of the SPOUT family enzymes. Because of this diversity, the challenge of generalizing features from one member of the superfamily to another is significant, often even among enzymes in a single organism (such as the case for human Trm10 paralogs). As such, structural determination of many more SPOUT methyltransferases in complex with their substrates will be essential to continue to reveal the full landscape of mechanisms and activities associated with these enzymes.

**Acknowledgements**

Research on SPOUT methyltransferases in the Conn and Jackman labs is supported by National Institute of General Medical Sciences award R01 GM130135 (to JEJ and GLC), NSF

GRFP award 1937971 (to SES) and the OSU Center for RNA Biology Graduate Fellowship (to IEB).

**Author Contributions**

S.E.S., I.E.B., G.L.C., and J.E.J. participated in conceptualization of manuscript. S.E.S. and I.E.B. wrote the original manuscript draft. D.D. provided formal analysis. S.E.S. and G.L.C. made figures. S.E.S., I.E.B., D.D., G.L.C., and J.E.J. reviewed and edited manuscript.

## Figures

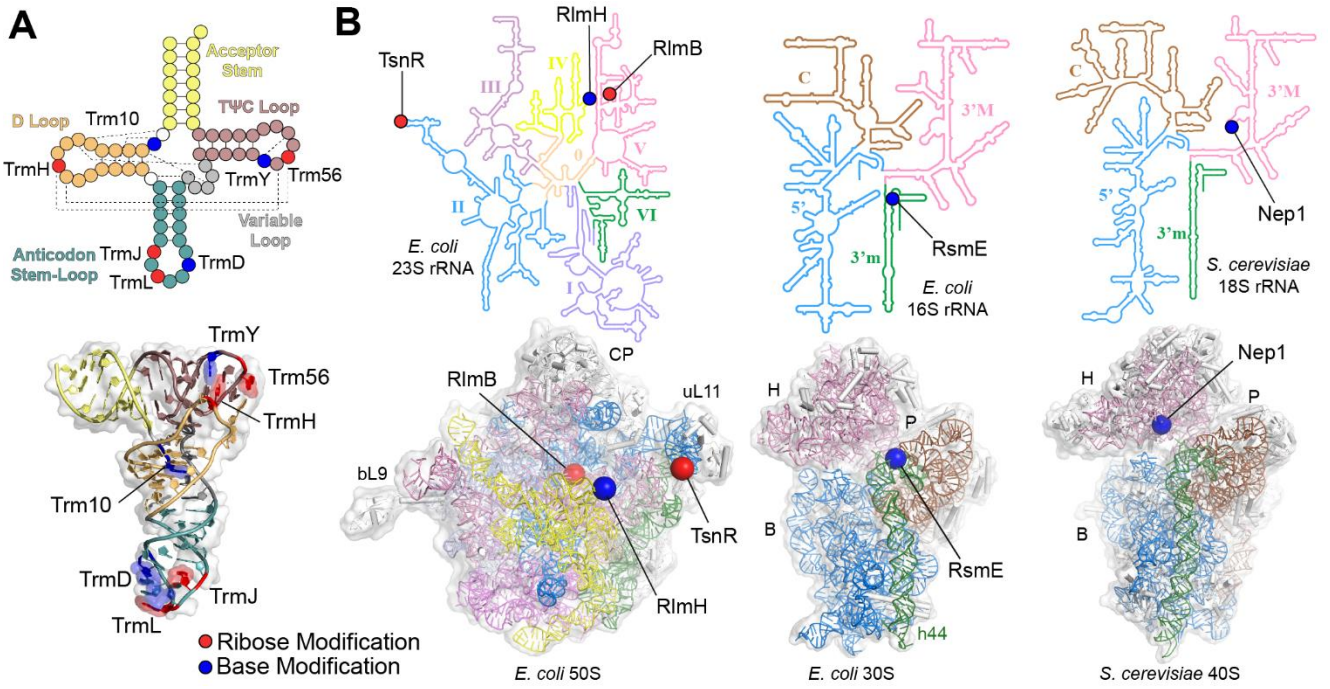


**Figure 2.1 RNA SPOUT methyltransferase target sites in tRNA and rRNA.** ***A,*** Sites of modification by tRNA-modifying SPOUT methyltransferases mapped onto the tRNA secondary (*top*) and tertiary (*bottom*) structures (shown for $tRNA^{Phe}$, PDB 6LVR). Each modification is colored based on the type of modification (red: ribose modification; blue: base modification) and labelled with the SPOUT methyltransferase responsible for the modification. Tertiary interactions which form the L-shaped three-dimensional structure are shown as dotted lines on the secondary structure. ***B,*** Sites of rRNA modification by SPOUT methyltransferases mapped onto the rRNA secondary structure (*top*) and structures of the applicable ribosomal subunit (*bottom*; shown for *E. coli* 30S and 50S (PDB 4V4Q) and *S. cerevisiae* 40S (PDB 4V88), as indicated). rRNA secondary structure maps were adapted from http://apollo.chemistry.gatech.edu/RibosomeGallery under a CC BY-SA 3.0 license (112). Ribosome structural features noted on the structures are central protuberance (CP), bacterial

ribosomal protein L9 domain (bL9), universal ribosomal protein L11 domain (uL11), head (H), platform (P) and body (B).

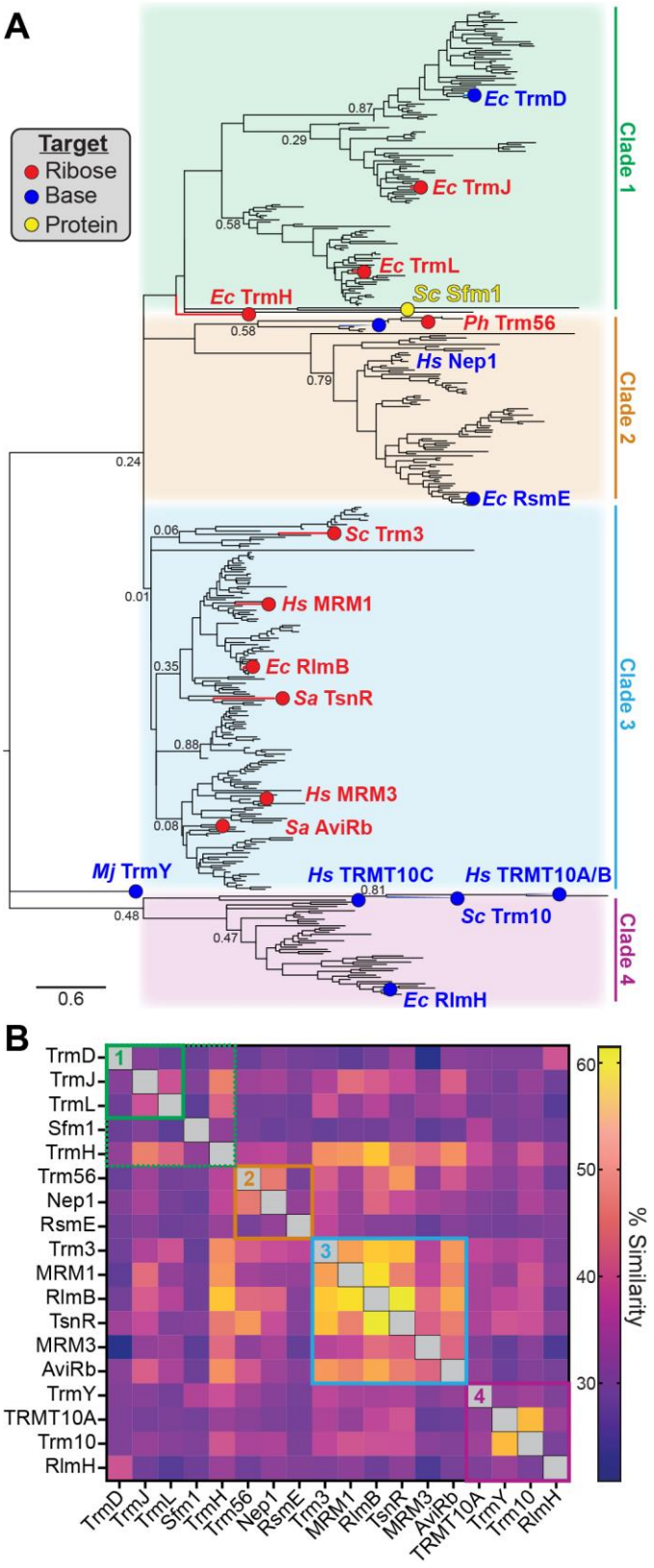


**Figure 2.2 Phylogenetic analysis of the SPOUT superfamily.** ***A***, The maximum likelihood

phylogenetic tree of SPOUT domains from diverse methyltransferases. The tree is clustered into four major clades (Clade 1- 4) and enzyme names are colored to indicate the type of modification. Bootstrap values are noted on select branches to highlight the low support for most deep nodes, but high support for the terminal nodes and thus composition of individual subclades. ***B***, Heat map comparison of sequence similarity (% similarity) for the SPOUT domain of the indicated SPOUT methyltransferases. Major Clades (1-4) from the tree are indicated by the color-coded boxes. The sequence similarity was calculated in the Geneious software based on BLOSUM 45 scoring matrix allowing consideration of similarities in residue physical or chemical properties.

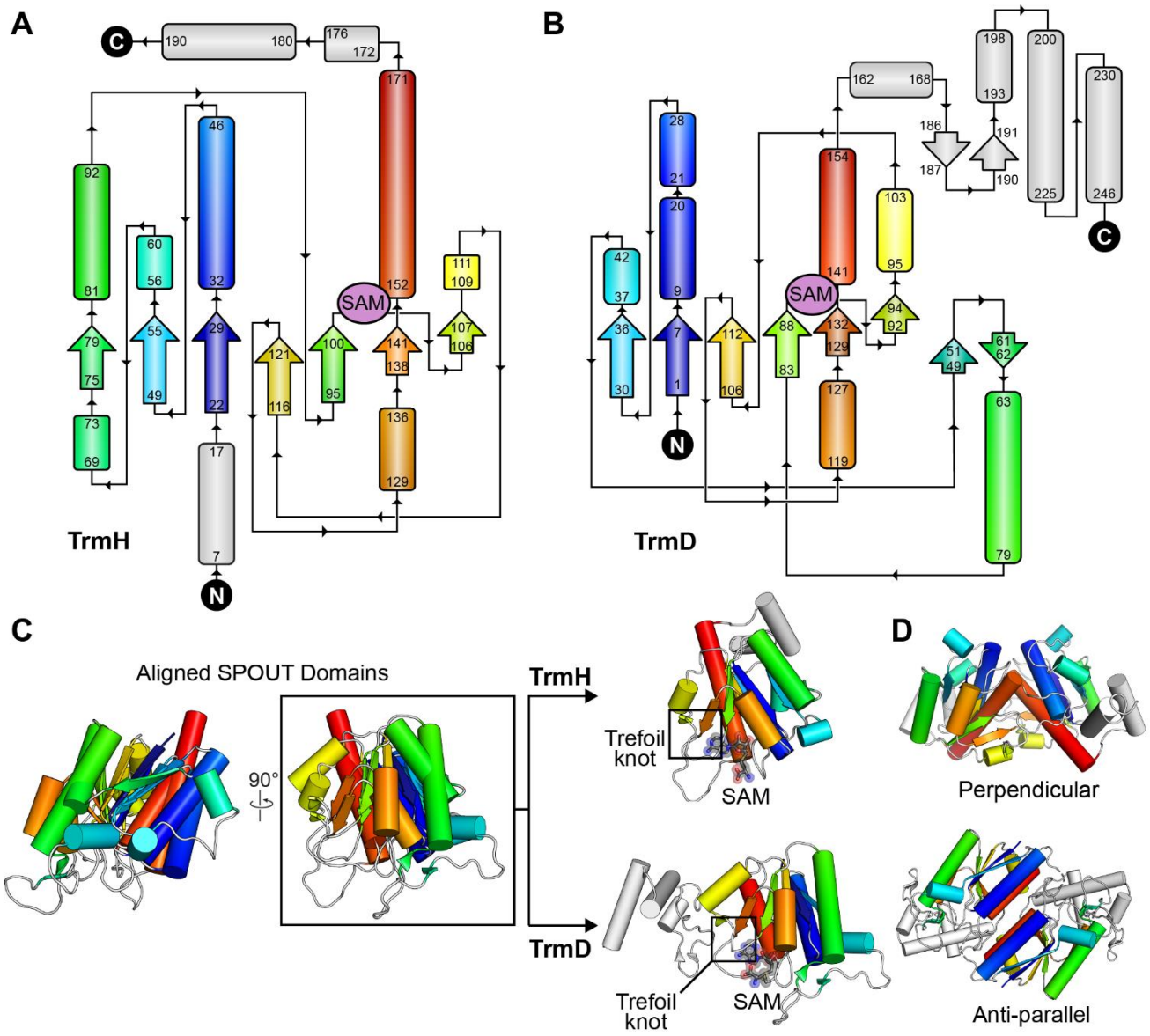


**Figure 2.3 Overview of SPOUT methyltransferase structure.** Topology maps of ***A***, TrmH (derived from *T. thermophilus;* PDB 1V2X) and ***B***, TrmD (derived from *H. influenzae;* PDB: 4YVG) are shown with α-helices represented by cylinders and β-sheets indicated by arrows. In both maps, the SAM-binding region is shown. The SPOUT domain is colored as a rainbow gradient (*blue to red*) from N- to C-terminal, with NTD and CTD extensions shown in grey. ***C,*** Two orthogonal views of the structures of TrmH and TrmD aligned by their SPOUT domain β-sheets (*left*) and the individual protomers of TrmH (*top right*) and TrmD (*bottom right*). The trefoil knot and the position of the bound cofactor SAM are indicated. ***D***, Perpendicular and

anti-parallel dimerization modes exemplified by TrmH (*top*) and TrmD (*bottom*); note the distinct, characteristic orientations of the red and blue α-helices in each dimer.

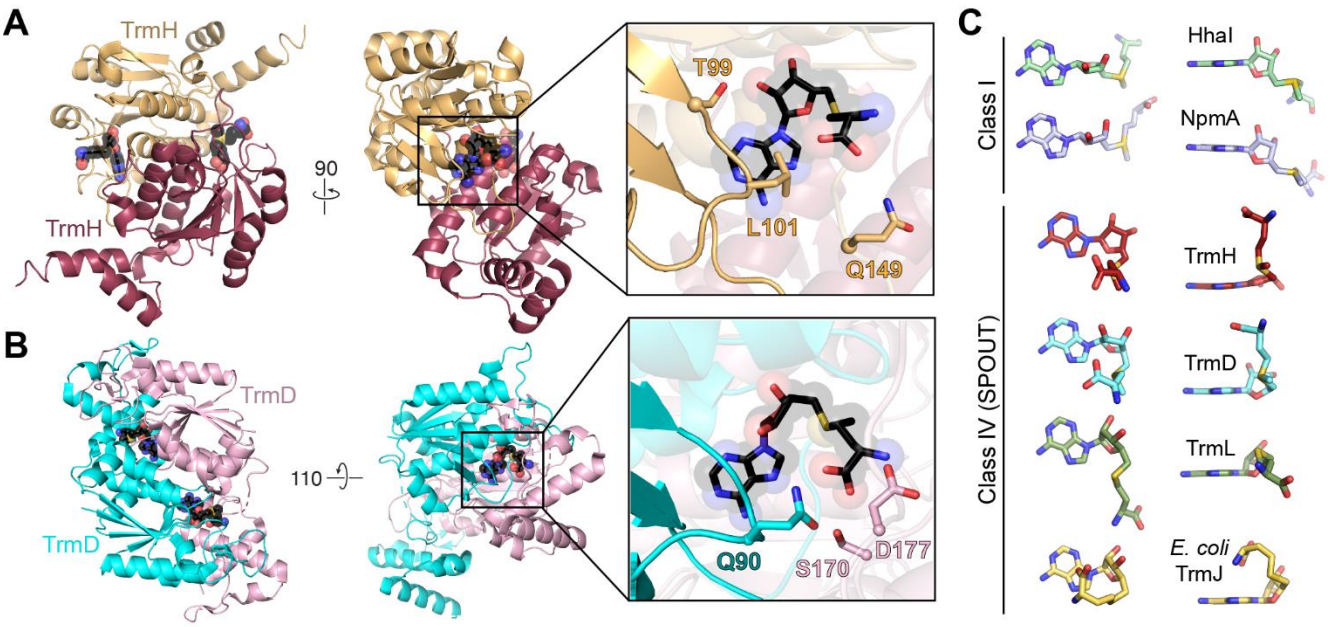


**Figure 2.4 SAM conformations and SAM-binding pockets of representative SPOUT methyltransferases.** ***A***, ***B***, Structural overview of the TrmD and TrmH dimers, respectively, showing a zoomed-in view of the SAM-binding pocket of each enzyme (*boxed, right*). The zoomed-in view highlights the proximity of the bound SAM to the characteristic SPOUT knot (solid cartoon), dimer interface (transparent cartoons, colored as in the structural overviews), and key residues whose side chains interact directly with SAM (shown in black in both structures). ***C***, The elongated conformation of SAM in two representative Class I methyltransferases, HhaI (PDB 2HMY) and NpmA (PDB 3MTE), is shown for comparison to the characteristic bent conformation in Class IV SPOUT methyltransferases, exemplified by TrmD (PDB 4YVG) and TrmH (PDB 1V2X). Two additional, distinct SPOUT co-substrate binding modes are also shown: a more extended form observed for one protomer in the TrmL

dimer (PDB 4JAL) and the super-bent conformation observed in *E. coli* TrmJ (PDB 4CNE). For both the TrmL and TrmJ structures, SAH was bound in the co-substrate binding pocket.

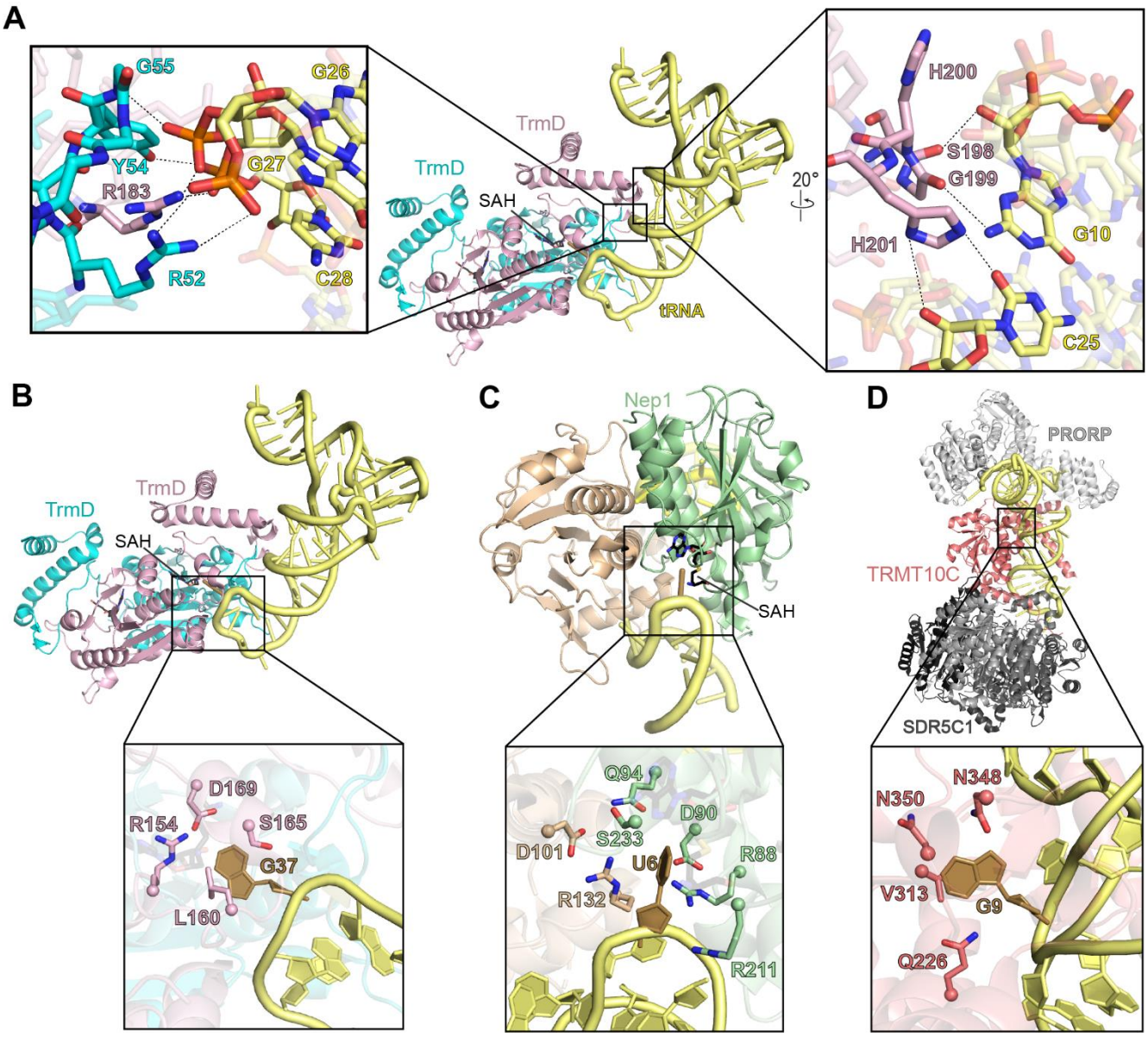


**Figure 2.5 Substrate Recognition and Base-flipping in SPOUT methyltransferase-RNA substrate complexes.** ***A***, Key interactions involved in tRNA substrate recognition by TrmD including phosphate groups in the anticodon branch of tRNA (*left*) and critical contacts along

the minor groove next to the G10:C25 pair (*right*) (PDB 4YVI). Target nucleotide base flipping observed in the structures of ***B,*** TrmD bound to substrate $tRNA^{Gln}$ (PDB 4YVI), ***C***, Nep1 bound to a model rRNA fragment (PDB 3OIJ), and ***D***, and TRMT10C as part of the mitochondrial RNase P complex with mitochondrial pre-$tRNA^{Tyr}$ (PDB 7ONU; other protein components are shown in gray). In each structure, the target nucleotide (gold) is flipped into the binding pocket and stabilized by multiple protein residues (shown as sticks). For both TrmD and Nep1, the flipped base is sequestered at the SPOUT the dimer interface. In all images the RNA is shown in yellow

## Tables

**Table 2.1** Properties, substrates, and modifications incorporated by SPOUT methyltransferases included in the phylogenetic analysis and discussed throughout this review.

| Clade[a] | Enzyme | PDB | Organism[b] | Substrate (Modification)[c] | Dimerization Mode | Domain Architecture | Domain Length (Amino Acids)[d] | | |
|---|---|---|---|---|---|---|---|---|---|
| | | | | | | | SPOUT | NTD | CTD |
| 1 | TrmD | 4YVG, 4YVI[n] | B | tRNA ($m^1G_{37}$) | Antiparallel | SPOUT–CTD | 160[e] | N/A | 86 |
| | TrmJ | 4XBO | B / A | tRNA ($Cm_{32}$/$Um_{32}$) | Perpendicular | SPOUT–CTD | 179[f] | N/A | 67 |
| | TrmL | 4JAL | B / A | tRNA ($Cm_{34}$; $Um_{34}$) | Perpendicular | SPOUT only | 157[f] | N/A | N/A |
| | TrmH | 1V2X | B | tRNA ($Gm_{18}$) | Perpendicular | NTD–SPOUT–CTD | 155[g] | 21 | 18 |
| | Sfm1 | 5C77 | E | r-protein eS3 (Ω-methylation Arg146)[e] | Monomer | SPOUT–CTD | 154[h] | N/A | 59 |
| 2 | Trm56 | 2YY8 | A | tRNA ($Cm_{56}$) | Perpendicular | SPOUT–CTD | 159[i] | N/A | 44 |
| | Nep1 | 3OII, 3OIJ[n] | A / E | 16S $m^1\Psi_{914}$[f]; 18S rRNA $m^1\Psi_{1189}$[e] | Perpendicular | NTD–SPOUT | 209[f] | 42 | N/A |
| | RsmE | 4E8B | B / E | 16S rRNA ($m^3U_{1498}$)[f] | Antiparallel | NTD–SPOUT | 172[f] | 71 | N/A |
| 3 | Trm3 | N/A | E | tRNA ($Gm_{18}$) | Perpendicular | NTD–SPOUT | 152[h] | 1284 | N/A |
| | MRM1 | N/A | E | 16S mitochondrial rRNA ($Gm_{1145}$)[g]; 21S mitochondrial rRNA ($Gm_{2270}$)[e] | ND[o] | NTD–SPOUT | 171[j] | 241 | N/A |
| | RlmB | 1GZ0 | B | 23S rRNA ($Gm_{2251}$)[f] | Perpendicular | NTD–SPOUT | 162[f] | 81 | N/A |
| | TsnR | 3GYQ | B | 23S rRNA ($Am_{1067}$)[i] | Perpendicular | NTD–SPOUT | 164[k] | 105 | N/A |
| | MRM3 | 7OI6 | E | 16S mitochondrial rRNA ($Gm_{1370}$)[g] | ND[o] | NTD–SPOUT | 211[j] | 209 | N/A |
| | AviRb | 1X7P | B | 23S rRNA ($Um_{2479}$)[j] | Perpendicular | NTD–SPOUT | 171[l] | 116 | N/A |
| | TrmY | N/A | A | tRNA ($m^1\Psi_{54}$) | Perpendicular | NTD–SPOUT or SPOUT–CTD | ND[o] | ND[o] | ND[o] |
| 4 | Trm10 | 4JWJ, 7ONU[n] | A / E | tRNA ($m^1G_9$ and/or $m^1A_9$) | Monomer | NTD–SPOUT–CTD | 158[m] | 88 | 46 |
| | | | | | | | 192[h] | 84 | 17 |
| | | | | | | | 191[j] | 94 | 54 |
| | | | | | | | 192[j] | 116 | 8 |
| | | | | | | | 202[j] | 142 | 20 |
| | RlmH | 5TWJ | B | 23S rRNA ($m^3\Psi_{1915}$)[f] | Antiparallel | SPOUT only | 155[f] | N/A | N/A |

[a] Representative clade for each SPOUT methyltransferase based upon the phylogenetic tree in Figure 2.
[b] Enzyme found in organisms among Bacteria (B), Archaea (A), and / or Eukaryotes (E).
[c] Because the numbering for site of modification for conserved for rRNA from different organisms, the organism is indicated for each rRNA modification site.
[d] Representative examples of domain lengths from organisms that have been characterized structurally or by multiple sequence alignment. If the length of the linker region connecting the SPOUT domain to its extended domain has been identified in the SPOUT methyltransferase structure, the numbering is included as part of the respective extended domain. Domain architecture for TrmY is not clear from available sequences.
Organisms: [e] *Haemophilus influenzae*; [f] *Escherichia coli*; [g] *Thermus thermophilus*; [h] *Saccharomyces cerevisiae*; [i] *Pyrococcus horikoshii*; [j] *Homo sapiens*; [k] *Streptomyces azureus*; [l] *Streptomyces viridochromogenes*; [m] *Sulfolobus acidocaldarius.*
[n] Structures include RNA substrate.
[o] ND: Not determined

## References


1. Schubert, H. L., Blumenthal, R. M., and Cheng, X. (2003) Many paths to methyltransfer: a chronicle of convergence. *Trends Biochem Sci* **28**, 329-335

2. Motorin, Y., and Helm, M. (2022) RNA nucleotide methylation: 2021 update. *Wiley Interdiscip Rev RNA* **13**, e1691

3. Hashimoto, H., Vertino, P. M., and Cheng, X. (2010) Molecular coupling of DNA methylation and histone methylation. *Epigenomics* **2**, 657-669

4. Phizicky, E. M., and Hopper, A. K. (2015) tRNA processing, modification, and subcellular dynamics: past, present, and future. *RNA* **21**, 483-485

5. Zhang, X., Walker, R. C., Phizicky, E. M., and Mathews, D. H. (2014) Influence of Sequence and Covalent Modifications on Yeast tRNA Dynamics. *J Chem Theory Comput* **10**, 3473-3483

6. Sun, Q., Huang, M., and Wei, Y. (2021) Diversity of the reaction mechanisms of SAM-dependent enzymes. *Acta Pharm Sin B* **11**, 632-650

7. Lennard, L. (2010) 4.21 - Methyltransferases. in *Comprehensive Toxicology* (McQueen, C. A. ed.), Elsevier Science. pp

8. Dixon, M. M., Huang, S., Matthews, R. G., and Ludwig, M. (1996) The structure of the C-terminal domain of methionine synthase: presenting S-adenosylmethionine for reductive methylation of B12. *Structure* **4**, 1263-1275

9. Schubert, H. L., Wilson, K. S., Raux, E., Woodcock, S. C., and Warren, M. J. (1998) The X-ray structure of a cobalamin biosynthetic enzyme, cobalt-precorrin-4 methyltransferase. *Nat Struct Biol* **5**, 585-592

10. Nureki, O., Shirouzu, M., Hashimoto, K., Ishitani, R., Terada, T., Tamakoshi, M., Oshima, T., Chijimatsu, M., Takio, K., Vassylyev, D. G., Shibata, T., Inoue, Y., Kuramitsu, S., and Yokoyama, S. (2002) An enzyme with a deep trefoil knot for the active-site architecture. *Acta Crystallogr D Biol Crystallogr* **58**, 1129-1137

11. Michel, G., Sauve, V., Larocque, R., Li, Y., Matte, A., and Cygler, M. (2002) The structure of the RlmB 23S rRNA methyltransferase reveals a new methyltransferase fold with a unique knot. *Structure* **10**, 1303-1315

12. Lim, K., Zhang, H., Tempczyk, A., Krajewski, W., Bonander, N., Toedt, J., Howard, A., Eisenstein, E., and Herzberg, O. (2003) Structure of the YibK methyltransferase from Haemophilus influenzae (HI0766): a cofactor bound at a site formed by a knot. *Proteins* **51**, 56-67

13. Ahn, H. J., Kim, H. W., Yoon, H. J., Lee, B. I., Suh, S. W., and Yang, J. K. (2003) Crystal structure of tRNA(m1G37)methyltransferase: insights into tRNA recognition. *EMBO J* **22**, 2593-2603

14. Anantharaman, V., Koonin, E. V., and Aravind, L. (2002) SPOUT: a class of methyltransferases that includes spoU and trmD RNA methylase superfamilies, and novel superfamilies of predicted prokaryotic RNA methylases. *J Mol Microbiol Biotechnol* **4**, 71-75

15. Ito, T., Masuda, I., Yoshida, K., Goto-Ito, S., Sekine, S., Suh, S. W., Hou, Y. M., and Yokoyama, S. (2015) Structural basis for methyl-donor-dependent and sequence-specific binding to tRNA substrates by knotted methyltransferase TrmD. *Proc Natl Acad Sci U S A* **112**, E4197-4205

16. Nureki, O., Watanabe, K., Fukai, S., Ishii, R., Endo, Y., Hori, H., and Yokoyama, S. (2004) Deep knot structure for construction of active site and cofactor binding site of tRNA modification enzyme. *Structure* **12**, 593-602

17. Tkaczuk, K. L., Dunin-Horkawicz, S., Purta, E., and Bujnicki, J. M. (2007) Structural and evolutionary bioinformatics of the SPOUT superfamily of methyltransferases. *BMC Bioinformatics* **8**, 73

18. Elkins, P. A., Watts, J. M., Zalacain, M., van Thiel, A., Vitazka, P. R., Redlak, M., Andraos-Selim, C., Rastinejad, F., and Holmes, W. M. (2003) Insights into catalysis by a knotted TrmD tRNA methyltransferase. *J Mol Biol* **333**, 931-949

19. Persson, B. C., Jager, G., and Gustafsson, C. (1997) The spoU gene of Escherichia coli, the fourth gene of the spoT operon, is essential for tRNA (Gm18) 2'-O-methyltransferase activity. *Nucleic Acids Res* **25**, 4093-4097

20. Lv, F., Zhang, T., Zhou, Z., Gao, S., Wong, C. C., Zhou, J. Q., and Ding, J. (2015) Structural basis for Sfm1 functioning as a protein arginine methyltransferase. *Cell Discov* **1**, 15037

21. Hori, H. (2017) Transfer RNA methyltransferases with a SpoU-TrmD (SPOUT) fold and their modified nucleosides in tRNA. *Biomolecules* **7**

22. Krishnamohan, A., Dodbele, S., and Jackman, J. E. (2019) Insights into Catalytic and tRNA Recognition Mechanism of the Dual-Specific tRNA Methyltransferase from Thermococcus kodakarensis. *Genes (Basel)* **10**

23. Liu, R. J., Zhou, M., Fang, Z. P., Wang, M., Zhou, X. L., and Wang, E. D. (2013) The tRNA recognition mechanism of the minimalist SPOUT methyltransferase, TrmL. *Nucleic Acids Res* **41**, 7828-7842

24. Somme, J., Van Laer, B., Roovers, M., Steyaert, J., Versees, W., and Droogmans, L. (2014) Characterization of two homologous 2'-O-methyltransferases showing different specificities for their tRNA substrates. *RNA* **20**, 1257-1271

25. Jackman, J. E., Montange, R. K., Malik, H. S., and Phizicky, E. M. (2003) Identification of the yeast gene encoding the tRNA m1G methyltransferase responsible for modification at position 9. *RNA* **9**, 574-585

26. Kempenaers, M., Roovers, M., Oudjama, Y., Tkaczuk, K. L., Bujnicki, J. M., and Droogmans, L. (2010) New archaeal methyltransferases forming 1-methyladenosine or 1-methyladenosine and 1-methylguanosine at position 9 of tRNA. *Nucleic Acids Res* **38**, 6533-6543

27. Purta, E., van Vliet, F., Tkaczuk, K. L., Dunin-Horkawicz, S., Mori, H., Droogmans, L., and Bujnicki, J. M. (2006) The yfhQ gene of Escherichia coli encodes a tRNA:Cm32/Um32 methyltransferase. *BMC Mol Biol* **7**, 23

28. Ochi, A., Makabe, K., Yamagami, R., Hirata, A., Sakaguchi, R., Hou, Y. M., Watanabe, K., Nureki, O., Kuwajima, K., and Hori, H. (2013) The catalytic domain of topological knot tRNA methyltransferase (TrmH) discriminates between substrate tRNA and nonsubstrate tRNA via an induced-fit process. *J Biol Chem* **288**, 25562-25574

29. Bjork, G. R., Wikstrom, P. M., and Bystrom, A. S. (1989) Prevention of translational frameshifting by the modified nucleoside 1-methylguanosine. *Science* **244**, 986-989

30. Robertus, J. D., Ladner, J. E., Finch, J. T., Rhodes, D., Brown, R. S., Clark, B. F., and Klug, A. (1974) Structure of yeast phenylalanine tRNA at 3 A resolution. *Nature* **250**, 546-551

31. Phizicky, E. M., and Hopper, A. K. (2010) tRNA biology charges to the front. *Genes Dev* **24**, 1832-1860

32. Alexandrov, A., Chernyakov, I., Gu, W., Hiley, S. L., Hughes, T. R., Grayhack, E. J., and Phizicky, E. M. (2006) Rapid tRNA decay can result from lack of nonessential modifications. *Mol Cell* **21**, 87-96

33. Gu, C., Begley, T. J., and Dedon, P. C. (2014) tRNA modifications regulate translation during cellular stress. *FEBS Lett* **588**, 4287-4296

34. Torres, A. G., and Marti, E. (2021) Toward an Understanding of Extracellular tRNA Biology. *Front Mol Biosci* **8**, 662620

35. Suzuki, T. (2021) The expanding world of tRNA modifications and their disease relevance. *Nat Rev Mol Cell Biol* **22**, 375-392

36. Gillis, D., Krishnamohan, A., Yaacov, B., Shaag, A., Jackman, J. E., and Elpeleg, O. (2014) TRMT10A dysfunction is associated with abnormalities in glucose homeostasis, short stature and microcephaly. *J Med Genet* **51**, 581-586

37. Igoillo-Esteve, M., Genin, A., Lambert, N., Desir, J., Pirson, I., Abdulkarim, B., Simonis, N., Drielsma, A., Marselli, L., Marchetti, P., Vanderhaeghen, P., Eizirik, D. L., Wuyts, W., Julier, C., Chakera, A. J., Ellard, S., Hattersley, A. T., Abramowicz, M., and Cnop, M. (2013) tRNA methyltransferase homolog gene TRMT10A mutation in young onset diabetes and primary microcephaly in humans. *PLoS Genet* **9**, e1003888

38. Jockel, S., Nees, G., Sommer, R., Zhao, Y., Cherkasov, D., Hori, H., Ehm, G., Schnare, M., Nain, M., Kaufmann, A., and Bauer, S. (2012) The 2'-O-methylation status of a single

guanosine controls transfer RNA-mediated Toll-like receptor 7 activation or inhibition. *J Exp Med* **209**, 235-241

39. Sloan, K. E., Warda, A. S., Sharma, S., Entian, K. D., Lafontaine, D. L. J., and Bohnsack, M. T. (2017) Tuning the ribosome: The influence of rRNA modification on eukaryotic ribosome biogenesis and function. *RNA Biol* **14**, 1138-1152

40. Burakovsky, D. E., Prokhorova, I. V., Sergiev, P. V., Milon, P., Sergeeva, O. V., Bogdanov, A. A., Rodnina, M. V., and Dontsova, O. A. (2012) Impact of methylations of m2G966/m5C967 in 16S rRNA on bacterial fitness and translation initiation. *Nucleic Acids Res* **40**, 7885-7895

41. Connolly, K., Rife, J. P., and Culver, G. (2008) Mechanistic insight into the ribosome biogenesis functions of the ancient protein KsgA. *Mol Microbiol* **70**, 1062-1075

42. Meyer, B., Wurm, J. P., Kotter, P., Leisegang, M. S., Schilling, V., Buchhaupt, M., Held, M., Bahr, U., Karas, M., Heckel, A., Bohnsack, M. T., Wohnert, J., and Entian, K. D. (2011) The Bowen-Conradi syndrome protein Nep1 (Emg1) has a dual role in eukaryotic ribosome biogenesis, as an essential assembly factor and in the methylation of Psi1191 in yeast 18S rRNA. *Nucleic Acids Res* **39**, 1526-1537

43. Eschrich, D., Buchhaupt, M., Kotter, P., and Entian, K. D. (2002) Nep1p (Emg1p), a novel protein conserved in eukaryotes and archaea, is involved in ribosome biogenesis. *Curr Genet* **40**, 326-338

44. Osterman, I. A., Dontsova, O. A., and Sergiev, P. V. (2020) rRNA Methylation and Antibiotic Resistance. *Biochemistry (Mosc)* **85**, 1335-1349

45. Mosbacher, T. G., Bechthold, A., and Schulz, G. E. (2005) Structure and function of the antibiotic resistance-mediating methyltransferase AviRb from Streptomyces viridochromogenes. *J Mol Biol* **345**, 535-545

46. Kuiper, E. G., and Conn, G. L. (2014) Binding induced RNA conformational changes control substrate recognition and catalysis by the thiostrepton resistance methyltransferase (Tsr). *J Biol Chem* **289**, 26189-26200

47. Howell, N. W., Jora, M., Jepson, B. F., Limbach, P. A., and Jackman, J. E. (2019) Distinct substrate specificities of the human tRNA methyltransferases TRMT10A and TRMT10B. *RNA* **25**, 1366-1376

48. Abascal, F., Zardoya, R., and Posada, D. (2005) ProtTest: selection of best-fit models of protein evolution. *Bioinformatics* **21**, 2104-2105

49. Sulkowska, J. I., Sulkowski, P., Szymczak, P., and Cieplak, M. (2008) Stabilizing effect of knots on proteins. *Proc Natl Acad Sci U S A* **105**, 19714-19719

50. Christian, T., Sakaguchi, R., Perlinska, A. P., Lahoud, G., Ito, T., Taylor, E. A., Yokoyama, S., Sulkowska, J. I., and Hou, Y. M. (2016) Methyl transfer by substrate signaling from a knotted protein fold. *Nat Struct Mol Biol* **23**, 941-948

51. Hou, Y. M., Matsubara, R., Takase, R., Masuda, I., and Sulkowska, J. I. (2017) TrmD: A Methyl Transferase for tRNA Methylation With m(1)G37. *Enzymes* **41**, 89-115

52. Shao, Z., Yan, W., Peng, J., Zuo, X., Zou, Y., Li, F., Gong, D., Ma, R., Wu, J., Shi, Y., Zhang, Z., Teng, M., Li, X., and Gong, Q. (2014) Crystal structure of tRNA m1G9 methyltransferase Trm10: insight into the catalytic mechanism and recognition of tRNA substrate. *Nucleic Acids Res* **42**, 509-525

53. Van Laer, B., Roovers, M., Wauters, L., Kasprzak, J. M., Dyzma, M., Deyaert, E., Kumar Singh, R., Feller, A., Bujnicki, J. M., Droogmans, L., and Versees, W. (2016) Structural and functional insights into tRNA binding and adenosine N1-methylation by an archaeal Trm10 homologue. *Nucleic Acids Res* **44**, 940-953

54. Benitez-Paez, A., Villarroya, M., Douthwaite, S., Gabaldon, T., and Armengod, M. E. (2010) YibK is the 2'-O-methyltransferase TrmL that modifies the wobble nucleotide in Escherichia coli tRNA(Leu) isoacceptors. *RNA* **16**, 2131-2143

55. Purta, E., Kaminska, K. H., Kasprzak, J. M., Bujnicki, J. M., and Douthwaite, S. (2008) YbeA is the m3Psi methyltransferase RlmH that targets nucleotide 1915 in 23S rRNA. *RNA* **14**, 2234-2244

56. Koh, C. S., Madireddy, R., Beane, T. J., Zamore, P. D., and Korostelev, A. A. (2017) Small methyltransferase RlmH assembles a composite active site to methylate a ribosomal pseudouridine. *Sci Rep* **7**, 969

57. Zhang, H., Wan, H., Gao, Z. Q., Wei, Y., Wang, W. J., Liu, G. F., Shtykova, E. V., Xu, J. H., and Dong, Y. H. (2012) Insights into the catalytic mechanism of 16S rRNA methyltransferase RsmE (m(3)U1498) from crystal and solution structures. *J Mol Biol* **423**, 576-589

58. Liu, R. J., Long, T., Zhou, M., Zhou, X. L., and Wang, E. D. (2015) tRNA recognition by a bacterial tRNA Xm32 modification enzyme from the SPOUT methyltransferase superfamily. *Nucleic Acids Res* **43**, 7489-7503

59. Zhou, M., Long, T., Fang, Z. P., Zhou, X. L., Liu, R. J., and Wang, E. D. (2015) Identification of determinants for tRNA substrate recognition by Escherichia coli C/U34 2'-O-methyltransferase. *RNA Biol* **12**, 900-911

60. Kumagai, I., Watanabe, K., and Oshima, T. (1982) A thermostable tRNA (guanosine-2')-methyltransferase from Thermus thermophilus HB27 and the effect of ribose methylation on the conformational stability of tRNA. *J Biol Chem* **257**, 7388-7395

61. Hori, H., Suzuki, T., Sugawara, K., Inoue, Y., Shibata, T., Kuramitsu, S., Yokoyama, S., Oshima, T., and Watanabe, K. (2002) Identification and characterization of tRNA (Gm18) methyltransferase from Thermus thermophilus HB8: domain structure and conserved amino acid sequence motifs. *Genes Cells* **7**, 259-272

62. Cavaille, J., Chetouani, F., and Bachellerie, J. P. (1999) The yeast Saccharomyces cerevisiae YDL112w ORF encodes the putative 2'-O-ribose methyltransferase catalyzing the formation of Gm18 in tRNAs. *RNA* **5**, 66-81

63. Wu, H., Min, J., Zeng, H., and Plotnikov, A. N. (2008) Crystal structure of the methyltransferase domain of human TARBP1. *Proteins* **72**, 519-525

64. Watanabe, K., Nureki, O., Fukai, S., Endo, Y., and Hori, H. (2006) Functional categorization of the conserved basic amino acid residues in TrmH (tRNA (Gm18) methyltransferase) enzymes. *J Biol Chem* **281**, 34630-34639

65. Ochi, A., Makabe, K., Kuwajima, K., and Hori, H. (2010) Flexible recognition of the tRNA G18 methylation target site by TrmH methyltransferase through first binding and induced fit processes. *J Biol Chem* **285**, 9018-9029

66. Pleshe, E., Truesdell, J., and Batey, R. T. (2005) Structure of a class II TrmH tRNA-modifying enzyme from Aquifex aeolicus. *Acta Crystallogr Sect F Struct Biol Cryst Commun* **61**, 722-728

67. Hori, H., Yamazaki, N., Matsumoto, T., Watanabe, Y., Ueda, T., Nishikawa, K., Kumagai, I., and Watanabe, K. (1998) Substrate recognition of tRNA (Guanosine-2'-)-methyltransferase from Thermus thermophilus HB27. *J Biol Chem* **273**, 25721-25727

68. Matsumoto, T., Nishikawa, K., Hori, H., Ohta, T., Miura, K., and Watanabe, K. (1990) Recognition sites of tRNA by a thermostable tRNA(guanosine-2'-)-methyltransferase from Thermus thermophilus HB27. *J Biochem* **107**, 331-338

69. Hori, H., Kubota, S., Watanabe, K., Kim, J. M., Ogasawara, T., Sawasaki, T., and Endo, Y. (2003) Aquifex aeolicus tRNA (Gm18) methyltransferase has unique substrate specificity. TRNA recognition mechanism of the enzyme. *J Biol Chem* **278**, 25081-25090

70. Renalier, M. H., Joseph, N., Gaspin, C., Thebault, P., and Mougin, A. (2005) The Cm56 tRNA modification in archaea is catalyzed either by a specific 2'-O-methylase, or a C/D sRNP. *RNA* **11**, 1051-1063

71. Clouet-d'Orval, B., Gaspin, C., and Mougin, A. (2005) Two different mechanisms for tRNA ribose methylation in Archaea: a short survey. *Biochimie* **87**, 889-895

72. Kawamura, T., Hirata, A., Ohno, S., Nomura, Y., Nagano, T., Nameki, N., Yokogawa, T., and Hori, H. (2016) Multisite-specific archaeosine tRNA-guanine transglycosylase (ArcTGT) from Thermoplasma acidophilum, a thermo-acidophilic archaeon. *Nucleic Acids Res* **44**, 1894-1908

73. Kuratani, M., Bessho, Y., Nishimoto, M., Grosjean, H., and Yokoyama, S. (2008) Crystal structure and mutational study of a unique SpoU family archaeal methylase that forms 2'-O-methylcytidine at position 56 of tRNA. *J Mol Biol* **375**, 1064-1075

74. Thompson, J., Schmidt, F., and Cundliffe, E. (1982) Site of action of a ribosomal RNA methylase conferring resistance to thiostrepton. *J Biol Chem* **257**, 7915-7917

75. Bechthold, A., and Floss, H. G. (1994) Overexpression of the thiostrepton-resistance gene from Streptomyces azureus in Escherichia coli and characterization of recognition sites of the 23S rRNA A1067 2'-methyltransferase in the guanosine triphosphatase center of 23S ribosomal RNA. *Eur J Biochem* **224**, 431-437

76. Dunstan, M. S., Hang, P. C., Zelinskaya, N. V., Honek, J. F., and Conn, G. L. (2009) Structure of the thiostrepton resistance methyltransferase.S-adenosyl-L-methionine complex and its interaction with ribosomal RNA. *J Biol Chem* **284**, 17013-17020

77. Yin, S., Jiang, H., Chen, D., and Murchie, A. I. (2015) Substrate recognition and modification by the nosiheptide resistance methyltransferase. *PLoS One* **10**, e0122972

78. O'Dwyer, K., Watts, J. M., Biswas, S., Ambrad, J., Barber, M., Brule, H., Petit, C., Holmes, D. J., Zalacain, M., and Holmes, W. M. (2004) Characterization of Streptococcus pneumoniae TrmD, a tRNA methyltransferase essential for growth. *J Bacteriol* **186**, 2346-2354

79. Redlak, M., Andraos-Selim, C., Giege, R., Florentz, C., and Holmes, W. M. (1997) Interaction of tRNA with tRNA (guanosine-1)methyltransferase: binding specificity determinants involve the dinucleotide G36pG37 and tertiary structure. *Biochemistry* **36**, 8699-8709

80. Juhling, F., Morl, M., Hartmann, R. K., Sprinzl, M., Stadler, P. F., and Putz, J. (2009) tRNAdb 2009: compilation of tRNA sequences and tRNA genes. *Nucleic Acids Res* **37**, D159-162

81. Takeda, H., Toyooka, T., Ikeuchi, Y., Yokobori, S., Okadome, K., Takano, F., Oshima, T., Suzuki, T., Endo, Y., and Hori, H. (2006) The substrate specificity of tRNA (m1G37) methyltransferase (TrmD) from Aquifex aeolicus. *Genes Cells* **11**, 1353-1365

82. Brule, H., Elliott, M., Redlak, M., Zehner, Z. E., and Holmes, W. M. (2004) Isolation and characterization of the human tRNA-(N1G37) methyltransferase (TRM5) and comparison to the Escherichia coli TrmD protein. *Biochemistry* **43**, 9243-9255

83. Christian, T., and Hou, Y. M. (2007) Distinct determinants of tRNA recognition by the TrmD and Trm5 methyl transferases. *J Mol Biol* **373**, 623-632

84. Perlinska, A. P., Kalek, M., Christian, T., Hou, Y. M., and Sulkowska, J. I. (2020) Mg(2+)-Dependent Methyl Transfer by a Knotted Protein: A Molecular Dynamics Simulation and Quantum Mechanics Study. *ACS Catal* **10**, 8058-8068

85. Sakaguchi, R., Lahoud, G., Christian, T., Gamper, H., and Hou, Y. M. (2014) A divalent metal ion-dependent N(1)-methyl transfer to G37-tRNA. *Chem Biol* **21**, 1351-1360

86. Wurm, J. P., Meyer, B., Bahr, U., Held, M., Frolow, O., Kotter, P., Engels, J. W., Heckel, A., Karas, M., Entian, K. D., and Wohnert, J. (2010) The ribosome assembly factor Nep1 responsible for Bowen-Conradi syndrome is a pseudouridine-N1-specific methyltransferase. *Nucleic Acids Res* **38**, 2387-2398

87. Chen, H. Y., and Yuan, Y. A. (2010) Crystal structure of Mj1640/DUF358 protein reveals a putative SPOUT-class RNA methyltransferase. *J Mol Cell Biol* **2**, 366-374

88. Thomas, S. R., Keller, C. A., Szyk, A., Cannon, J. R., and Laronde-Leblanc, N. A. (2011) Structural insight into the functional mechanism of Nep1/Emg1 N1-specific pseudouridine methyltransferase in ribosome biogenesis. *Nucleic Acids Res* **39**, 2445-2457

89. Basturea, G. N., Rudd, K. E., and Deutscher, M. P. (2006) Identification and characterization of RsmE, the founding member of a new RNA base methyltransferase family. *RNA* **12**, 426-434

90. Basturea, G. N., and Deutscher, M. P. (2007) Substrate specificity and properties of the Escherichia coli 16S rRNA methyltransferase, RsmE. *RNA* **13**, 1969-1976

91. Dunkle, J. A., Vinal, K., Desai, P. M., Zelinskaya, N., Savic, M., West, D. M., Conn, G. L., and Dunham, C. M. (2014) Molecular recognition and modification of the 30S ribosome by the aminoglycoside-resistance methyltransferase NpmA. *Proc Natl Acad Sci U S A* **111**, 6275-6280

92. Chatterjee, K., Blaby, I. K., Thiaville, P. C., Majumder, M., Grosjean, H., Yuan, Y. A., Gupta, R., and de Crecy-Lagard, V. (2012) The archaeal COG1901/DUF358 SPOUT-methyltransferase members, together with pseudouridine synthase Pus10, catalyze the formation of 1-methylpseudouridine at position 54 of tRNA. *RNA* **18**, 421-433

93. Swinehart, W. E., and Jackman, J. E. (2015) Diversity in mechanism and function of tRNA methyltransferases. *RNA Biol* **12**, 398-411

94. Vilardo, E., Amman, F., Toth, U., Kotter, A., Helm, M., and Rossmanith, W. (2020) Functional characterization of the human tRNA methyltransferases TRMT10A and TRMT10B. *Nucleic Acids Res* **48**, 6157-6169

95. Vilardo, E., Nachbagauer, C., Buzet, A., Taschner, A., Holzmann, J., and Rossmanith, W. (2012) A subcomplex of human mitochondrial RNase P is a bifunctional methyltransferase--extensive moonlighting in mitochondrial tRNA biogenesis. *Nucleic Acids Res* **40**, 11583-11593

96. Krishnamohan, A., and Jackman, J. E. (2017) Mechanistic features of the atypical tRNA m1G9 SPOUT methyltransferase, Trm10. *Nucleic Acids Res* **45**, 9019-9029

97. Singh, R. K., Feller, A., Roovers, M., Van Elder, D., Wauters, L., Droogmans, L., and Versees, W. (2018) Structural and biochemical analysis of the dual-specificity Trm10 enzyme from Thermococcus kodakaraensis prompts reconsideration of its catalytic mechanism. *RNA* **24**, 1080-1092

98. Bhatta, A., Dienemann, C., Cramer, P., and Hillen, H. S. (2021) Structural basis of RNA processing by human mitochondrial RNase P. *Nat Struct Mol Biol* **28**, 713-723

99. Ero, R., Peil, L., Liiv, A., and Remme, J. (2008) Identification of pseudouridine methyltransferase in Escherichia coli. *RNA* **14**, 2223-2233

100. Ero, R., Leppik, M., Liiv, A., and Remme, J. (2010) Specificity and kinetics of 23S rRNA modification enzymes RlmH and RluD. *RNA* **16**, 2075-2084

101. Schapira, M. (2016) Structural Chemistry of Human RNA Methyltransferases. *ACS Chem Biol* **11**, 575-582

102. Kurowski, M. A., Sasin, J. M., Feder, M., Debski, J., and Bujnicki, J. M. (2003) Characterization of the cofactor-binding site in the SPOUT-fold methyltransferases by computational docking of S-adenosylmethionine to three crystal structures. *BMC Bioinformatics* **4**, 9

103. Taylor, A. B., Meyer, B., Leal, B. Z., Kotter, P., Schirf, V., Demeler, B., Hart, P. J., Entian, K. D., and Wohnert, J. (2008) The crystal structure of Nep1 reveals an extended SPOUT-class methyltransferase fold and a pre-organized SAM-binding site. *Nucleic Acids Res* **36**, 1542-1554

104. Nosrati, M., Dey, D., Mehrani, A., Strassler, S. E., Zelinskaya, N., Hoffer, E. D., Stagg, S. M., Dunham, C. M., and Conn, G. L. (2019) Functionally critical residues in the aminoglycoside resistance-associated methyltransferase RmtC play distinct roles in 30S substrate recognition. *J Biol Chem* **294**, 17642-17653

105. Vinal, K., and Conn, G. L. (2017) Substrate Recognition and Modification by a Pathogen-Associated Aminoglycoside Resistance 16S rRNA Methyltransferase. *Antimicrob Agents Chemother* **61**

106. Oerum, S., Roovers, M., Rambo, R. P., Kopec, J., Bailey, H. J., Fitzpatrick, F., Newman, J. A., Newman, W. G., Amberger, A., Zschocke, J., Droogmans, L., Oppermann, U., and Yue, W. W. (2018) Structural insight into the human mitochondrial tRNA purine N1-methyltransferase and ribonuclease P complexes. *J Biol Chem* **293**, 12862-12876

107. Cheng, X., and Roberts, R. J. (2001) AdoMet-dependent methylation, DNA methyltransferases and base flipping. *Nucleic Acids Res* **29**, 3784-3795

108. Laughlin, Z. T., Dey, D., Zelinskaya, N., Witek, M. A., Srinivas, P., Nguyen, H. A., Kuiper, E. G., Comstock, L. R., Dunham, C. M., and Conn, G. L. (2021) 50S subunit recognition and modification by the Mycobacterium tuberculosis ribosomal RNA methyltransferase TlyA. *bioRxiv*, 2021.2011.2011.467980

109. Conn, G. L., Draper, D. E., Lattman, E. E., and Gittis, A. G. (1999) Crystal structure of a conserved ribosomal protein-RNA complex. *Science* **284**, 1171-1174

110. Hori, H., Saneyoshi, M., Kumagai, I., Miura, K., and Watanabe, K. (1989) Effects of modification of 4-thiouridine in E. coli tRNA(fMet) on its methyl acceptor activity by thermostable Gm-methylases. *J Biochem* **106**, 798-802

111. Bai, Y., Fox, D. T., Lacy, J. A., Van Lanen, S. G., and Iwata-Reuyl, D. (2000) Hypermodification of tRNA in Thermophilic archaea. Cloning, overexpression, and characterization of tRNA-guanine transglycosylase from Methanococcus jannaschii. *J Biol Chem* **275**, 28731-28738

112. Petrov, A. S., Bernier, C. R., Gulen, B., Waterbury, C. C., Hershkovits, E., Hsiao, C., Harvey, S. C., Hud, N. V., Fox, G. E., Wartell, R. M., and Williams, L. D. (2014) Secondary structures of rRNAs from all three domains of life. *PLoS One* **9**, e88222

# CHAPTER THREE:

## tRNA $m^1G9$ modification depends on substrate-specific RNA conformational changes induced by the methyltransferase Trm10

The following chapter is under review at the *Journal of Biological Chemistry* and is available on bioRxiv:

Strassler SE, Bowles IE, Krishnamohan A, Kim H, Edgington CB, Kuiper EG, Hancock CJ, Comstock LR, Jackman JE, Conn GL. (2023). tRNA $m^1$ G9 modification depends on substrate-specific RNA conformational changes induced by the methyltransferase Trm10. *J Biol Chem.* (In Press)

*BioRxiv*. doi: 10.1101/2023.02.01.526536. (PMID: 36778341)

**Abstract**

The methyltransferase Trm10 modifies a subset of tRNAs on the base N1 position of the 9th nucleotide in the tRNA core. Trm10 is conserved throughout Eukarya and Archaea, and mutations in the human gene (*TRMT10A*) have been linked to neurological disorders such as microcephaly and intellectual disability, as well as defects in glucose metabolism. Of the 26 tRNAs in yeast with guanosine at position 9, only 13 are substrates for Trm10. However, no common sequence or other posttranscriptional modifications have been identified among these substrates, suggesting the presence of some other tRNA feature(s) which allow Trm10 to distinguish substrate from nonsubstrate tRNAs. Here, we show that substrate recognition by *Saccharomyces cerevisiae* Trm10 is dependent on both intrinsic tRNA flexibility and the ability of the enzyme to induce specific tRNA conformational changes upon binding. Using the sensitive RNA structure-probing method SHAPE, conformational changes upon binding to Trm10 in tRNA substrates, but not nonsubstrates, were identified and mapped onto a model of Trm10-bound tRNA. These changes may play an important role in substrate recognition by allowing Trm10 to gain access to the target nucleotide. Our results highlight a novel mechanism of substrate recognition by a conserved tRNA modifying enzyme. Further, these studies reveal a strategy for substrate recognition that may be broadly employed by tRNA-modifying enzymes which must distinguish between structurally similar tRNA species.

**Introduction**

RNA modifications are central to proper RNA function and are highly conserved across all kingdoms of life (1). Of all major RNA classes, tRNAs are the most highly modified with 10-20% of tRNA nucleotides containing a modification (2-4). These modifications are critical in determining tRNA fate and tight regulation is crucial for proper cell function due to their roles in ensuring correct

codon-anticodon interaction (5, 6), fine-tuning tRNA structure and stability (7, 8), and regulating tRNA charging with cognate aminoacyl groups (9, 10). Because of the abundance of possible tRNA modifications and variations in modification patterns, the mechanisms employed by tRNA modification enzymes to identify their correct tRNA substrates from the large pool of structurally similar tRNAs are still being uncovered.

The Trm10 family of tRNA methyltransferases modify the N1 position of purine nucleotides at position 9 in the core region of tRNA (11). This enzyme family is evolutionarily conserved throughout Eukarya and Archaea, with the first Trm10 enzyme being discovered in *Saccharomyces cerevisiae* (11). Humans express three Trm10 enzymes, with the direct homolog of *S. cerevisiae* Trm10 referred to as TRMT10A and two additional enzymes, TRMT10B and TRMT10C that are distinct in their cellular localization and pool of tRNA substrates. While Trm10/TRMT10A and TRMT10B are both believed to be nuclear/ cytosolic, TRMT10C is localized to the mitochondria as part of the mitochondrial RNase P complex and is the only member of the Trm10 family which is known to function as part of a larger complex (12). Each human Trm10 enzyme also methylates a unique subset of tRNAs, modifying only G9 (Trm10/TRMT10A), only A9 (TRMT10B), or exhibiting bifunctional activity to modify either G9 or A9 (TMRT10C) (13-15).

The importance of Trm10/TRMT10A has been highlighted by its connection to distinct disease phenotypes. In humans, mutations in the *TRMT10A* gene are linked to microcephaly and intellectual disability, as well as defects in glucose metabolism (16-20). Additionally, the *S. cerevisiae trm10* deletion strain exhibits hypersensitivity to the anti-tumor drug 5-fluorouracil (21). While the mechanistic basis of these phenotypes is not fully defined, loss of the $m^1G9$ modification increases tRNA fragmentation, which is consistent with the role of core modifications in maintaining optimal tRNA stability (22).

Trm10 is a member of the SPOUT family of *S*-adenosyl-L-methionine (SAM)-dependent methyltransferases which are characterized by an α/β fold with a deep topological knot (23-25). Many SPOUT methyltransferases are involved in RNA posttranscriptional modification (25), including the well-characterized methyltransferase TrmD which modifies G37 of tRNA, catalyzing the same guanosine N1-methylation as Trm10 (11, 14). However, TrmD and Trm10 employ very different mechanisms of catalysis. For example, Trm10 does not require a divalent metal ion for catalysis and does not possess the same catalytic residues as demonstrated for TrmD (26-29). Further, in contrast to TrmD and most other SPOUT enzymes, Trm10 is catalytically active as a monomer (30). These differences suggest that Trm10 uses a distinct mechanism of substrate recognition and catalysis.

Trm10 modifies only 13 of 26 possible tRNA substrates in yeast that contain a G9 nucleotide (4, 11, 14), but no common sequence or posttranscriptional modification(s) have been identified that can explain this substrate specificity (29, 30). Trm10 has been shown to efficiently modify *in vitro* transcribed substrate tRNAs, indicating that prior modifications are not necessary for methylation (14). Finally, among tRNAs which do not contain $m^1G9$ *in vivo*, there are some which can be modified by Trm10 *in vitro* (hereafter, termed “partial substrates”) and others which are never modified, either *in vitro* or *in vivo* (14). Therefore, some other inherent tRNA property (or properties) must be exploited by Trm10 to discriminate between substrate and nonsubstrate.

Here, we use selective 2’-OH-acylation analyzed by primer extension (SHAPE) to probe inherent tRNA dynamics and their changes upon interaction of Trm10 with substrate and nonsubstrate tRNAs. Our studies demonstrate that there are differences in inherent dynamics in free tRNAs that may allow initial discrimination by Trm10 between substrate and nonsubstrate tRNAs. Using a mutational approach to query the predicted tRNA binding surface of *S. cerevisiae* Trm10, we identify three highly conserved basic residues that are implicated in forming the

catalytically productive conformation of the Trm10-tRNA complex. Specifically, the variant protein in which all three residues are altered (Trm10-KRR) is capable of binding tRNAs equivalently to the wild-type enzyme, but fails to significantly modify any substrate tRNA tested, suggesting that formation of the catalytically productive enzyme-substrate complex requires features that were previously unknown. By comparing SHAPE data of tRNA bound to wild-type Trm10 and Trm10-KRR, we show that productive substrate recognition is dependent on the ability of wild-type Trm10 to induce specific tRNA conformational changes to support methylation. These conformational changes are not observed for nonsubstrate tRNA and cannot be induced by the inactive Trm10-KRR variant. Collectively, these studies identify the role of intrinsic and induced tRNA conformational changes and reveal a novel mechanism of RNA substrate recognition by a tRNA-modifying enzyme.

## Materials and Methods

*RNA in vitro transcription and purification*

Genes encoding $tRNA^{Gly\text{-}GCC}$, $tRNA^{Trp\text{-}CCA}$, $tRNA^{Val\text{-}UAC}$, $tRNA^{Leu\text{-}CAA}$, and $tRNA^{Ser\text{-}UGA}$ were cloned into plasmids for production of *in vitro* transcripts with 5'- and 3'-end hairpins to improve structure probing resolution at the 5' and 3' ends of the tRNA sequence (31). All tRNAs were *in vitro* transcribed from *Xho*I linearized plasmid DNA using T7 RNA polymerase as previously described (32). Briefly, *in vitro* transcription was performed for 5 hours at 37˚C in 200 mM HEPES-KOH (pH 7.5) buffer containing 28 mM $MgCl_2$, 2 mM spermidine, 40 mM dithiothreitol (DTT), 6 mM each rNTP, and 100 μg/mL DNA template. At the end of the reaction, following addition of EDTA to clear pyrophosphate-magnesium precipitates and dialysis against 1×Tris–EDTA buffer, RNAs were purified by denaturing polyacrylamide gel electrophoresis (50% urea, 1×Tris–Borate–EDTA

buffer). RNA bands were identified by UV shadowing, excised, eluted from the gel by crushing and soaking in 0.3 M sodium acetate, and ethanol precipitated as previously described (32).

*Trm10 expression and purification*

Trm10 and Trm10-KRR proteins with an N-terminal 6xHis-tag were expressed from the pET-derived plasmid pJEJ12-3 encoding full-length wild-type Trm10 or Trm10-KRR in *E. coli* BL21(DE3) pLysS grown in lysogeny broth as described previously (11). Briefly, protein expression was induced by addition of 1 mM β-D-1-thiogalactopyranoside at mid-log phase growth ($OD_{600}$ ~0.6) and growth continued at 37˚C for an additional 5 hours. To ensure removal of co-purifying SAM, cells were lysed in buffer containing 1M NaCl and 0.5% TritonX-100, and the lysate dialyzed three times in buffer containing 2M NaCl before dialysis back into original buffer (20 mM HEPES pH 7.5, 0.25 M NaCl, 4 mM $MgCl_2$, 1 mM β-mercaptoethanol, 10 mM imidazole, 5% glycerol). Protein was purified by sequential $Ni^{2+}$-affinity (HisTrap HP), heparin-affinity (HiPrep Heparin 16/10), and gel filtration (Superdex 75 16/600) chromatographies on an ÄKTApurifier10 system (GE Healthcare). Trm10 was eluted from the gel filtration column in 20 mM Tris (pH 7.5) buffer containing 100 mM NaCl, 1 mM $MgCl_2$, 5 mM β-mercaptoethanol, and 5% glycerol.

*NM6 preparation*

The SAM analog NM6 (5’-(diaminobutyric acid)-N-iodoethyl-5’-deoxyadenosine ammoniumhydrochloride) was prepared as previously described (33) and purified by semi-preparative reverse-phase HPLC. Before use, NM6 was dissolved in protein buffer (20 mM Tris pH 7.5, 100 mM NaCl, 1 mM $MgCl_2$, 5 mM β-mercaptoethanol, and 5% glycerol). NM6 was included in SHAPE reactions at a final concentration of 5 μM at the same time as Trm10, prior to incubation at 30˚C. *In situ* activation of NM6 results in a Trm10 cosubstrate that is covalently

attached by the enzyme to RNA (**Supplemental Figure S3.2A**), as shown previously (34, 35) and confirmed by mass spectrometry (**Supplemental Figure S3.2B**).

*tRNA SHAPE analysis*

SHAPE RNA probing was carried out following previously described procedures (36). Each tRNA was annealed at 95˚C for 2 minutes and incubated on ice for 2 minutes, and addition of folding buffer (333 mM HEPES pH 8.0, 20 mM $MgCl_2$, and 333 mM NaCl) followed by incubation at 30˚C for 20 minutes. For samples containing Trm10 or Trm10-KRR, the protein (final concentration of 750 nM) and SAM-analog NM6 or SAH (final concentration 5 μM) were added after RNA folding (33, 34). The complex was incubated at 30˚C for 30 minutes before introducing either the SHAPE reagent 1M7 (75 mM), or DMSO control, for 1.5 minutes at 37˚C (37). Trm10 was removed (where required) via phenol chloroform and RNAs recovered by ethanol precipitation.

Reverse transcription (RT) was carried for each product ([+] and [-] SHAPE reagent and one sequencing reaction) with a fluorescently (VIC) labelled primer corresponding to the sequence of the 3' end of the SHAPE hairpin (**Figure 3.1A**). Modified RNA was incubated with labeled DNA primer for 5 minutes at 95˚C and cooled to room temperature. The reverse transcription enzyme mix (10 mM dNTPs, 0.1 M DTT, SuperScript III Reverse Transcriptase, and SuperScript III Reverse Transcriptase buffer) was added to the RNA solution and incubated at 55˚C for 1 hour, followed by inactivation at 70˚C for 15 minutes. The resulting cDNA was ethanol precipitated, washed with 70% ethanol, and analyzed by capillary electrophoresis. For capillary electrophoresis, cDNA pellets were resuspended in formamide and mixed with GeneScan™ 600 LIZ® Size Standard (Applied Biosystems) for intercapillary alignment. Samples were resolved on an Applied Biosystems 3730 DNA Analyzer (Genomics Shared Resource Facility, Ohio State University).

Raw electropherograms were converted to normalized SHAPE reactivity using the RNA capillary-electrophoresis analysis tool (RiboCAT) (38). For samples containing the $m^1G9$ modification (wild-type-bound substrate and partial substrate tRNAs), a large peak was observed at the modification site (for example, **Supplemental Figure S3.2C**), blocking the reverse transcriptase and limiting reactivity information 3' of the site of modification (nucleotides indicated in grey in relevant figures). The SHAPE reactivities were normalized by dividing each value by the average of the reactivities of the highest 8%, after omitting the highest 2% (39).The values from two replicates were then averaged for each nucleotide and the resulting reactivities classified as ≤0.20, 0.20–0.49, 0.50–0.79, and ≥0.80. To compare unbound tRNA, Trm10-bound tRNA, and KRR-bound tRNA, the scaled, averaged reactivities for each nucleotide were subtracted as indicated for each data set. The difference in reactivity for each nucleotide was then classified as decreased (≤ -0.50, or -0.49 to -0.19), no change (-0.20 to 0.19) or increased (0.20 to 0.49, or ≥0.50).

*Isothermal titration calorimetry*

Trm10 was dialyzed twice at 4˚C against 20 mM Tris buffer (pH 7.5) containing 150 mM NaCl and concentrated to 50 µM. The final dialysis buffer was used to resuspend SAM and SAH (Sigma-Aldrich) to a final concentration of 1 mM. Experiments were performed on an Auto-$iTC_{200}$ at 25˚C and involved 16 injections of 2.4 µl of SAM or SAH into the cell containing protein. Titrations were performed twice for each combination of protein and ligand. The data were fit to a model for one-binding site in Origin software supplied with the instrument after subtraction of residual heats yielding individual equilibrium association constant ($K_a$) values for replicate titrations (reported in **Supplemental Table 1**). A representative titration for each protein-ligand combination is also shown in **Figure 3.3E,F**.

*Mass Spectrometry (MS)*

Samples were prepared for MS by incubating 1 µg of $tRNA^{Gly\text{-}GCC}$ with 1.3 µg of wild-type Trm10 alone, or with 100 ng of NM6 prepared in water. Samples were incubated for 1 hour at 37˚C and then digested with 1 unit of RNase T1 (Life Technologies) for 1 hour at 37˚C, and allowed to dry overnight at 40˚C. Samples were resuspended in 0.5% triethylamine in MS grade water before being manually injected for analysis by electrospray MS on a Q Exactive Orbitrap Mass Spectrometer calibrated in negative ion mode. MS spectra were centered on the m/z range corresponding to the masses expected for the unmodified and modified (+393 Da) target site fragment (**Supplemental Figure S3.3B**).

*Fluorescence anisotropy*

tRNA binding was measured by fluorescence anisotropy using wild-type and Trm10-KRR variant proteins and 5'-6-carboxyfluorescein-labeled $tRNA^{Gly\text{-}GCC}$ transcripts, prepared, and measured as previously described (17). Reactions containing varied concentration of enzyme (50-300 nM) and 15 nM fluorescently-labeled tRNA were incubated for 30 minutes at room temperature prior to measuring anisotropy using an Infinite M1000 PRO fluorometer (Tecan). Anisotropy was measured and plotted as a function of concentration of each Trm10 enzyme. The data were fit to equation 1 (a modified Hill equation) using Kaleidagraph (Synergy Software) to yield the observed $K_D$, the minimum anisotropy ($FA_{min}$), and maximum anisotropy ($FA_{max}$) for each enzyme. The results are plotted from three independent assays performed with each enzyme, with the indicated standard error for the resulting fit.

$$FA = FA_{min} + (FA_{max} - FA_{min})/(1 + (K_D/[E])) \qquad \text{(eq. 1)}$$

*Electromobility Shift Assay*–$tRNA^{Gly}$ was incubated at 80˚C for 10 minutes and then slow cooled to room temperature. The Trm10-tRNA complexes were formed by combining $tRNA^{Gly}$ (4 μM) with final concentrations of wild-type Trm10 or Trm10-KRR ranging from 0 to 10 μM. These mixed components were incubated at 30˚C for 30 minutes to form the complex and then run at 4˚C on a 10% nondenaturing polyacrylamide gel. The gel was incubated with a solution containing ethidium bromide for visualization by UV illumination.

*Trm10 methyltransferase activity assay*

Single turnover kinetics were performed as described previously (13, 14). Briefly, uniformly labeled transcripts were generated by *in vitro* transcription in the presence of [α-$^{32}$P]-GTP, resulting in labeling of all the G-nucleotides in the tRNA, including at G9. Single turnover reactions (at least 10-fold excess [Enzyme] over [Substrate]) were performed at 30°C with 50 mM Tris pH 8.0, 1.5 mM $MgCl_2$, and 0.5 mM SAM. Either 1.5 μM Trm10 ($tRNA^{Gly\text{-}GCC}$) or 7 μM Trm10 ($tRNA^{Trp\text{-}CCA}$ and $tRNA^{Val\text{-}UAC}$) was added to initiate each reaction. At each timepoint, an aliquot of the reaction was quenched by adding to a mixture of excess yeast tRNA and phenol: chloroform: isoamyl alcohol (PCA, 25:24:1 v:v:v). Following PCA extraction and ethanol precipitation, the resulting tRNA was digested to single nucleotides using nuclease P1 (Sigma-Aldrich). Resulting 5'-$^{32}$P labelled p*G or p*$m^1$G were resolved by thin layer chromatography on cellulose plates in an isobutyric acid: $H_2O$: $NH_4OH$ solvent (66:33:1, v:v:v). Plates were exposed to a phosphor screen and imaged using a Typhoon imaging system (GE Healthcare). The percent of $m^1$G9 conversion at each timepoint was quantified using ImageQuant TL software (GE Healthcare) and the average percent from replicate experiments were plotted versus time using Kaleidagraph (Synergy Software). A $k_{obs}$ value was determined by fitting the plot to a single exponential equation 2, also yielding the $P_{max}$, or maximal amount of product observed for each assay.

$$\%P = P_{max}(1^{-(-kobs*t)}) \qquad \text{(eq. 2)}$$

Methyltransferase assays of wild-type Trm10 and Trm10-KRR (**Figure 3.4D**) were performed essentially identically to the single turnover kinetic assays described above, except that these enzyme titration assays were not performed under enzyme excess conditions and also utilized a $tRNA^{Gly\text{-}GCC}$ substrate that was uniquely-labeled with $^{32}P$ at the phosphate immediately 5' to the G9 nucleotide, as previously prepared and described (27). Reactions were carried out for 2 hours before quenching and processing as described above.

**Results**

*SHAPE analysis reveals differences in inherent flexibility of Trm10 substrate and nonsubstrate tRNAs*

To assess whether inherent tRNA flexibility might play a role in substrate recognition by Trm10, SHAPE RNA structure probing was performed on five different tRNAs representing substrate ($tRNA^{Gly\text{-}GCC}$ and $tRNA^{Trp\text{-}CCA}$), nonsubstrate ($tRNA^{Leu\text{-}CAA}$ and $tRNA^{Ser\text{-}UGA}$), and partial substrate ($tRNA^{Val\text{-}UAC}$) (14). These tRNAs were *in vitro* transcribed with short hairpin sequences appended to the 5’ and 3’ ends (**Figure 3.1A**) to allow measurement of SHAPE reactivities for the full tRNA sequence (31, 36, 40). The substrate tRNAs are efficiently modified by Trm10 both *in vivo* and *in vitro* and the nonsubstrate tRNAs are never modified by Trm10 (*in vivo* or *in vitro*). The partial substrate is not modified by Trm10 *in vivo* but modification has been observed *in vitro* with similar reaction kinetics to substrate tRNAs (**Figure 3.1B**) (14). Additionally, Trm10 activity was not significantly altered by the addition of hairpins to both ends (**Figure 3.1B**), which is consistent with

previous studies showing that SHAPE structure probing of tRNA with similar appended hairpin structures yields consistent results with the authentic tRNA sequences (40).

SHAPE structure probing was performed on each tRNA using the SHAPE reagent 1-methyl-7-nitroisatoic anhydride (1M7) and analyzed using capillary electrophoresis. The resulting reactivities were determined using RiboCAT software (38) and normalized to the average of the highest reactivities for each sample (**Figure 3.2A**, and see *Materials and Methods* for details of the process used). The results were then mapped onto the secondary and tertiary structures of tRNA (**Figure 3.2B**) and reveal that both substrate and partial substrate tRNAs have high SHAPE reactivity in the 3'-side of the D-loop and the anticodon loop, indicating regions of higher intrinsic tRNA flexibility. These tRNAs also both have low reactivities for nucleotides in the 5'-half of the anticodon stem, core region, acceptor stem, and T-loop indicating more rigid and/ or inaccessible regions. Thus, the intrinsic tRNA dynamics of both substrate and partial substrate tRNAs in the absence of Trm10 appear indistinguishable. In contrast, very different trends for SHAPE reactivity were observed for nonsubstrate tRNAs which exhibit more extensive regions of high SHAPE reactivity for the full D-loop and stem, as well as the core region around the Trm10 target site and parts of the acceptor stem and T-loop.

These results thus reveal clear differences in inherent tRNA flexibility between substrate and nonsubstrate tRNA which may contribute to substrate discrimination by Trm10. Interestingly, the distinct behavior of the nonsubstrate tRNAs is consistent with the distinct structural nature of nonsubstrate tRNAs, including $tRNA^{Leu\text{-}CAA}$ and $tRNA^{Ser\text{-}UGA}$, as Type II tRNA species contain an extended variable loop sequence. The observed differences in flexibility for this, and possibly other Type II tRNAs may contribute to the inability of Trm10 to modify any of the tRNAs in this group in any organism studied to date (2, 14). The similar inherent flexibility observed with both substrate and partial substrate tRNA is also consistent with the ability of Trm10 to methylate both

species *in vitro*. However, these studies with free tRNAs can offer no additional insight into the basis of the substrate preference difference between full and partial substrate *in vivo*. We therefore assessed SHAPE reactivity of the same set of tRNAs in the presence of wild-type Trm10.

*Trm10 induces specific conformational changes in substrate tRNAs that are not observed in nonsubstrate tRNA*

To identify changes in tRNA conformation and nucleotide dynamics that occur during Trm10 binding and G9 modification, the same set of five tRNAs ($tRNA^{Gly\text{-}GCC}$, $tRNA^{Trp\text{-}CCA}$, $tRNA^{Leu\text{-}CAA}$, $tRNA^{Ser\text{-}UGA}$, and $tRNA^{Val\text{-}UAC}$) was pre-incubated with excess Trm10 (at least five times the $K_D$ for the protein-RNA interaction; **Supplemental Figure S3.1**) before adding 1M7 for tRNA SHAPE probing. Additionally, to ensure capture of a homogeneous and catalytically relevant tRNA conformation for the full and partial substrate tRNAs, the SAM cosubstrate-analog “N-mustard 6” (NM6) (33) was included in all SHAPE reactions. *In situ* activation of NM6 results in its covalent attachment to substrates during methyltransferase-catalyzed alkylation reactions, thus trapping the enzyme-substrate-cosubstrate analog complex (33, 34, 41) (**Supplemental Figure S3.2A**). The enzyme-dependent incorporation of NM6 on RNA has been shown previously (34, 35) and NM6 was confirmed to be a suitable cosubstrate for tRNA modification by Trm10 using mass spectrometry (**Supplemental Figure S3.2B**). Thus, NM6 is covalently attached to the tRNA by Trm10 at the N1 base position of G9 such that the Trm10-tRNA complex is trapped in a state immediately following catalysis by virtue of Trm10’s affinity for both the tRNA and the cosubstrate analog which is covalently linked to G9. However, as the SAM analog is only covalently attached to tRNA, Trm10 was removed from the sample after SHAPE modification via phenol:chloroform extraction so that bound protein did not interfere with the subsequent primer extension and

capillary electrophoresis analysis. The capillary electrophoresis chromatogram following SHAPE probing shows a large peak at the site of modification (**Supplemental Figure S3.2C**), providing additional evidence that the SAM analog is incorporated and very efficiently prevents further primer extension (thus no information on reactivity can be determined for subsequent nucleotides 1-8). From these observations we conclude that inclusion of NM6 in SHAPE reactions supports specific capture of an immediate post-catalytic state of the tRNA that accurately reflects changes induced by Trm10.

Analysis and normalization of SHAPE reactivities for each Trm10-bound tRNA was determined as before (**Supplemental Figure S3.3A** and **S3.4A,B**) and the corresponding free tRNA values were subtracted. The resulting difference reactivity (Trm10-bound minus free) for each tRNA was then mapped onto the tRNA secondary and tertiary structures (**Figure 3.3**). Despite being able to bind all tRNAs with similar affinity (**Supplemental Figure S3.1**), there are significant differences in the conformational changes induced by Trm10 in substrate and nonsubstrate tRNAs. When bound to Trm10, substrates ($tRNA^{Gly\text{-}GCC}$ and $tRNA^{Trp\text{-}CCA}$) exhibit increased reactivity in the D-loop, particularly in the D-stem immediately adjacent to G9. These changes, which presumably increase accessibility to the target site in the tRNA core, are less pronounced in partial substrate ($tRNA^{Val\text{-}UAC}$) and absent in the nonsubstrate tRNAs ($tRNA^{Leu\text{-}CAA}$ and $tRNA^{Ser\text{-}UGA}$). Additionally, both substrate tRNAs exhibit strong decreases in reactivity in the anticodon stem-loop. This finding was unexpected given the large distance between the anticodon loop and the site of modification, and may be indicative of more global changes in the tRNA structure. This change in the anticodon stem-loop SHAPE reactivity is not observed in partial substrate $tRNA^{Val\text{-}UAC}$ or the nonsubstrate tRNAs ($tRNA^{Leu\text{-}CAA}$ and $tRNA^{Ser\text{-}UGA}$) further suggesting that the corresponding changes in tRNA are important for modification by Trm10. In the former

case, we speculate that the observed differences in this region may play a role in this tRNA's lack of modification *in vivo* where other modifications or interactions may also limit Trm10 activity.

The SHAPE reactivities may provide some insight into the molecular basis for the observed differences in single turnover rates of modification with the three *in vitro* substrate tRNAs ($k_{obs}$ $tRNA^{Gly\text{-}GCC}$ > $tRNA^{Trp\text{-}CCA}$/ $tRNA^{Val\text{-}UAC}$; **Figure 3.1B**). We note that for these three tRNAs, there are differences observed in the variable loop which may be important for Trm10 to access and modify G9, as this region is nearby in the folded tRNA structure. Although $tRNA^{Trp\text{-}CCA}$ and $tRNA^{Val\text{-}UAC}$ exhibit localized increases in SHAPE reactivity, $tRNA^{Gly\text{-}GCC}$ exhibits no change in this region upon Trm10 binding. Interestingly, $tRNA^{Gly\text{-}GCC}$ has the shortest variable loop (4 nts) of the tRNAs tested, while $tRNA^{Trp\text{-}CCA}$ and $tRNA^{Val\text{-}UAC}$ are both one nucleotide longer. Thus, the observed changes may reflect a scenario where Trm10 can access G9 of $tRNA^{Gly\text{-}GCC}$ without the need to alter its variable loop structure, whereas this region must be altered to allow modification of the other two modified tRNAs ($tRNA^{Trp\text{-}CCA}$ and $tRNA^{Val\text{-}UAC}$), resulting in the observed differences in activity on these substrate tRNAs. In contrast, with the much longer variable loops of nonsubstrate tRNAs ($tRNA^{Leu\text{-}CAA}$ and $tRNA^{Ser\text{-}UGA}$), Trm10 is unable to access G9 regardless of its ability to induce conformational changes in this region of the tRNA.

To confirm that the observed differences in SHAPE reactivity between substrate and nonsubstrate are not due to the covalent attachment of NM6 only in substrate tRNA, SHAPE experiments were also performed for a substrate ($tRNA^{Trp}$) and nonsubstrate ($tRNA^{Leu}$) bound to wild-type Trm10 in the presence of the methylation reaction byproduct, S-adenosylhomocysteine (SAH). SAH was selected for this experiment in place of NM6 because it does not result in any modification or covalent attachment of the cosubstrate to the tRNA. The results recapitulate the key observations of the prior experiments for both substrate and nonsubstrate tRNAs, including both increased reactivity in the D-loop and decreased reactivity in the anticodon loop of substrate

$tRNA^{Trp}$ (**Supplemental Figure S3.5**). Interestingly, however, two distinctions are apparent for substrate tRNA with Trm10 in the presence of SAH compared to NM6. First, the reactivity of nucleotide G10 is dramatically reduced. This observation is consistent with major changes in the position of the target nucleotide G9, and thus its interaction with G10, via specific distortions to the tRNA that only occur when G9 is positioned for modification (and, here, trapped in that state by NM6). Second, in the presence of SAH, substrate $tRNA^{Trp}$ shows additional increases in SHAPE reactivity compared to free tRNA and samples with Trm10 and NM6. These additional changes may reflect conformational heterogeneity (e.g. a mixture of free and different bound states) in the presence of SAH, supporting the use of NM6 as a cosubstrate to stabilize a catalytically relevant Trm10-tRNA complex for SHAPE experiments.

Together, these observations suggest that the specific conformational changes observed in both substrate tRNAs, i.e. increased flexibility in the D-loop and decreased anticodon stem-loop flexibility, are essential for substrate recognition by Trm10. Additionally, the variable loop, and Trm10's ability to induce alterations in its structure where required, may serve as a negative determinant in substrate selection and thus a major reason why $tRNA^{Leu\text{-}CAA}$ and other Type II tRNAs are not substrates for Trm10. However, from these data it is not possible to distinguish conformational or nucleotide flexibility changes resulting from Trm10 binding to tRNA vs. those necessary for $m^1G9$ methylation.

*Comparison of tRNA bound to Trm10 and Trm10-KRR highlights conformational changes specifically necessary for methylation*

Previous structural studies on Trm10 identified a positively charged surface containing conserved residues K110, R121, and R127 as a putative tRNA binding surface (30). Initial binding assays performed with a variant of *Schizosaccharomyces pombe* Trm10 in which all three residues were

converted to glutamic acid (K11E/R121E/R127E) indicated that the enzyme completely lost the ability to bind to tRNA, but the impact on catalytic activity was not determined (30). We reconstructed this variant protein in the context of *S. cerevisiae* Trm10 where the same three residues are substituted to glutamic acid (Trm10-KRR; **Figure 3.4A,B**), and analyzed both tRNA binding and methylation activity. Interestingly, in contrast to the complete loss of tRNA affinity of the *S. pombe* Trm10 variant observed in the previous study, we observed binding of *S. cerevisiae* Trm10-KRR to substrate $tRNA^{Gly\text{-}GCC}$ via electromobility shift assay (**Supplemental Figure S3.6**). While the basis for these distinct impacts of the KRR amino acid changes in the two enzymes is not readily apparent, Trm10 enzymes from *S. pombe* and *S. cerevisiae* only have ~40% sequence identity and differences in behavior of the "same enzyme" from different organisms have been well documented for other SPOUT methyltransferases (42). The binding of Trm10-KRR to tRNA was further quantified via fluorescence anisotropy-based binding assays which revealed that binding of this Trm10-KRR variant to substrate $tRNA^{Gly\text{-}GCC}$ remains essentially identical to that of wild-type Trm10 (**Figure 3.4C**). However, methylation activity of Trm10-KRR is abolished with $tRNA^{Gly\text{-}GCC}$ (**Figure 3.4D**). Moreover, activity of Trm10-KRR also appears to be decreased significantly compared to wild-type with $tRNA^{Trp\text{-}CCA}$ and $tRNA^{Val\text{-}UAC}$ tRNAs, based on the loss of the strong stop in primer extension in the SHAPE analyses described below.

Given its comparable tRNA binding affinity to wild-type Trm10, we reasoned that the defect in Trm10-KRR activity could arise either through a defect in enzyme-cosubstrate interaction (e.g. reduced SAM affinity), or an inability to induce changes in the tRNA structure necessary for methylation. To first test the former possibility, we used isothermal titration calorimetry to determine that the affinities of both SAM and SAH are essentially the same (2- to 3-fold differences) for the wild-type Trm10 and Trm10-KRR protein (**Figure 3.4E,F**). Thus, loss of activity in Trm10-KRR is not due to a defect in SAM/ SAH binding and we propose that the observed

impact on enzymatic activity is instead due to an inability to induce some, or all, of the conformational change(s) which are necessary for methylation in these substrate tRNAs after initial Trm10-tRNA binding. As such, Trm10-KRR is a useful probe to dissect changes in tRNA SHAPE reactivity arising from binding and those mechanistically required for modification in tRNA substrates.

To define the tRNA conformational changes specifically necessary for methylation, the same set of tRNAs was pre-incubated with Trm10-KRR before adding 1M7 SHAPE reagent. NM6 was included in these reactions to remain consistent with wild-type Trm10 reactions. Following the same procedures for processing and normalization, SHAPE reactivity of each Trm10-KRR-bound tRNA was mapped onto the tRNA secondary structures (**Supplemental Figure S3.3** and **S3.4**). Reactivity differences were calculated for free tRNA and Trm10-KRR bound tRNA (Trm10-KRR-bound minus free; **Supplemental Figure S3.7**) and both protein-bound states (Trm10-bound minus Trm10-KRR-bound; **Figure 3.5A,B**). Trm10-KRR appears to induce only a small number of changes in nucleotide flexibility in contrast to wild-type Trm10 (**Supplemental Figure S3.7**). As such, the calculated differences in tRNA SHAPE reactivities when bound to Trm10-KRR *vs*. Trm10 and Trm10 *vs*. free tRNA are essentially identical (**Figures 3.3B** and **3.5B**). Specifically for the protein-bound comparison, the same increases in D-loop and decreases in anticodon stem-loop reactivity are observed. These changes are again absent for nonsubstrate tRNAs and only present in the D-loop of the partial substrate. The variable loop shows an identical trend to the previous comparison for substrate and partial substrate with increased ($tRNA^{Trp\text{-}CCA}$ and $tRNA^{Val\text{-}UAC}$) or unchanged ($tRNA^{Gly\text{-}GCC}$) reactivity in this region. Thus, these results confirm that the conformational changes in the D-loop and anticodon loop observed upon wild-type Trm10 binding to substrate tRNAs are specifically necessary for adoption of a catalytically competent complex for tRNA methylation by Trm10.

*Mapping of SHAPE reactivity onto a Trm10-tRNA model highlights interactions critical for required conformational changes*

To further understand the role of tRNA conformational changes in correct substrate recognition and the interactions which support them, a model of Trm10 bound to tRNA was generated using the structure of TRMT10C bound to pre-tRNA as part of the RNase P complex (PDB: 7ONU) (43) (**Figure 3.5C,D**). This structure was used to guide our modeling as it is currently the only available structure of any Trm10 family member bound to tRNA. The $tRNA^{Phe}$ structure (PDB: 6LVR) was first fit into the binding pocket of TRMT10C by aligning it with the pre-tRNA. Next, the structure of *S. cerevisiae* Trm10 (PDB: 4JWJ) was aligned with TRMT10C to show the placement of this protein with respect to the tRNA. Because the structure of Trm10 lacks the N-terminal domain, the N-terminal domain of TRMT10C was retained in the model to show its approximate location and how the analogous domain of *S. cerevisiae* Trm10 might be positioned to bind the tRNA. Finally, SHAPE reactivity differences corresponding to conformational changes necessary for methylation (i.e. KRR-bound tRNA subtracted from Trm10-bound tRNA reactivity) were mapped onto the structure of the tRNA (**Figure 3.5C,D**). Although limited due to differences in sequence and the requirement for partner proteins between Trm10 and TRMT10C, this model provides a useful framework for visualizing and interpreting SHAPE reactivity changes observed in the tRNA.

Regions of increased SHAPE reactivity cluster around the site of modification (G9) in the folded tRNA, consistent with an essential role of these Trm10-binding induced conformational changes in allowing accessibility to the target nucleotide. Such changes are also consistent with a mechanism of catalysis that requires the target nucleotide to be rotated 180˚ around its phosphodiester bond (“base-flip") to allow the base to enter the catalytic pocket (44). In further support of this mechanism, we note that the adjacent nucleotide, G10, displays very high reactivity when NM6 is included in the SHAPE reaction (but is absent in the presence of SAH), thus

suggesting G9 is secured in the flipped conformation immediately after modification. In our model, the anticodon stem-loop is predicted to interact with the Trm10 N-terminal domain; these interactions may distort the tRNA structure in a way that leads to stabilization or occlusion of this region (decreased SHAPE reactivity) while supporting the changes elsewhere in the tRNA necessary for methylation. Previous studies with a truncated Trm10 protein lacking the N-terminal domain showed a drastic reduction in methylation activity (30), further supporting a model where conformational changes to the anticodon stem-loop induced by the N-terminal domain are essential for catalysis.

**Discussion**

One challenge faced by all tRNA-modifying enzymes is how to recognize specific substrates from a pool of tRNAs with a similar overall structure. Sequence and modification recognition elements have been identified for some enzymes, but many key aspects of molecular recognition are still being uncovered (42, 45). Trm10 methylates a subset of tRNAs with a guanosine at position 9 and these tRNAs appear to have no common sequence or other posttranscriptional modifications that result in selection of some, but not all, G9-containing tRNAs for modification. Moreover, we previously demonstrated that the long variable loop of Type II tRNAs is a defining feature of nonsubstrate tRNAs (14), but the molecular basis for this distinction had not been demonstrated. Thus, some other common structural feature(s) among substrate tRNAs or among nonsubstrate tRNAs that affect modification, must underpin Trm10's observed specificity.

Here, we used the SAM-analog NM6 to capture the Trm10-tRNA complex in a catalytically relevant state and showed that methylation by Trm10 is dependent on specific conformational changes to the substrate tRNA that are induced by binding of the enzyme. Our SHAPE structure probing revealed distinct conformational changes in substrate tRNA that are necessary for

methylation and which are not observed in Trm10-bound nonsubstrate tRNA. These changes are also not observed for any tRNA in the presence of the tRNA-binding competent but catalytically inactive Trm10-KRR variant. The changes include increased reactivity in the D-loop of the tRNA and decreased reactivity in the anticodon loop, which are consistent with a model in which local conformational changes position the target nucleotide in its binding pocket, while distant conformational changes are related to specific interactions with the N-terminal domain of Trm10.

Considering the inaccessibility of the G9 target nucleotide in the core region of the tRNA, the increased reactivity for nucleotides in the D-loop which surround the site of modification is likely to be necessary for access to the target base and to position it for methylation. Based on the observed nucleotide reactivity changes surrounding G9 in the Trm10-bound substrate tRNA and lack of G10 SHAPE reactivity in the presence of wild-type Trm10 with SAH compared to NM6, we speculate that methylation may require a process known as base-flipping, which is common among DNA and RNA methyltransferases that act on an inaccessible nucleotide. First observed in the methyltransferase *M.HhaI* DNA C5-methyltransferase complexed with a synthetic DNA complex (46), all structures solved since for base-modifying SPOUT methyltransferases in complex with substrate RNAs (TrmD (47), Nep1 (48), and TRMT10C (43)) exhibit this process as part of the modification mechanism. Considering that nonsubstrate tRNAs bound to wild-type Trm10 and substrate tRNAs bound to the inactive Trm10-KRR variant do not show these same increases in reactivity around the site of modification, base-flipping presumably only occurs after initial binding and directly prior to methylation once the correct structural elements have been recognized. The inability of the inactive Trm10-KRR variant to induce the tRNA changes that we propose are necessary to flip the target base into position implies that one or more of the mutated residues is likely essential for driving and/ or recognizing these alterations in the tRNA core region. This idea is supported by comparison of the electrostatic surface potential of wild-type Trm10 and

Trm10-KRR (**Supplemental Figure S3.8**). The observation of tRNA binding to the Trm10 variant suggests that Trm10-KRR maintains enough positive residues around the putative binding surface. Moreover, the replacement of arginine and lysine residues around the catalytic center may prevent the necessary distortion of the tRNA around the site of modification, rendering the target nucleotide inaccessible. As precedence for such a mechanism, basic residues that are critical for RNA distortion, but which do not contribute measurably to RNA substrate binding, have been identified in other RNA-modifying enzymes such as the aminoglycoside-resistance 16S ribosomal RNA methyltransferase RmtC (49, 50). However, a precise understanding of the role of these residues in Trm10 requires further detailed investigation.

The decreased reactivity in the anticodon loop distant from the site of modification was more surprising. However, these changes can potentially be explained in the context of our model for Trm10-tRNA interaction (**Figure 3.5C,D**) which provides a useful framework to visualize tRNA conformational changes and to predict how the tRNA may be interacting with different regions of Trm10. The conformational changes in the anticodon loop may be related to specific interactions made by the N-terminal domain of Trm10 with the opposite surface of the tRNA to that used for C-terminal domain binding. Despite the lower sequence conservation and likely structural differences between the TRMT10C and Trm10 N-terminal domains compared to the C-terminal SPOUT fold, both are enriched in positively charged residues and have been implicated in tRNA binding (30, 43). Thus, a reasonable expectation is that the Trm10 N-terminal domain wraps around the anticodon stem-loop to make similar interactions with tRNA as for TRMT10C. Therefore, the region linking the two Trm10 domains may directly interact with the anticodon loop of tRNA, leading to the reduction in reactivity in this region of the tRNA. However, we note that as Trm10 is not known to function as part of larger complexes, there are limitations to the information that can be inferred from this model which was generated using the structure of TRMT10C as part

of the larger mitochondrial RNase P complex. Further direct structural information is needed to draw specific conclusions about the interactions between the Trm10 and tRNA. Nonetheless, an essential role for the N-terminal domain in distorting the anticodon loop during recognition would also explain why a truncated Trm10 enzyme which is lacking the N-terminal domain shows a drastic reduction in methylation activity (30). Recognition of the tRNA as a whole and of regions distant from the modification site is common amongst tRNA-modifying SPOUT methyltransferases, including TrmD (51), TrmJ (52, 53), and TrmH (54), as well as other tRNA modifying enzymes such as human pseudouridine synthase PUS7 (55). Each of these enzymes require full-length tRNA for efficient modification, implying that they recognize structural elements of the tRNA outside of just the modification site, in a manner similar to Trm10.

It is additionally possible that the interactions between Trm10 and the anticodon loop of substrate tRNA directly contribute to recognition by helping to propagate long distance changes in the tRNA conformation which are necessary for methylation. Conformational changes to the substrate which are distant from the site of modification have been observed for other SPOUT methyltransferases including thiostrepton-resistance methyltransferase, which unfolds the tertiary structure of its substrate ribosomal RNA to cause a more global conformational change (56, 57). Similar unfolding processes have also been observed for tRNA-modifying SPOUT methyltransferases, including TrmH (54, 58) which modifies the D-loop of tRNA and Trm56 (59) which modifies the T-loop. Both enzymes require disruptions to the tertiary structure of the tRNA for methylation to occur.

Our findings on RNA conformational changes necessary for methylation by Trm10 shed light on a novel component to substrate recognition and can explain why no apparent trends in sequences have been identified to date among substrate or nonsubstrate tRNAs. Very different RNA sequences can result in similar inherent flexibilities in the tRNA structure and/ or capacity to

be appropriately reconfigured upon Trm10 binding, as is observed for substrates $tRNA^{Gly\text{-}GCC}$ and $tRNA^{Trp\text{-}CCA}$. Therefore, consideration of RNA flexibility and deformability as potential recognition elements for a specific RNA-modifying enzyme may be critical in fully defining the recognition process. This may be especially true for other RNA-modifying enzymes which modify an inaccessible region or other tRNA-modifying enzymes which need to be able to discriminate between structurally similar tRNA species.

Thus, while a high-resolution structure is still needed to uncover the details of the interaction between Trm10 and substrate tRNA, the current study has revealed new insights into how Trm10 discriminates between structurally similar tRNAs to select the correct substrate for methylation. Considering the similar overall tertiary structure for all tRNAs, identifying the mechanism of substrate recognition by Trm10 may prove to be critical for understanding substrate recognition for other tRNA-binding proteins as well.

**Acknowledgements**

We thank Drs. Duc Duong and Nick Seyfried for their assistance with MS analysis. This research was supported by the National Institute of General Medical Sciences award R01 GM130135 (to J. E. J. and G. L. C.), the NSF GRFP award 1937971 (to S. E. S.), and the OSU Center for RNA Biology Graduate Fellowship (to I. E. B.). Research reported in this publication was also supported by the Office of the Director, NIH, under award number S10 OD023582.

**Author Contributions**

S.E.S., G.L.C., and J.E.J. participated in research design. L.R.C. synthesized reagents. S.E.S.*, I.E.B, A.K., H.K., C.B.E., E.G.K., and C.J.H. performed experiments. S.E.S. analyzed data. S.E.S. and G.L.C wrote the manuscript. I.E.B. and J.E.J. provided feedback on the manuscript.

[*S.E.S. performed the majority of experiments shown in Figures 3.2-3.5]

## Figures

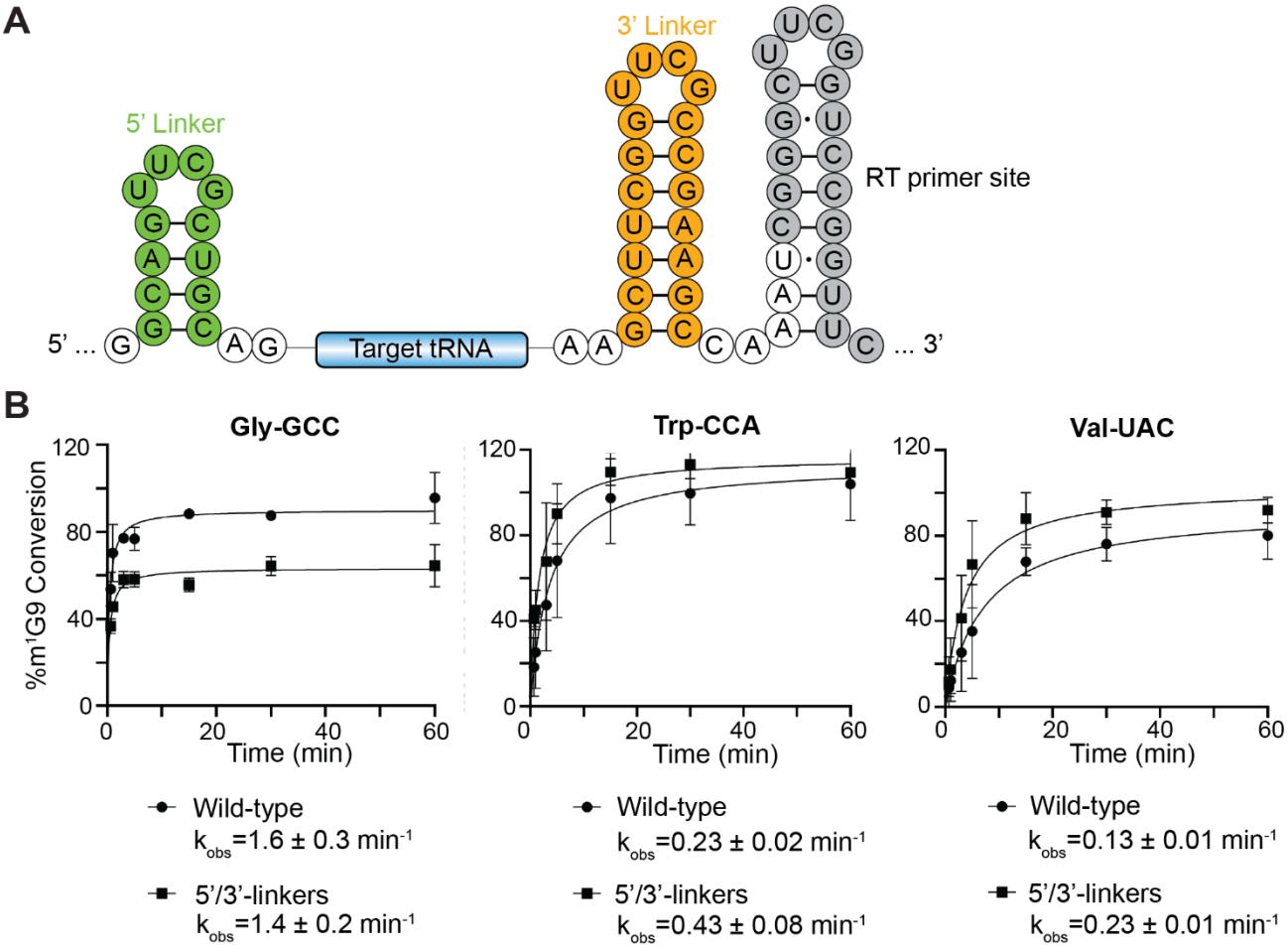


**Figure 3.1 Comparison of modification reaction kinetics for authentic tRNA transcripts and tRNAs embedded within 5'- and 3'-end hairpins.** ***A***, Structure and sequence of the *in vitro* transcription template containing 5'- and 3'-hairpins on each side of the tRNA. The RT primer binding site in the 3'-region is also indicated ***B***, Single-turnover reaction plots for authentic tRNA transcripts (wild-type; circles) and SHAPE tRNAs (5'/3'-linkers; squares) for $tRNA^{Gly\text{-}GCC}$ (*left*), $tRNA^{Trp\text{-}CCA}$ (*middle*), and $tRNA^{Val\text{-}UAC}$ (*right*).

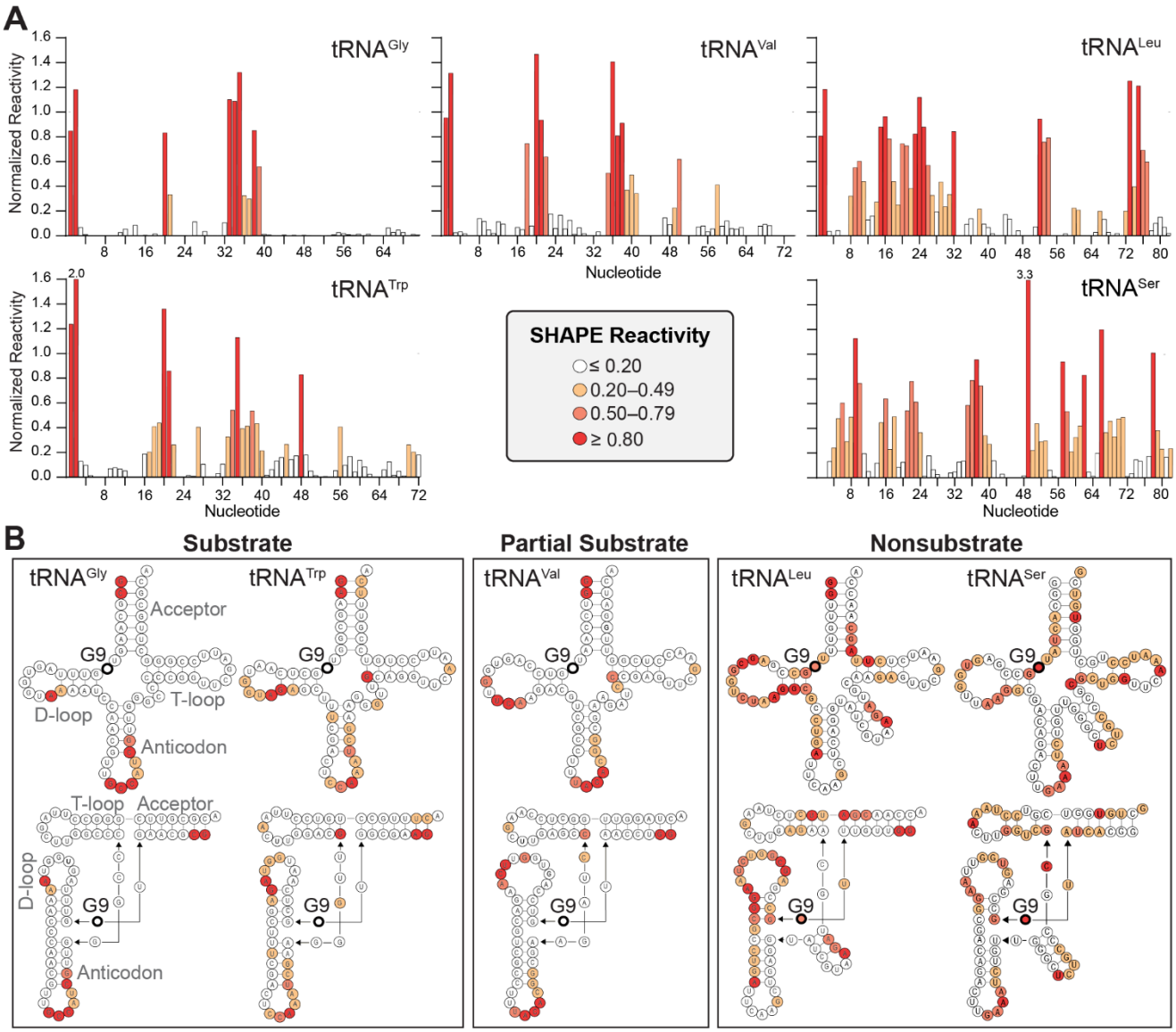


**Figure 3.2 SHAPE analysis reveals differences in inherent flexibility of substrate and nonsubstrate tRNAs.** ***A***, SHAPE reactivities for each nucleotide of free $tRNA^{Gly\text{-}GCC}$ (substrate), $tRNA^{Trp\text{-}CCA}$ (substrate), $tRNA^{Val\text{-}UAC}$ (partial substrate), $tRNA^{Leu\text{-}CAA}$ (nonsubstrate), and $tRNA^{Ser\text{-}UGA}$ (nonsubstrate) were normalized by dividing each value by the average of the reactivities of the highest 8%, omitting the highest 2% (39). The averaged values from two replicates are shown as plots of normalized reactivity vs. nucleotide number. Note that due to the nature of the normalization process, some values

may be above 1. The color scale for SHAPE reactivity for both panels is shown in center of the bottom row. ***B***, Averaged SHAPE reactivities for each free tRNA mapped onto their secondary (top) and tertiary (bottom) structures.

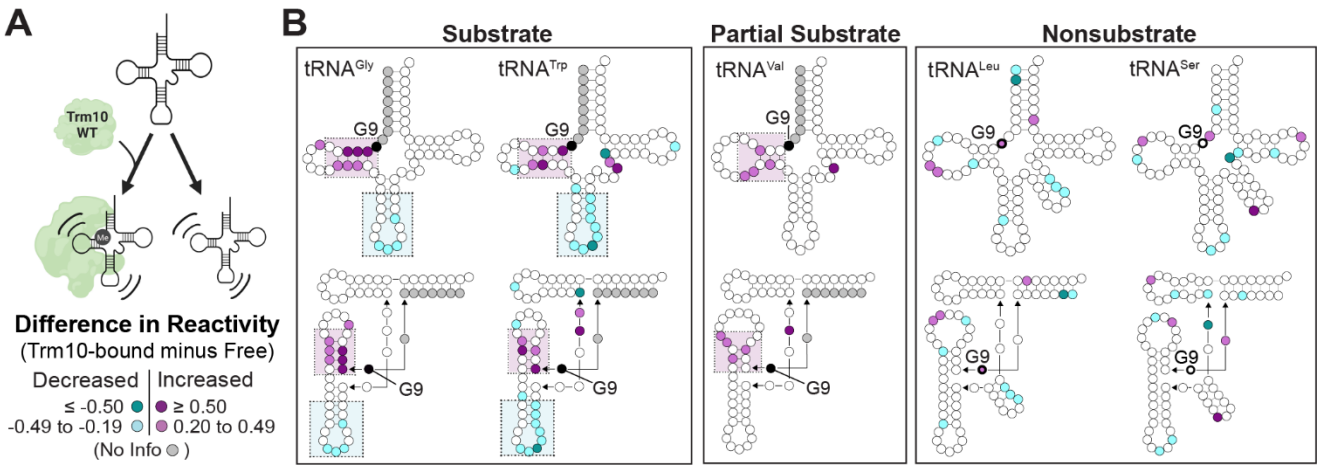


**Figure 3.3 Trm10 induces specific conformational changes in substrate tRNAs that are not observed in nonsubstrate tRNAs.** ***A***, Schematic of comparison being made between free tRNA and tRNA bound to wild-type Trm10. ***B***, Difference SHAPE reactivities between Trm10-bound and free tRNAs mapped onto secondary (*top*) and tertiary (*bottom*) structures for (*left* to *right*): $tRNA^{Gly\text{-}GCC}$ (substrate), $tRNA^{Trp\text{-}CCA}$ (substrate), $tRNA^{Val\text{-}UAC}$ (partial substrate), and $tRNA^{Leu\text{-}CAA}$ (nonsubstrate), and $tRNA^{Ser\text{-}UGA}$ (nonsubstrate). The color scale for difference in SHAPE reactivity (Trm10-bound minus free tRNA) is shown in the *bottom left*.

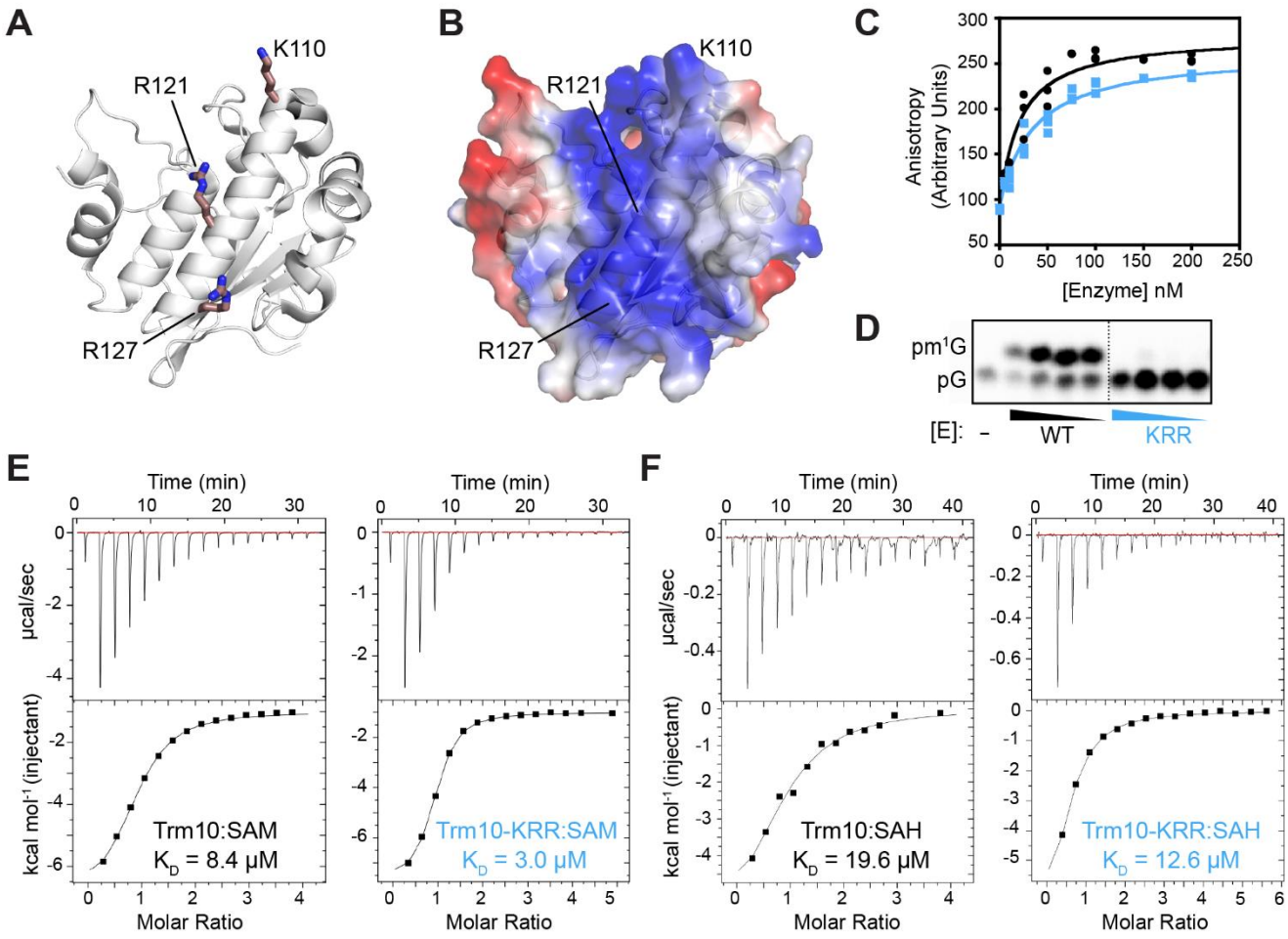


**Figure 3.4 S. cerevisiae Trm10-KRR has similar substrate and cosubstrate binding affinities as the wild-type enzyme but lacks catalytic activity.** Trm10 C-terminal domain structure (PDB: 4JWJ) shown as ***A***, cartoon and ***B***, electrostatic surface potential highlighting the lysine (K) and arginine (R) residues substituted with glutamic acid in the Trm10-KRR variant. ***C***, Fluorescence anisotropy determination of substrate $tRNA^{Gly\text{-}GCC}$ binding affinities ($K_D$) for wild-type Trm10 (*black circles*; $K_D = 20 \pm 4$ nM) and Trm10-KRR (*blue squares*; $K_D = 34 \pm 5$ nM). Results shown are for three independent assays plotted together and fit to equation 1, as described in the Materials and Methods. ***D***, Thin-layer chromatography methylation assay to determine methylation efficiency of wild-type Trm10 and Trm10-KRR with substrate $tRNA^{Gly\text{-}GCC}$. Reactions contained 10-fold serial

dilutions of purified enzyme, as indicated by triangles, or no enzyme (-). Representative isothermal titration calorimetry (ITC) analysis of wild-type Trm10 and Trm10-KRR binding to ***E***, SAM cosubstrate and ***F***, methylation reaction by-product SAH. Binding affinities derived from fits to both replicates are given in **Supplemental Table S1**.

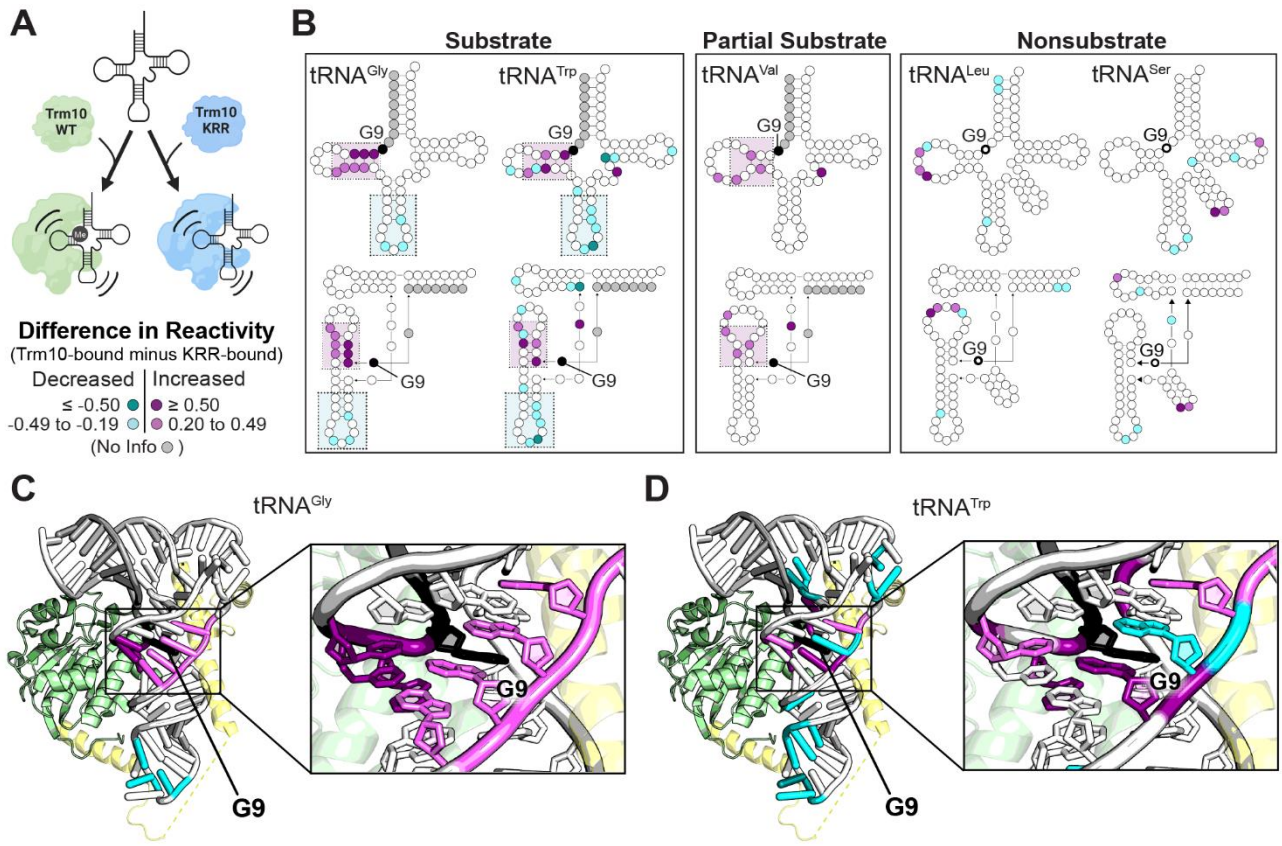


**Fig. 3.5. Comparison of SHAPE reactivities when bound to wild-type Trm10 and Trm10-KRR variant reveals the tRNA conformational changes necessary for methylation.** ***A***, Schematic of comparison being made between KRR-bound tRNA and Trm10-bound tRNA. ***B***, Difference SHAPE reactivities between Trm10-bound and KRR-bound tRNAs mapped onto secondary (*top*) and tertiary (*bottom*) structures for (*left* to *right*): $tRNA^{Gly\text{-}GCC}$ (substrate), $tRNA^{Trp\text{-}CCA}$ (substrate), $tRNA^{Val\text{-}UAC}$ (partial substrate), $tRNA^{Leu\text{-}CAA}$ (nonsubstrate), and $tRNA^{Ser\text{-}UGA}$ (nonsubstrate). Difference in reactivity for ***C***, $tRNA^{Gly\text{-}GCC}$ and ***D***, $tRNA^{Trp\text{-}CCA}$ mapped onto a model of the Trm10-tRNA complex, highlighting conformational changes necessary for methylation. The model of the Trm10-tRNA complex was generated using the structure of TRMT10C bound to pre-tRNA (PDB: 7ONU) and $tRNA^{Phe}$ (PDB: 6LVR), and is comprised of: the Trm10 C-terminal domain

(PDB: 4JWJ; *green*), tRNA (*white)* and the N-terminal domain of TRMT10C (*yellow*). The color scale for difference in SHAPE reactivity (Trm10-bound minus KRR-bound tRNA) is shown in the *bottom of panel A*.

## Supplemental Figures

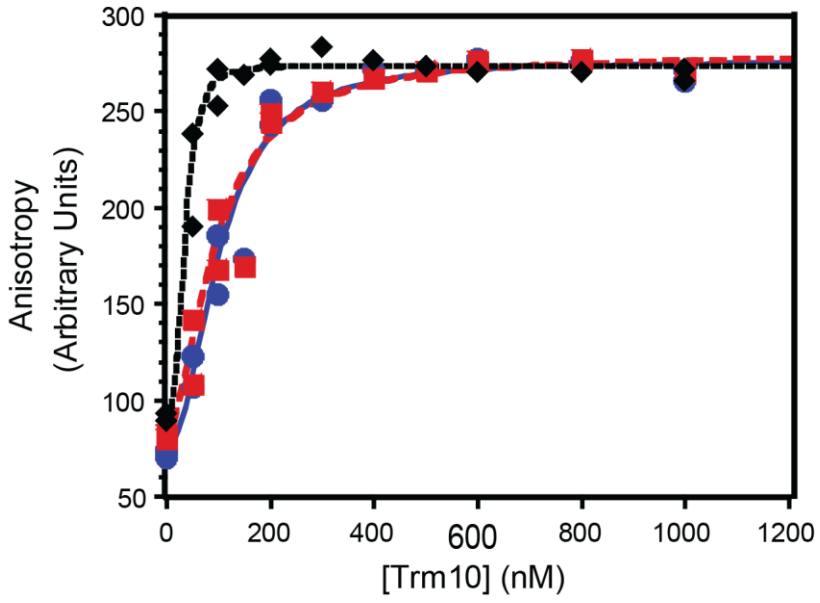


**Supplemental Figure S3.1 Binding affinity of tRNAs with Trm10.** Wild-type Trm10 binding affinity was determined by fluorescence anisotropy for $tRNA^{Gly\text{-}GCC}$ (*blue circles*; $K_D$ = 100 ± 8 nM), $tRNA^{Val\text{-}UAC}$ (*red squares*; $K_D$ = 96 ± 10 nM), and $tRNA^{Leu\text{-}CAA}$ (*black diamonds*; $K_D$ = 38 ± 5 nM). Data from three independent experiments were plotted together and fit to equation 1 (see *Materials and Methods*).

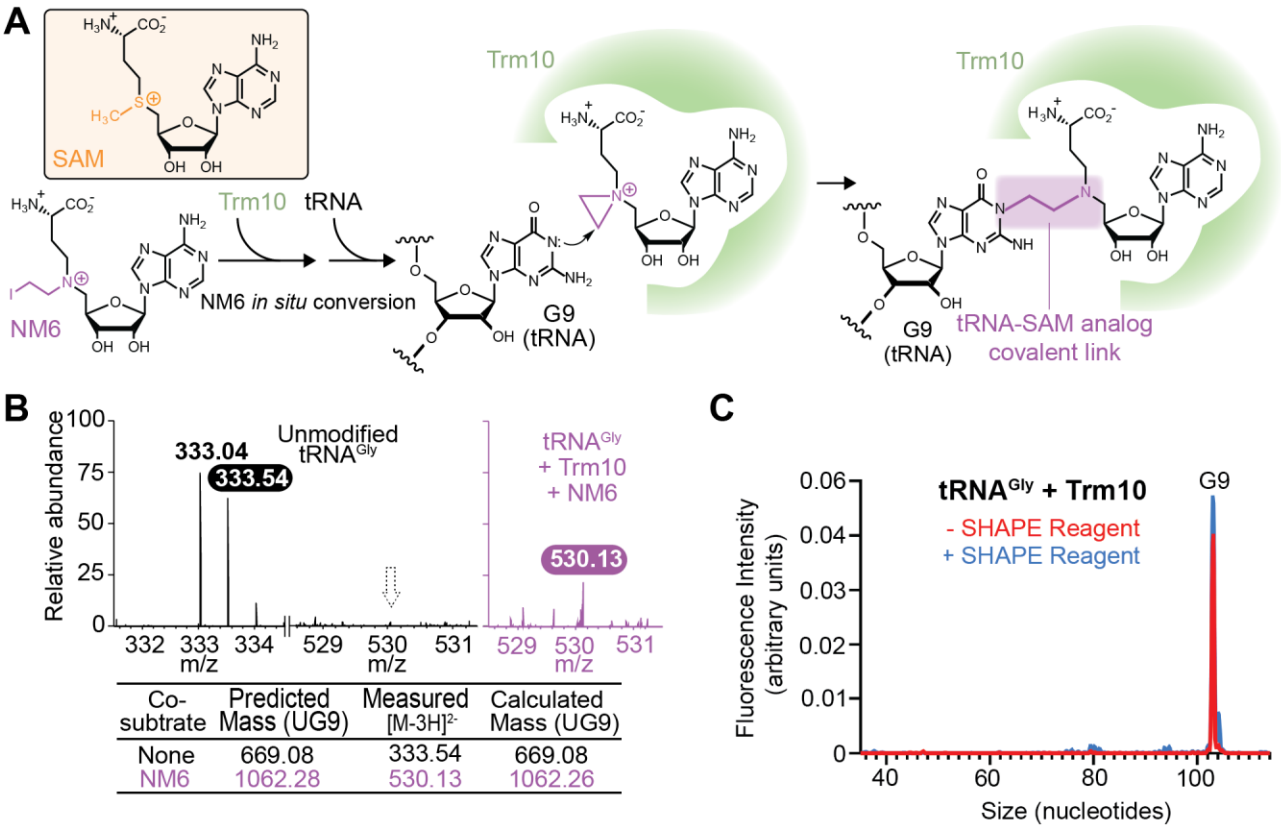


**Supplemental Figure S3.2. Stabilization of the Trm10-tRNA complex using the SAM analog NM6.** ***A***, N-mustard 6 (NM6; *bottom left*) is an analog of S-adenosyl-L-methionine (SAM; *top left box*) that Trm10 can use as a cosubstrate for modification of tRNA. In this enzymatic reaction, NM6 becomes covalently attached to the tRNA at the N1 base position of G9. The Trm10-tRNA complex is thus stabilized in a state immediately following catalysis by virtue of Trm10's affinity for both tRNA subunit and the cosubstrate analog covalently attached to G9. ***B***, The covalent attachment of NM6 to G9 of $tRNA^{Gly}$ is confirmed by MS analysis showing a peak at an m/z of 530.13 representing the $UG_9$-NM6 fragment. This peak is not observed in the sample in which NM6 is absent (dotted arrow). ***C***, Example capillary electrophoresis chromatogram of $tRNA^{Gly\text{-}GCC}$ in the presence of Trm10 and NM6 displaying a large peak at the modification site, indicating that the attachment of NM6 prevents further reverse transcription.

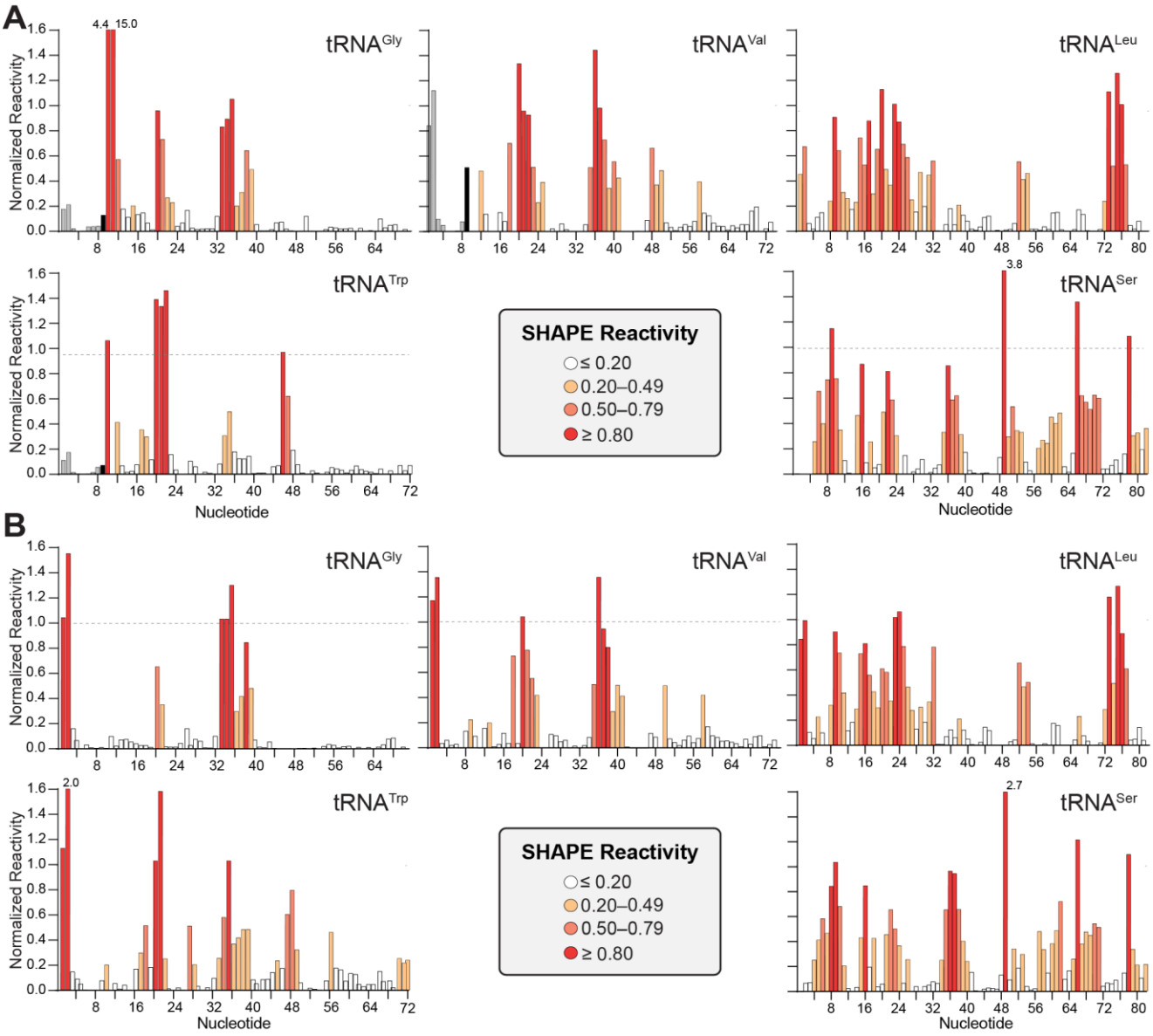


**Supplemental Figure S3.3 Normalized reactivities of tRNAs bound to wild-type Trm10 and Trm10-KRR.** SHAPE reactivities of tRNA bound to ***A***, wild-type Trm10 or ***B***, Trm10-KRR were normalized by dividing each value by the average of the reactivities of the highest 8%, omitting the highest 2%. The values from two replicates were then averaged and classified as shown in the key in the center of the bottom row of each panel.

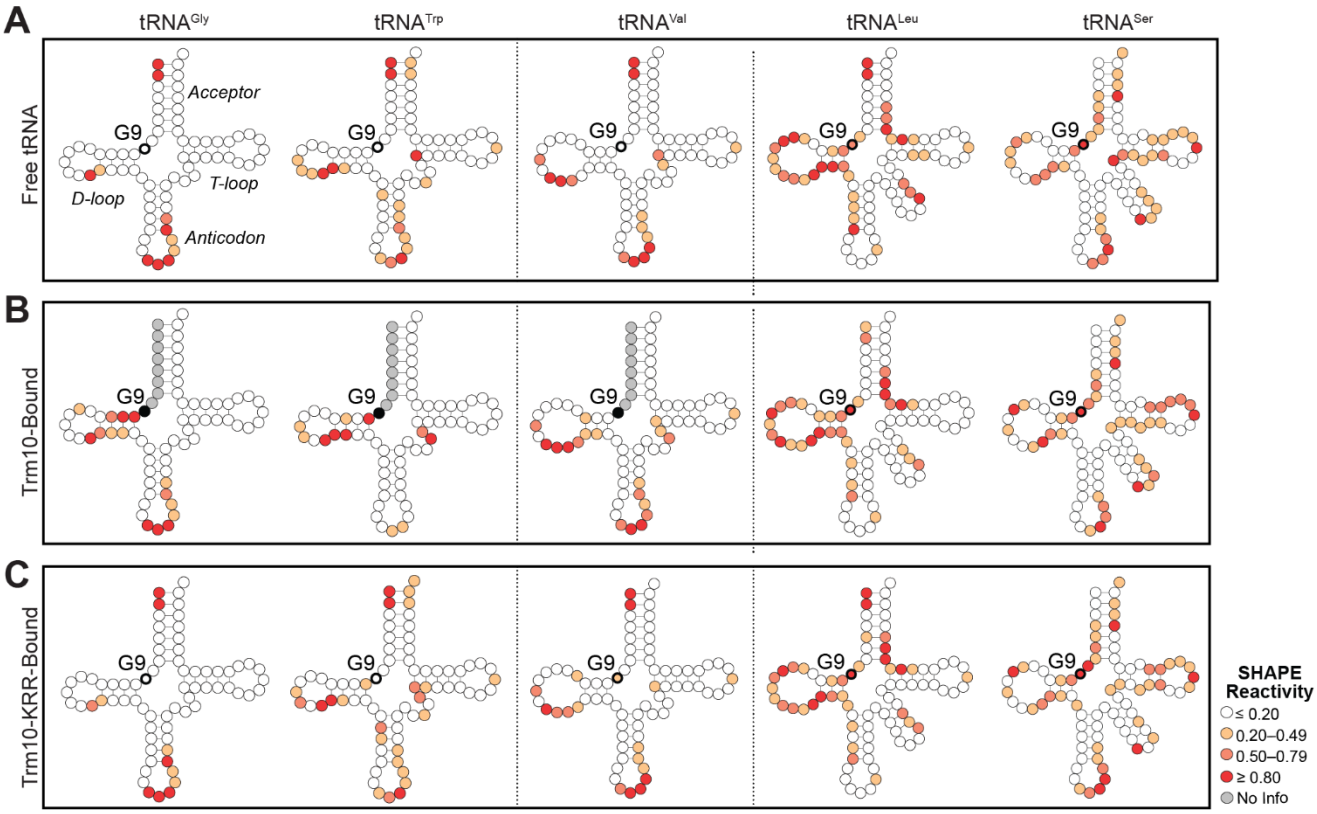


**Supplemental Figure S3.4 Nucleotide SHAPE reactivities in free and Trm10-bound tRNAs.** SHAPE reactivities mapped onto tRNA secondary structures for: ***A***, free tRNA (note, these data are the same as shown in **Fig. 3.2B**), ***B***, tRNA bound to wild-type Trm10, and ***C***, tRNA bound to Trm10-KRR. The color scale for SHAPE reactivity is shown in the *bottom right.*

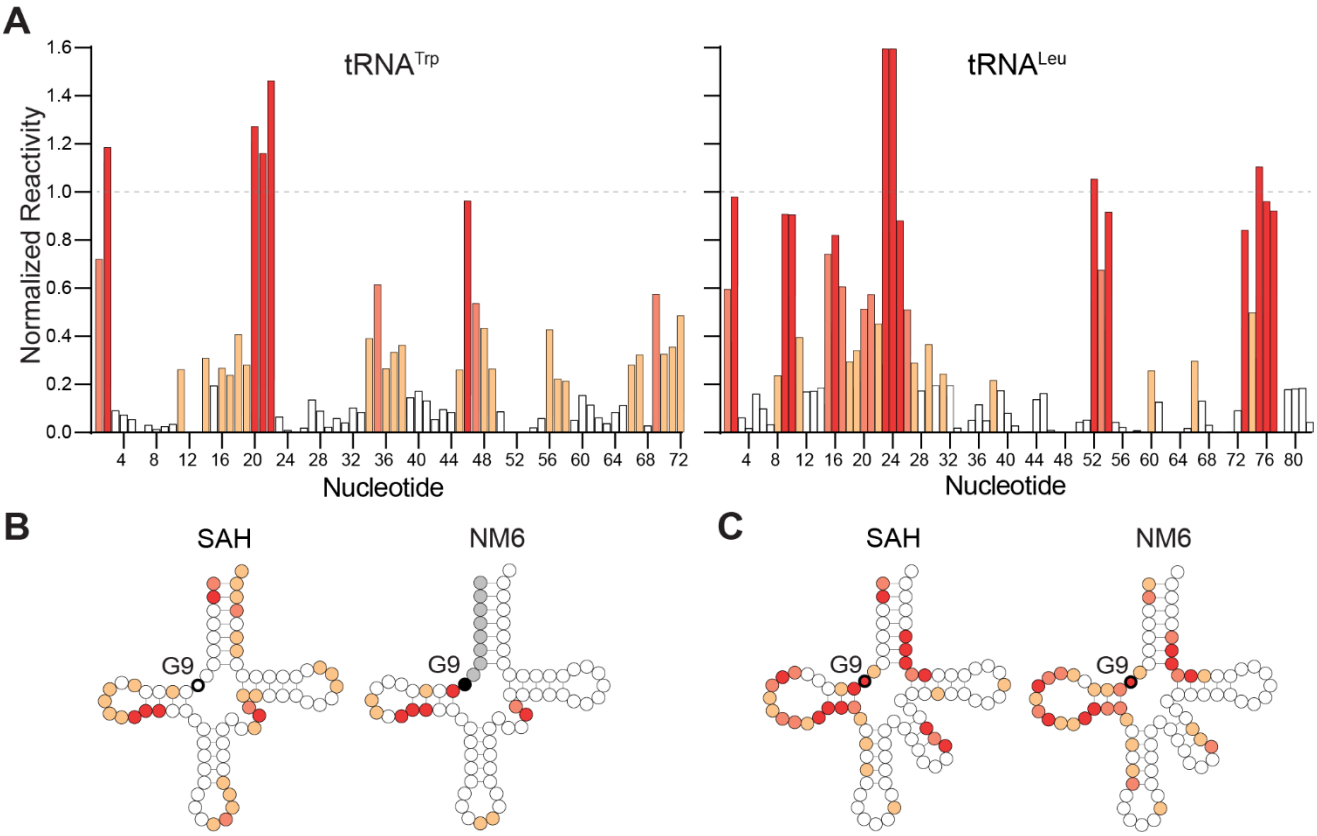


**Supplemental Figure S3.5 SHAPE reactivities of substrate tRNA$^{Trp}$ and nonsubstrate tRNA$^{Leu}$ bound to wild-type Trm10 in the presence of SAH.** ***A***, SHAPE reactivities of tRNA$^{Trp}$ (substrate) and tRNA$^{Leu}$ (nonsubstrate) bound to wild-type Trm10 in the presence of SAH were normalized and the values for two replicates were averaged. SHAPE reactivities of ***B***, tRNA$^{Trp}$ and ***C***, tRNA$^{Leu}$ bound to wild-type Trm10 in the presence of cosubstrate SAH or NM6 (note, these data for NM6 are the same as shown in **Supplemental Figure S3.4B**) are mapped onto the tRNA secondary structure. The color scale for SHAPE reactivity is shown for both panels in the *bottom right.*

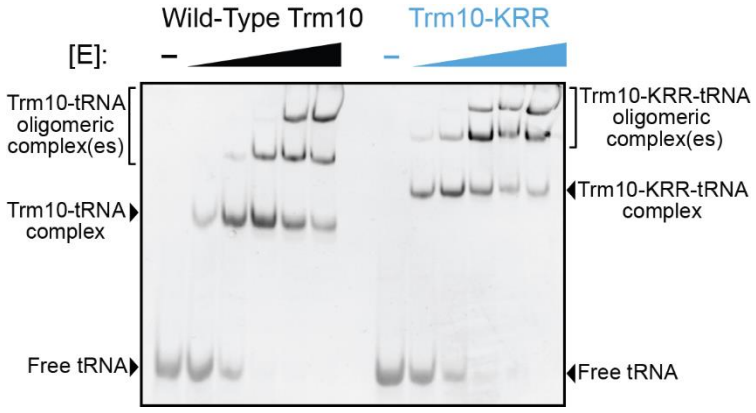


**Supplemental Figure S3.6 Electromobility shift assay (EMSA) of substrate $tRNA^{Gly}$ with wild-type Trm10 and Trm10-KRR.** $tRNA^{Gly}$ was incubated with increasing concentrations of wild-type Trm10 or Trm10-KRR and samples were run on a non-denaturing 10% polyacrylamide gel. The apparent differences in mobility of the mutant complex are likely due to the different electrostatics of the enzyme-tRNA complex(es) but overall similar binding affinities and patterns of complex formation are observed between wild-type Trm10 and Trm10-KRR.

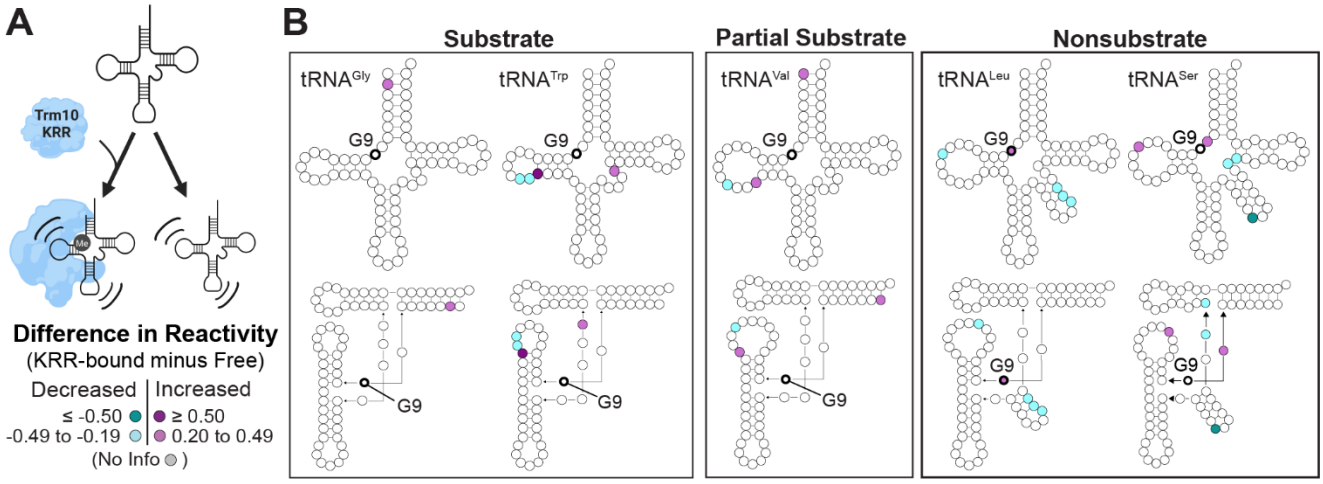


**Supplemental Figure S3.7 Comparison of unbound tRNA and KRR-bound tRNA.** ***A***, Schematic of comparison being made between free tRNA and KRR-bound tRNA. ***B***, Difference SHAPE reactivities between KRR-bound and free tRNAs mapped onto secondary (*top*) and tertiary (*bottom*) structures for (*left* to *right*): $tRNA^{Gly\text{-}GCC}$ (substrate), $tRNA^{Trp\text{-}CCA}$ (substrate), $tRNA^{Val\text{-}UAC}$ (partial substrate), $tRNA^{Leu\text{-}CAA}$ (nonsubstrate), and $tRNA^{Ser\text{-}UGA}$ (nonsubstrate). The color scale for difference in SHAPE reactivity (KRR-bound minus free tRNA) is shown in the *bottom left*.

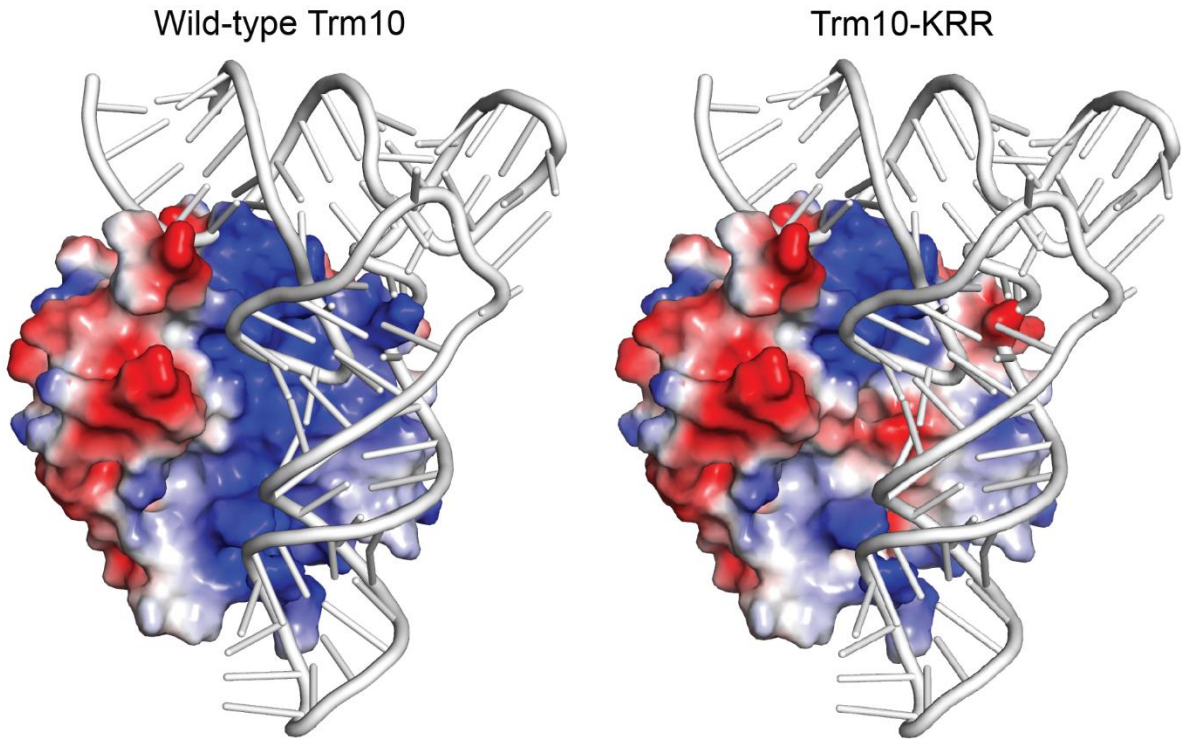


**Supplemental Figure S3.8 Electrostatic surface potential of wild-type Trm10 and Trm10-KRR shown on a Trm10-tRNA model.** Amino acid substitutions to *S. cerevisiae* Trm10 C-terminal domain (PDB 4JWJ) were made using the PyMol mutagenesis tool to generate the Trm10-KRR variant. Protein electrostatics were then generated for wild-type Trm10 and Trm10-KRR in PyMol and are shown on a semi-transparent surface representation for each protein. The placement of tRNA was predicted from the structure of TRMT10C in complex with pre-tRNA (PDB: 7ONU) and is shown using $tRNA^{Phe}$ (PDB: 6LVR).

## Supplemental Table

**Supplemental Table 3.1 Association constants ($K_A$) for Trm10 binding SAM and SAH determined by ITC.**

| | | SAM[a] | SAH[a] |
|---|---|---|---|
| $K_A$ ($M^{-1}$) | Wild-Type Trm10 | $8.90 \pm 0.27 \times 10^4$ | $5.1 \pm 1.42 \times 10^4$ |
| | | $11.9 \pm 0.87 \times 10^4$ | $4.62 \pm 1.33 \times 10^4$ |
| | Trm10-KRR | $32.5 \pm 1.83 \times 10^4$ | $10.7 \pm 1.92 \times 10^4$ |
| | | $33.1 \pm 0.88 \times 10^4$ | $7.96 \pm 0.70 \times 10^4$ |

[a]Replicate measurements shown with the direct fit error determined using a model for one-binding site in Origin software after subtraction of residual heats.

## References


1. Nachtergaele, S., andHe, C. (2017) The emerging biology of RNA post-transcriptional modifications RNA Biol **14**, 156-163 10.1080/15476286.2016.1267096

2. Machnicka, M. A., Milanowska, K., Osman Oglou, O., Purta, E., Kurkowska, M., Olchowik, A. *et al.* (2013) MODOMICS: a database of RNA modification pathways--2013 update Nucleic Acids Res **41**, D262-267 10.1093/nar/gks1007

3. Phizicky, E. M., andHopper, A. K. (2010) tRNA biology charges to the front Genes Dev **24**, 1832-1860 10.1101/gad.1956510

4. Juhling, F., Morl, M., Hartmann, R. K., Sprinzl, M., Stadler, P. F., andPutz, J. (2009) tRNAdb 2009: compilation of tRNA sequences and tRNA genes Nucleic Acids Res **37**, D159-162 10.1093/nar/gkn772

5. Han, L., andPhizicky, E. M. (2018) A rationale for tRNA modification circuits in the anticodon loop RNA **24**, 1277-1284 10.1261/rna.067736.118

6. Bjork, G. R., Wikstrom, P. M., andBystrom, A. S. (1989) Prevention of translational frameshifting by the modified nucleoside 1-methylguanosine Science **244**, 986-989 10.1126/science.2471265

7. Motorin, Y., andHelm, M. (2010) tRNA stabilization by modified nucleotides Biochemistry **49**, 4934-4944 10.1021/bi100408z

8. Helm, M., andAlfonzo, J. D. (2014) Posttranscriptional RNA Modifications: playing metabolic games in a cell's chemical Legoland Chem Biol **21**, 174-185 10.1016/j.chembiol.2013.10.015

9. Sylvers, L. A., Rogers, K. C., Shimizu, M., Ohtsuka, E., andSoll, D. (1993) A 2-thiouridine derivative in tRNAGlu is a positive determinant for aminoacylation by Escherichia coli glutamyl-tRNA synthetase Biochemistry **32**, 3836-3841 10.1021/bi00066a002

10. Suzuki, T., Ueda, T., andWatanabe, K. (1997) The 'polysemous' codon--a codon with multiple amino acid assignment caused by dual specificity of tRNA identity EMBO J **16**, 1122-1134 10.1093/emboj/16.5.1122

11. Jackman, J. E., Montange, R. K., Malik, H. S., andPhizicky, E. M. (2003) Identification of the yeast gene encoding the tRNA m1G methyltransferase responsible for modification at position 9 RNA **9**, 574-585 10.1261/rna.5070303

12. Vilardo, E., Nachbagauer, C., Buzet, A., Taschner, A., Holzmann, J., andRossmanith, W. (2012) A subcomplex of human mitochondrial RNase P is a bifunctional methyltransferase--extensive moonlighting in mitochondrial tRNA biogenesis Nucleic Acids Res **40**, 11583-11593 10.1093/nar/gks910

13. Howell, N. W., Jora, M., Jepson, B. F., Limbach, P. A., andJackman, J. E. (2019) Distinct substrate specificities of the human tRNA methyltransferases TRMT10A and TRMT10B RNA **25**, 1366-1376 10.1261/rna.072090.119

14. Swinehart, W. E., Henderson, J. C., andJackman, J. E. (2013) Unexpected expansion of tRNA substrate recognition by the yeast m1G9 methyltransferase Trm10 RNA **19**, 1137-1146 10.1261/rna.039651.113

15. Vilardo, E., Amman, F., Toth, U., Kotter, A., Helm, M., andRossmanith, W. (2020) Functional characterization of the human tRNA methyltransferases TRMT10A and TRMT10B Nucleic Acids Res **48**, 6157-6169 10.1093/nar/gkaa353

16. Igoillo-Esteve, M., Genin, A., Lambert, N., Desir, J., Pirson, I., Abdulkarim, B. *et al.* (2013) tRNA methyltransferase homolog gene TRMT10A mutation in young onset diabetes and primary microcephaly in humans PLoS Genet **9**, e1003888 10.1371/journal.pgen.1003888

17. Gillis, D., Krishnamohan, A., Yaacov, B., Shaag, A., Jackman, J. E., andElpeleg, O. (2014) TRMT10A dysfunction is associated with abnormalities in glucose homeostasis, short stature and microcephaly J Med Genet **51**, 581-586 10.1136/jmedgenet-2014-102282

18. Yew, T. W., McCreight, L., Colclough, K., Ellard, S., andPearson, E. R. (2016) tRNA methyltransferase homologue gene TRMT10A mutation in young adult-onset diabetes with intellectual disability, microcephaly and epilepsy Diabet Med **33**, e21-25 10.1111/dme.13024

19. Zung, A., Kori, M., Burundukov, E., Ben-Yosef, T., Tatoor, Y., andGranot, E. (2015) Homozygous deletion of TRMT10A as part of a contiguous gene deletion in a syndrome of failure to thrive, delayed puberty, intellectual disability and diabetes mellitus Am J Med Genet A **167A**, 3167-3173 10.1002/ajmg.a.37341

20. Narayanan, M., Ramsey, K., Grebe, T., Schrauwen, I., Szelinger, S., Huentelman, M. *et al.* (2015) Case Report: Compound heterozygous nonsense mutations in TRMT10A are associated with microcephaly, delayed development, and periventricular white matter hyperintensities F1000Res **4**, 912 10.12688/f1000research.7106.1

21. Gustavsson, M., andRonne, H. (2008) Evidence that tRNA modifying enzymes are important in vivo targets for 5-fluorouracil in yeast RNA **14**, 666-674 10.1261/rna.966208

22. Cosentino, C., Toivonen, S., Diaz Villamil, E., Atta, M., Ravanat, J. L., Demine, S. *et al.* (2018) Pancreatic beta-cell tRNA hypomethylation and fragmentation link TRMT10A deficiency with diabetes Nucleic Acids Res **46**, 10302-10318 10.1093/nar/gky839

23. Anantharaman, V., Koonin, E. V., andAravind, L. (2002) SPOUT: a class of methyltransferases that includes spoU and trmD RNA methylase superfamilies, and novel superfamilies of predicted prokaryotic RNA methylases J Mol Microbiol Biotechnol **4**, 71-75, https://www.ncbi.nlm.nih.gov/pubmed/11763972

24. Kurowski, M. A., Sasin, J. M., Feder, M., Debski, J., andBujnicki, J. M. (2003) Characterization of the cofactor-binding site in the SPOUT-fold methyltransferases

by computational docking of S-adenosylmethionine to three crystal structures BMC Bioinformatics **4**, 9 10.1186/1471-2105-4-9

25. Tkaczuk, K. L., Dunin-Horkawicz, S., Purta, E., andBujnicki, J. M. (2007) Structural and evolutionary bioinformatics of the SPOUT superfamily of methyltransferases BMC Bioinformatics **8**, 73 10.1186/1471-2105-8-73

26. Sakaguchi, R., Lahoud, G., Christian, T., Gamper, H., andHou, Y. M. (2014) A divalent metal ion-dependent N(1)-methyl transfer to G37-tRNA Chem Biol **21**, 1351-1360 10.1016/j.chembiol.2014.07.023

27. Krishnamohan, A., andJackman, J. E. (2017) Mechanistic features of the atypical tRNA m1G9 SPOUT methyltransferase, Trm10 Nucleic Acids Res **45**, 9019-9029 10.1093/nar/gkx620

28. Perlinska, A. P., Kalek, M., Christian, T., Hou, Y. M., andSulkowska, J. I. (2020) Mg(2+)-Dependent Methyl Transfer by a Knotted Protein: A Molecular Dynamics Simulation and Quantum Mechanics Study ACS Catal **10**, 8058-8068 10.1021/acscatal.0c00059

29. Van Laer, B., Roovers, M., Wauters, L., Kasprzak, J. M., Dyzma, M., Deyaert, E. *et al.* (2016) Structural and functional insights into tRNA binding and adenosine N1-methylation by an archaeal Trm10 homologue Nucleic Acids Res **44**, 940-953 10.1093/nar/gkv1369

30. Shao, Z., Yan, W., Peng, J., Zuo, X., Zou, Y., Li, F. *et al.* (2014) Crystal structure of tRNA m1G9 methyltransferase Trm10: insight into the catalytic mechanism and recognition of tRNA substrate Nucleic Acids Res **42**, 509-525 10.1093/nar/gkt869

31. Vachon, V. K., andConn, G. L. (2012) Plasmid template design and in vitro transcription of short RNAs within a "structure cassette" for structure probing experiments Methods Mol Biol **941**, 157-169 10.1007/978-1-62703-113-4_12

32. Linpinsel, J. L., andConn, G. L. (2012) General protocols for preparation of plasmid DNA template, RNA in vitro transcription, and RNA purification by denaturing PAGE Methods Mol Biol **941**, 43-58 10.1007/978-1-62703-113-4_4

33. Weller, R. L., andRajski, S. R. (2006) Design, synthesis, and preliminary biological evaluation of a DNA methyltransferase-directed alkylating agent Chembiochem **7**, 243-245 10.1002/cbic.200500362

34. Stanevich, V., Jiang, L., Satyshur, K. A., Li, Y., Jeffrey, P. D., Li, Z. *et al.* (2011) The structural basis for tight control of PP2A methylation and function by LCMT-1 Mol Cell **41**, 331-342 10.1016/j.molcel.2010.12.030

35. Laughlin, Z. T., Nandi, S., Dey, D., Zelinskaya, N., Witek, M. A., Srinivas, P. *et al.* (2022) 50S subunit recognition and modification by the Mycobacterium tuberculosis ribosomal RNA methyltransferase TlyA Proc Natl Acad Sci U S A **119**, e2120352119 10.1073/pnas.2120352119

36. Wilkinson, K. A., Merino, E. J., andWeeks, K. M. (2006) Selective 2'-hydroxyl acylation analyzed by primer extension (SHAPE): quantitative RNA structure

analysis at single nucleotide resolution Nat Protoc **1**, 1610-1616 10.1038/nprot.2006.249

37. Rice, G. M., Busan, S., Karabiber, F., Favorov, O. V., andWeeks, K. M. (2014) SHAPE analysis of small RNAs and riboswitches Methods Enzymol **549**, 165-187 10.1016/B978-0-12-801122-5.00008-8

38. Cantara, W. A., Hatterschide, J., Wu, W., andMusier-Forsyth, K. (2017) RiboCAT: a new capillary electrophoresis data analysis tool for nucleic acid probing RNA **23**, 240-249 10.1261/rna.058404.116

39. Low, J. T., andWeeks, K. M. (2010) SHAPE-directed RNA secondary structure prediction Methods **52**, 150-158 10.1016/j.ymeth.2010.06.007

40. Merino, E. J., Wilkinson, K. A., Coughlan, J. L., andWeeks, K. M. (2005) RNA structure analysis at single nucleotide resolution by selective 2'-hydroxyl acylation and primer extension (SHAPE) J Am Chem Soc **127**, 4223-4231 10.1021/ja043822v

41. Hymbaugh Bergman, S. J., andComstock, L. R. (2015) N-mustard analogs of S-adenosyl-L-methionine as biochemical probes of protein arginine methylation Bioorg Med Chem **23**, 5050-5055 10.1016/j.bmc.2015.05.001

42. Strassler, S. E., Bowles, I. E., Dey, D., Jackman, J. E., andConn, G. L. (2022) Tied up in knots: Untangling substrate recognition by the SPOUT methyltransferases J Biol Chem **298**, 102393 10.1016/j.jbc.2022.102393

43. Bhatta, A., Dienemann, C., Cramer, P., andHillen, H. S. (2021) Structural basis of RNA processing by human mitochondrial RNase P Nat Struct Mol Biol **28**, 713-723 10.1038/s41594-021-00637-y

44. Schubert, H. L., Blumenthal, R. M., andCheng, X. (2003) Many paths to methyltransfer: a chronicle of convergence Trends Biochem Sci **28**, 329-335 10.1016/S0968-0004(03)00090-2

45. McKenney, K. M., Rubio, M. A. T., andAlfonzo, J. D. (2017) The Evolution of Substrate Specificity by tRNA Modification Enzymes Enzymes **41**, 51-88 10.1016/bs.enz.2017.03.002

46. Klimasauskas, S., Kumar, S., Roberts, R. J., andCheng, X. (1994) HhaI methyltransferase flips its target base out of the DNA helix Cell **76**, 357-369 10.1016/0092-8674(94)90342-5

47. Ito, T., Masuda, I., Yoshida, K., Goto-Ito, S., Sekine, S., Suh, S. W. *et al.* (2015) Structural basis for methyl-donor-dependent and sequence-specific binding to tRNA substrates by knotted methyltransferase TrmD Proc Natl Acad Sci U S A **112**, E4197-4205 10.1073/pnas.1422981112

48. Thomas, S. R., Keller, C. A., Szyk, A., Cannon, J. R., andLaronde-Leblanc, N. A. (2011) Structural insight into the functional mechanism of Nep1/Emg1 N1-specific pseudouridine methyltransferase in ribosome biogenesis Nucleic Acids Res **39**, 2445-2457 10.1093/nar/gkq1131

49. Srinivas, P., Nosrati, M., Zelinskaya, N., Dey, D., Comstock, L. R., Dunham, C. M. *et al.* (2023) 30S subunit recognition and G1405 modification by the aminoglycoside-resistance 16S ribosomal RNA methyltransferase RmtC Proc Natl Acad Sci U S A **120**, e2304128120 10.1073/pnas.2304128120

50. Nosrati, M., Dey, D., Mehrani, A., Strassler, S. E., Zelinskaya, N., Hoffer, E. D. *et al.* (2019) Functionally critical residues in the aminoglycoside resistance-associated methyltransferase RmtC play distinct roles in 30S substrate recognition J Biol Chem **294**, 17642-17653 10.1074/jbc.RA119.011181

51. Redlak, M., Andraos-Selim, C., Giege, R., Florentz, C., andHolmes, W. M. (1997) Interaction of tRNA with tRNA (guanosine-1)methyltransferase: binding specificity determinants involve the dinucleotide G36pG37 and tertiary structure Biochemistry **36**, 8699-8709 10.1021/bi9701538

52. Liu, R. J., Long, T., Zhou, M., Zhou, X. L., andWang, E. D. (2015) tRNA recognition by a bacterial tRNA Xm32 modification enzyme from the SPOUT methyltransferase superfamily Nucleic Acids Res **43**, 7489-7503 10.1093/nar/gkv745

53. Somme, J., Van Laer, B., Roovers, M., Steyaert, J., Versees, W., andDroogmans, L. (2014) Characterization of two homologous 2'-O-methyltransferases showing different specificities for their tRNA substrates RNA **20**, 1257-1271 10.1261/rna.044503.114

54. Matsumoto, T., Nishikawa, K., Hori, H., Ohta, T., Miura, K., andWatanabe, K. (1990) Recognition sites of tRNA by a thermostable tRNA(guanosine-2'-)-methyltransferase from Thermus thermophilus HB27 J Biochem **107**, 331-338 10.1093/oxfordjournals.jbchem.a123047

55. Guegueniat, J., Halabelian, L., Zeng, H., Dong, A., Li, Y., Wu, H. *et al.* (2021) The human pseudouridine synthase PUS7 recognizes RNA with an extended multi-domain binding surface Nucleic Acids Res **49**, 11810-11822 10.1093/nar/gkab934

56. Conn, G. L., Draper, D. E., Lattman, E. E., andGittis, A. G. (1999) Crystal structure of a conserved ribosomal protein-RNA complex Science **284**, 1171-1174 10.1126/science.284.5417.1171

57. Kuiper, E. G., andConn, G. L. (2014) Binding induced RNA conformational changes control substrate recognition and catalysis by the thiostrepton resistance methyltransferase (Tsr) J Biol Chem **289**, 26189-26200 10.1074/jbc.M114.574780

58. Hori, H., Saneyoshi, M., Kumagai, I., Miura, K., andWatanabe, K. (1989) Effects of modification of 4-thiouridine in E. coli tRNA(fMet) on its methyl acceptor activity by thermostable Gm-methylases J Biochem **106**, 798-802 10.1093/oxfordjournals.jbchem.a122933

59. Renalier, M. H., Joseph, N., Gaspin, C., Thebault, P., andMougin, A. (2005) The Cm56 tRNA modification in archaea is catalyzed either by a specific 2'-O-methylase, or a C/D sRNP RNA **11**, 1051-1063 10.1261/rna.2110805

# CHAPTER FOUR:

## Cryo-EM structure of the tRNA methyltransferase Trm10 bound to substrate tRNA

This work is unpublished.

**Abstract**

The methyltransferase Trm10 modifies a subset of tRNAs on the base N1 position of the 9th nucleotide in the tRNA core. Trm10 is conserved throughout Eukarya and Archaea, and mutations in the human gene (*TRMT10A*) have been linked to neurological disorders such as microcephaly and intellectual disability, as well as defects in glucose metabolism. However, little is known about the specific interactions between Trm10 and tRNA that allow for the unique substrate specificities seen by Trm10 enzymes. To define the molecular basis of tRNA recognition and $m^1G9$ modification by Trm10, we used a *S*-adenosyl-L-methionine (SAM) analog to trap the complex in a post-catalytic state to enable determination of a cryogenic electron microscopy (cryo-EM) structure of Trm10 from *Saccharomyces cerevisiae* bound to substrate $tRNA^{Gly}$. The current 3D reconstruction provides the first snapshot of a monomeric SPOUT methyltransferase bound to its substrate in the absence of any additional binding partners. Our model reveals the positioning of Trm10 in relation to the tRNA and pinpoints specific regions of the tRNA which interact with Trm10 during substrate recognition. Additionally, the 2D classes reveal the presence of a small population of dimeric Trm10 bound to substrate tRNA which may be important for initial substrate recognition and/ or catalysis. These studies shed light on a novel mechanism of substrate recognition by a conserved tRNA methyltransferase and expand our knowledge of substrate recognition by tRNA-modifying enzymes.

## Introduction

Methylation is one of the most common cellular modifications and can play an important role in gene expression, small molecule metabolism, and regulation of macromolecule structure and function (1-4). The SpoU-TrmD (SPOUT) enzymes comprise one of five families of SAM-dependent methyltransferases which was designated when structural similarity was identified between the transfer RNA (tRNA)-modifying enzymes TrmH (SpoU) and TrmD (5-10). SPOUT methyltransferases are characterized by a unique α/β fold and a deep trefoil knot in the C-terminal half of the SPOUT methyltransferase catalytic domain. This knot stabilizes SAM in a bent conformation that is necessary for methyl transfer by this family of enzymes (7, 11-13).

The tRNA methyltransferase Trm10 was first predicted to be a member of the SPOUT family in 2007 by a bioinformatics study before any structural information was known about the enzyme (9). Trm10 modifies the N1 base position of the 9$^{th}$ nucleotide in the core region of tRNA and is evolutionarily conserved across Eukarya and Archaea (14). Humans express three Trm10 enzymes that are distinct in their cellular localization and pool of tRNA substrates: TRMT10A (the direct homolog of Trm10 from *S. cerevisiae*), TRMT10B and TRMT10C. While Trm10/TRMT10A and TRMT10B are both believed to be nuclear/ cytosolic, TRMT10C is localized to the mitochondria as part of the mitochondrial RNase P complex and is the only member of the Trm10 family which is known to function as part of a larger complex (15). Each human Trm10 enzyme also methylates a unique subset of tRNAs, modifying only G9 (TRMT10A), only A9 (TRMT10B), or exhibiting bifunctional activity to modify either G9 or A9 (TMRT10C) (16-18). Of all the Trm10 enzymes in humans, the biological importance of TRMT10A has

been highlighted the most by studies that link loss of TRMT10A function to diseases related to neurological and endocrine function (19-23).

In 2014, the first structure of any Trm10 protein was solved using x-ray crystallography (24): The structures of Trm10 from *Schizosaccharomyces pombe* and *S. cerevisiae* which are lacking the N-terminal domains (NTD). These structures confirmed that Trm10 contains a typical SPOUT fold and is therefore a member of the SPOUT family of methyltransferases. However, Trm10 was observed as a monomer in the crystal structure which was different from the other known RNA-modifying SPOUT enzymes that require dimerization to be catalytically active. Additionally, the structural information is limited by the absence of the NTD which has been shown to be important for substrate recognition (24). Structures of archaeal Trm10 enzymes from *Sulfolobus acidocaldarius* and *Thermococcus kodakarensis* were solved shortly after (in 2016 and 2018, respectively) (25, 26), which both appeared monomeric as well. As the catalytic site of other SPOUT methyltransferases occurs at the dimer interface, it remains unclear how Trm10 is able to efficiently methylate a tRNA substrate without dimerization. The only other monomeric SPOUT methyltransferase is Sfm1 which is also unique in many other ways, such as acting on a protein substrate and containing a negatively-charged surface surrounding the active site (27).

In 2021, the first structure of a Trm10 enzyme in complex with substrate tRNA was solved using cryo-EM. The structure of the mitochondrial RNase P complex was solved in complex with the pre-tRNA and includes TRMT10C as one of the RNase P subunits responsible for tRNA binding and recognition (28). The structure shows the NTD of TRMT10C wrapping around the tRNA so that the tRNA is encased by the catalytic C-

terminal domain (CTD) and the NTD, with the target A9 base flipped into the active site of the CTD. However, multiple domains of the protein-only RNase P (PRORP) subunit of RNase P also contact the pre-tRNA, including the pentatricopeptide repeat (PPR) and nuclease domains. This is not surprising considering that PPR domain has a known role in RNA recognition and the nuclease domain makes direct contact with the RNA for cleavage of the 5' end. TRMT10C is the only SPOUT methyltransferase known to function as part of a larger complex which may explain why it is also one of the few SPOUT enzymes which is functional with only one protomer present, as PRORP aids in recognition. The other Trm10 enzymes, however, do not have any known binding partners and it remains unclear how they are able to recognize the correct substrate without dimerization or the presence of additional proteins.

Here, we use cryo-EM to gain structural insight into the mechanism of substrate $tRNA^{Gly}$ recognition by the full-length Trm10 protein from *S. cerevisiae*. For this structural analysis, the Trm10-tRNA complex is stabilized by a SAM-analog which becomes covalently attached to tRNA during the modification reaction and thus captures the complex in a relevant state immediately after catalysis. Our studies shed light on the conformation of Trm10 during substrate recognition and allow us to make important comparisons to the mechanism of substrate recognition by TRMT10C. Future work to improve the resolution of the 3D reconstruction will allow us to identify residues critical for substrate recognition by Trm10 and will shed light on how the similar SPOUT domains of TRMT10C and Trm10/TRMT10A are able to methylate bases with differing specificities.

## Materials and Methods

*Trm10 expression and purification*

Full-length wild-type *S. cerevisiae* Trm10 with an N-terminal 6xHis-tag was expressed from the pET-derived plasmid pJEJ12-3 in *E. coli* BL21(DE3)-pLysS grown in lysogeny broth as described previously (14). Briefly, protein expression was induced by addition of 1 mM β-D-1-thiogalactopyranoside at mid-log phase growth ($OD_{600}$ ~0.6) and growth continued at 37˚C for an additional 5 hours. All steps during lysis and initial purification were performed in 20 mM HEPES pH 7.5, 4 mM $MgCl_2$, 1.0 mM BME, 10 mM imidazole, and 5% glycerol. To ensure removal of co-purifying SAM, cells were lysed in this buffer additionally containing 1 M NaCl and 0.5% TritonX-100, and the lysate dialyzed three times in the same buffer but containing 2 M NaCl and no TritonX-100. A final dialysis was used to reduce the NaCl to 0.25 M for protein purification. Protein was purified by sequential $Ni^{2+}$-affinity (HisTrap HP), heparin-affinity (HiPrep Heparin 16/10), and gel filtration (Superdex 75 16/600) chromatographies on an ÄKTApurifier10 system (GE Healthcare). Trm10 was eluted from the gel filtration column in 20 mM Tris (pH 7.5) buffer containing 100 mM NaCl, 1 mM $MgCl_2$, 5 mM BME, and 5% glycerol and flash frozen in liquid nitrogen before storage at -80˚C.

*RNA in vitro transcription and purification*

$tRNA^{Gly\text{-}GCC}$ was *in vitro* transcribed from *BstNI* linearized plasmid DNA using T7 RNA polymerase as previously described (29). Briefly, *in vitro* transcription was performed for 5 hours at 37˚C in 200 mM HEPES-KOH (pH 7.5) buffer containing 28 mM $MgCl_2$, 2 mM spermidine, 40 mM dithiothreitol (DTT), 6 mM each rNTP, and 100 μg/mL DNA template.

At the end of the reaction, following addition of EDTA to clear pyrophosphate-magnesium precipitates and dialysis against 1×Tris–EDTA buffer, RNAs were purified by denaturing polyacrylamide gel electrophoresis (50% urea, 1×Tris–Borate–EDTA buffer). RNA bands were identified by UV shadowing, excised, eluted from the gel by crushing and soaking in 0.3 M sodium acetate, and ethanol precipitated as previously described (29).

*NM6 preparation*

The SAM analog NM6 (5'-(diaminobutyric acid)-N-iodoethyl-5'-deoxyadenosine ammoniumhydrochloride) was prepared as previously described (30) and purified by semi-preparative reverse-phase HPLC. Before use, NM6 was dissolved in protein buffer (20 mM Tris pH 7.5, 100 mM NaCl, 1 mM $MgCl_2$, and 5 mM BME). NM6 was added to cryo-EM samples at a final concentration of 5 μM at the same time as Trm10, prior to incubation at 30˚C. *In situ* activation of NM6 results in a Trm10 cosubstrate that is covalently attached by the enzyme to RNA as shown previously (31, 32).

*Trm10-tRNA complex formation and grid preparation*

Prior to preparation of Trm10-tRNA complex for cryo-EM studies, Trm10 was dialyzed (to remove glycerol) into 20 mM Tris buffer (pH 7.5) containing 100 mM NaCl, 1 mM $MgCl_2$, and 5 mM BME. $tRNA^{Gly\text{-}GCC}$ was incubated at 65˚C for 10 minutes and then slow cooled to room temperature. The Trm10-tRNA complex was formed by mixing components in a 2:1:20 ratio of Trm10:tRNA:NM6 followed by incubation at 30˚C for 30 minutes. The sample was diluted in Trm10 buffer (100 mM NaCl, 1 mM $MgCl_2$, and 5 mM BME) to a Trm10 concentration of 0.125 mg/ml or 0.25 mg/ml. The diluted complex (3 μl) was

applied to freshly glow-discharged grids (0.6/1 300 mesh UltrAuFoil), with blotting for 2 s or 3 s at 100% humidity at room temperature before freezing in liquid ethane using a Vitrobot Mark IV System (Thermo Scientific). Grids were stored in liquid nitrogen until used for data collection.

*Screening grid types and preparation conditions*

In order to identify the optimal conditions that would result in different orientations of the Trm10-tRNA complex while maintaining sample integrity, we tried various grid types and detergents. Each grid was screened at the National Center for CryoEM Access and Training (NCCAT) on a Glacios microscope operating at 200 keV. For each grid type and detergent, the sample concentration (noted as the concentration of Trm10 in the sample) and blot force were optimized. Samples were prepared using graphene grids (0.025 mg/ml, wait time 60 seconds, blot time 4 seconds), graphene oxide grids (0.125 mg/ml, wait time 60 seconds, blot time 5 seconds), UltrAufoil 0.6 grids (0.125 mg/ml, wait time 0 seconds, blot time 3 seconds), and nanowire grids which required the use of a Chameleon instrument (0.625 mg/ml, 100 millisecond wait time). For graphene and nanowire grids, aggregation of the sample was observed. For graphene oxide grids, collection of a small dataset (~2,000 micrographs) on the Glacios microscope yielded poor quality 2D classes which may be indicative of a decrease in the sample quality on the graphene oxide surface. Applying the sample to UltrAufoil 0.6 grids yielded very thin ice and optimal sample quality and distribution. However, the complex was still only visible in a limited number of orientations.

Adding detergents to the sample prior to freezing the grid is another method to capture the complex in a variety of orientations. Detergent (0.2 µl) was added to the sample immediately before applying the sample to the grid. Chapso and FOM detergents were used with a sample concentration of 0.75 mg/ml and 0.5 mg/ml, respectively and each detergent was used at a final concentration of 0.12%. Samples containing detergent were applied to UltrAuFoil 0.6 grids with a blot time of 4 seconds and a blot force of 2. These grids were screened by collecting datasets of ~2,000 micrographs on the Glacios microcrope. The datasets produced blurry 2D classes which indicated that the detergents may be negatively impacting the integrity of the sample. Based on these results, the UltrAuFoil 0.6 grids containing the Trm10-tRNA complex were prioritized for further data collection.

*Cryo-EM image collection, processing and analysis*

Data were collected at NCCAT on a Titan Krios microscope (FEI) operating at 300 keV with a K3 direct electron detector (Gatan). A total of 26,656 micrographs were collected using a defocus range of -0.8 to -2.0 µm at 105,000x magnification with a 0.412 Å/pixel size. The dataset contains micrographs that were collected from tilting the sample 0°, 30°, and 45°. Micrographs were collected as 50 frames with a dose rate of 25.05 $e^-/Å^2/s$ and a total exposure of 2.50 seconds, for an accumulated dose of 62.64 $e^-/Å^2$. Image processing (including motion correction) was conducted in cryoSPARC (33) and contrast transfer function parameters estimated by patch CTF estimation. CryoSPARC's Blob Picker was used for autopicking. A random subset of 1,000 micrographs was selected and particles were 4x-binned before further processing. Incorrectly selected particles

were discarded after reference-free 2D class averaging. An *ab initio* model with C1 symmetry was created and used as a reference map for 3D homogenous refinement. Analysis of the angular distribution of particles comprising the final map indicates that the distribution of orientations was significantly improved by tilting the grids.

*Electromobility shift assay (EMSA)*

$tRNA^{Gly}$ was incubated at 80˚C for 10 minutes and then slow cooled to room temperature. The Trm10-tRNA complexes were formed by combining $tRNA^{Gly}$ (4 μM) with final concentrations of wild-type Trm10 ranging from 0 to 10 μM in a final volume of 10 μL. The reaction was carried out in a 20 mM Tris (pH 7.5) buffer containing 100 mM NaCl, 1 mM $MgCl_2$, 5 mM BME, and 5% glycerol These mixed components were incubated at 30˚C for 30 minutes to form the complex and then run at 4˚C on a 10% nondenaturing polyacrylamide gel. The gel was incubated with a solution containing ethidium bromide for visualization by UV illumination.

*BS3 crosslinking assay*

Trm10 and $tRNA^{Gly}$ were dialyzed into buffer containing 20 mM HEPES pH 7.5, 150 mM NaCl, and 5 mM BME. Bis(sulfosuccinimidyl)suberate (BS3) crosslinking reagent was prepared immediately before use in water to a final concentration of 12.5 mM. BS3 was added in 50-fold molar excess to samples containing 6 μM Trm10 in the presence or absence of $tRNA^{Gly}$ and cofactor SAM. Samples were incubated at room temperature for 30 minutes and quenched with Tris pH 7.5 to a final concentration of 50 mM. Samples

were run on a 9% sodium dodecyl-sulfate polyacrylamide gel electrophoresis gel and visualized by staining with Coomassie blue.

## Results

*Tilted UltrAuFoil grids provide optimal ice thickness and range of orientations for structural analysis using Cryo-EM*

Trm10 from *S. cerevisiae* and $tRNA^{Gly\text{-}GCC}$ were purified as previously described (14, 29). A SAM analog, N-mustard 6 (NM6), that is transferred in its entirety to N1 base position of G9 by the enzymatic action of Trm10, was used to trap the Trm10-tRNA complex in an immediately post-catalytic state (**Fig. 4.1**) (31, 32). This complex was then used to prepare grids and a dataset was collected on a 300 kV Krios microscope (**Fig. 4.2A**).

Previous attempts to solve the structure of this ~60 kDa Trm10-tRNA complex were limited by ice thickness and preferred orientation of the complex. The ice thickness was significantly improved to <50 nm thickness by using 0.6/1 300 mesh UltrAuFoil grids. Several methods were used in efforts to capture the complex in a wider distribution of orientations including the addition of detergents (FOM and Chapso), changing the grid type (Quantifoil, C-flat, graphene, graphene oxide, and UltrAuFoil), and using a Chameleon instrument to prepare samples using nanowire grids. None of these methods were successful in capturing the complex in new orientations while also preserving the integrity of the sample. Therefore, UltrAuFoil grids were tilted at 30° and 45° which allowed us to capture the complex in new orientations (**Fig. 4.2B**).

From working with a small subset of micrographs from this dataset which was 4x binned, a 6-8 Å 3D reconstruction of the Trm10-tRNA complex was generated which

provides useful insight into the Trm10-tRNA interaction (**Fig. 4.3**). The full dataset will be processed further in order to improve the resolution and identify specific interactions between the tRNA nucleotides and Trm10 residues.

*Trm10-tRNA model shows protein binding to tRNA in a 1:1 ratio*

Previous structures of Trm10 solved using x-ray crystallography show a monomeric Trm10 protein which has been used to justify claims that Trm10 is catalytically active as a monomer (24). However, structural studies have never been done on Trm10 bound to substrate tRNA. Our structural studies provide the first 3D reconstruction of the Trm10-tRNA complex to confirm that Trm10 binds to substrate tRNA in a 1:1 ratio (**Fig. 4.4**). As such, our new structure represents the first time a monomeric SPOUT methyltransferase is seen bound to an RNA substrate without the presence of binding partners.

*Trm10 makes specific contacts with different regions of the tRNA*

Trm10 is observed making extensive contacts with the core of the tRNA and the D-arm, with the α1 helix interacting directly with the target nucleotide (**Fig. 4.4**). This confirms the predicted binding surface of Trm10 and positions the SAM-binding pocket close to the site of modification. This alpha helix contains residues K110, R121, and R127 which, when substituted with glutamic acid, cause the enzyme to lose all methylation activity (34). These residues have also been shown to play an important role in distorting the tRNA to make the target nucleotide accessible for modification by Trm10 (see **Chapter 3**).

The anticodon loop and the acceptor stem of tRNA appear to remain largely unbound and highly dynamic during substrate recognition by Trm10. The movement of the anticodon loop and acceptor stem is apparent from 2D classes in which these regions consistently appear blurry (**Fig. 4.2B**). The movement of the anticodon loop and acceptor stem towards and away from the Trm10 protein may indicate transient or dynamic interactions between Trm10 and these regions of the tRNA which, although short-lived, could aid in recognition of the tRNA as a whole.

The previously unresolved NTD of Trm10 which been shown to be essential for catalytic activity is not observed in our current model, indicating that this region of the protein may be highly flexible. Improving upon the resolution through further processing may uncover where the NTD is positioned in relation to the tRNA.

*Trm10 binds to substrate tRNA in a manner similar to TRMT10C*

A comparison between the Trm10-tRNA model and the structure of the Trm10 paralog, TRMT10C, bound to pre-tRNA highlights similarities and differences in the mechanism of substrate recognition (**Fig. 4.5**). The structure of TRMT10C was solved as part of the 257 kDa mitochondrial RNase P complex using cryo-EM. TRMT10C is also observed binding to substrate pre-tRNA as a monomer, albeit aided by its additional protein binding partners. The CTDs of Trm10 and TRMT10C are positioned similarly along the tRNA, contacting the core region and the D-loop (**Fig. 4.5B**). Both Trm10 and TRMT10C have a conserved alpha helix involved in catalysis which is positioned facing the site of modification. As the NTD of Trm10 is not visible in our current model, it is unclear whether

the NTD of Trm10 is positioned similarly to the NTD of TRMT10C to wrap around the tRNA to aid in substrate recognition.

In the mitochondrial RNase P complex, other proteins aid in substrate recognition such as PRORP which is positioned above the pre-tRNA and makes contacts with both the acceptor stem and the T-loop. PRORP also appears to interact with the NTD of TRMT10C which could potentially stabilize this flexible region of the protein in its observed position. Considering that Trm10 does not require any additional binding partners for methylation, it remains unclear how it is able to recognize substrate tRNA without the addition of other protein to interact with the acceptor stem and T-loop of tRNA or to stabilize the NTD in the necessary position.

*Trm10 dimerization observed upon binding to substrate tRNA*

Despite the monomeric nature of Trm10 in our 3D reconstruction and in the majority of the 2D classes, there was a small subset of particles which appear to contain two Trm10 proteins for each tRNA molecule (**Fig. 4.6A**). This is apparent from inspection of the 2D classes in which clear additional density can be observed on the opposite side of the tRNA anticodon loop, corresponding well with the size and shape of Trm10. This density is only clear in one class but can be seen faintly in others, indicating that the interaction between this additional Trm10 protomer and the monomeric Trm10-tRNA complex is short-lived or dynamic. This additional Trm10 molecule was only observed in about 5% of particles from the initial 1000 micrographs processed and we were unable to generate a 3D reconstruction in which the density of this second Trm10 is clearly observed. However, by further processing of the full dataset (~26,000 micrographs), a 3D

reconstruction may be obtained. Even at lower resolution, such a map should be sufficient to accurately dock a second Trm10 protein to shed light on how Trm10 dimerizes and the position of the second Trm10 protomer in relation to the tRNA.

The potential dimerization of Trm10 has been observed through additional assays, such as protein crosslinking, in which Trm10 appears to dimerize only in the presence of substrate tRNA (**Fig. 4.6B**). tRNA dependence in dimerization would explain why Trm10 dimerization was not observed in previous structural studies in which tRNA was absent. Additionally, we have observed multiple bands corresponding to the Trm10-tRNA complex when running EMSAs of tRNA in the presence of increasing amounts of Trm10 (**Fig. 4.6C**). Considering that this higher molecular weight species only appears after increasing the concentration of Trm10, it may correspond with Trm10 binding to tRNA in a 2:1 ratio. Since both monomeric and dimeric Trm10 have been observed bound to substrate tRNA, it remains unclear which conformation of Trm10 is necessary for catalytic activity. However, we speculate that transient interaction of a second Trm10 protein may be required to promote catalysis of modification by the Trm10 protomer already bound to substrate tRNA.

## Discussion

Trm10 is an evolutionarily conserved tRNA methyltransferase that modifies the N1 base position of guanosine at position 9 in the core region of tRNA. In this work, we used cryo-EM to generate a 6-8 Å 3D reconstruction of the yeast Trm10-tRNA complex. In our structure, Trm10 is seen binding to substrate tRNA in a 1:1 ratio. This is the first time a monomeric SPOUT methyltransferase has been observed binding to its substrate in the

absence of any additional binding partners. Although the resolution of our model is currently too low to make conclusions about specific interactions, we observe Trm10 binding to the core region of the tRNA in the expected position with the α1 helix near the target nucleotide. Additionally, a dimeric Trm10 bound-tRNA complex can be seen in a small number of the 2D classes.

The current structure was generated by working with a small subset of micrographs (1,000 of 26,565 collected). The largest improvement to the overall resolution came from decreasing the ice thickness, with the best grid having ice less than 40 nm thick in most regions. Because the majority of particles are still present in a preferred orientation in our small subset of micrographs, we anticipate that processing the full dataset will allow us to capture enough particles in the rarer orientations to significantly improve the resolution. Improvements to the overall resolution through further processing and unbinning the data may allow us to see regions of the protein and tRNA which are currently unresolved, including the NTD of Trm10. The NTD has been shown to play an essential role in substrate recognition (24) which was further confirmed by the structure of TRMT10C as part of the mitochondrial RNase P complex, in which the NTD can be seen wrapping about the tRNA to encase the molecule and make contacts with regions distant from the site of modification (28). A high-resolution structure of the Trm10-tRNA complex will confirm if the NTD of Trm10 behaves in a similar manner and how the NTD is stabilized in position without the presence of additional binding partners.

Further processing and refinement will also allow us to gain insight into specific interactions between Trm10 and tRNA. Although the CTD of Trm10 appears to be positioned similarly in relation to the tRNA as TRMT10C, Trm10 and TRMT10C to not

modify the same pools of tRNA. While TRMT10C is able to modify tRNAs with a G or A at position 9, Trm10 is only able to modify tRNAs with a G at position 9. Therefore, there must be subtle differences between how Trm10 and TRMT10C recognize their target nucleotides which can only be understood through further structural analysis. By solving a high-solution structure of Trm10 bound to substrate tRNA, we will be able to make important comparisons to the TRMT10C structure in order to uncover the molecular basis behind these differences in substrate selectivity.

While our current structure clearly shows one Trm10 protein docked onto the tRNA, it remains unclear how Trm10 is able to compensate for the lack of additional binding partners or an additional protomer. The presence of an additional Trm10 protomer in a small percentage of 2D classes introduces the possibility of a potential role for dimeric Trm10 action on substrate tRNA. Although this interaction appears to be short-lived, it may be an important intermediate during the process of tRNA methylation by Trm10. For example, it's possible that the second Trm10 protomer binds transiently to the Trm10-tRNA complex in order to activate catalysis of this first Trm10 enzyme.

By processing the full dataset, we anticipate that enough particles and resulting 2D classes will be obtained with two proteins to allow for a 3D reconstruction of dimeric Trm10 bound to tRNA. This 3D reconstruction would allow us to visualize the dimer interface to guide further biochemical studies on the role of the Trm10 dimer during catalysis. We anticipate that we will be able to identify residues involved in dimerization that are far from the active site and that we will be able to decrease (or eliminate) catalytic activity by making mutations to Trm10 that disrupt dimerization. This disruption to dimerization could be assessed using crosslinking assays and EMSAs, where the bands

corresponding to a Trm10 dimer in the presence of tRNA would be expected to disappear. These experiments would provide further insight into the role of the Trm10 dimer during catalysis.

In conclusion, our studies show that cryo-EM is a useful tool for structural studies of the Trm10-tRNA complex to gain insight into the mechanism of substrate recognition by Trm10. While our current structure remains limited in resolution, we are confident that a high-resolution structure can be obtained through further processing and refinement of the larger dataset that is now available. These studies will shed light on a unique mechanism of substrate recognition by Trm10, a highly conserved atypical SPOUT methyltransferase.

**Acknowledgements**

We thank Drs. Ed Eng, Eugene Chua, Aaron Owji, and Misha Kopylov from the New York Structural Biology Center for their help with cryo-EM sample preparation and data processing. Some of this work was performed at NCCAT and the Simons Electron Microscopy Center located at the New York Structural Biology Center, supported by the NIH Common Fund Transformative High Resolution Cryo-Electron Microscopy program (U24 GM129539), and by grants from the Simons Foundation (SF349247) and NY State Assembly. We also thank Drs. Srihari Koripella and Ricardo Guerrero-Ferreira from Emory University's Robert P. Apkarian Integrated Electron Microscopy Core for their guidance with sample preparation and usage of the facility's electron microscopes. This research was supported by the National Institute of General Medical Sciences award R01 GM130135 (to G.L.C.) and the NSF GRFP award 1937971 (to S. E. S.). Research

reported in this publication was also supported by the Office of the Director, NIH, under award number S10 OD023582.

## Figures

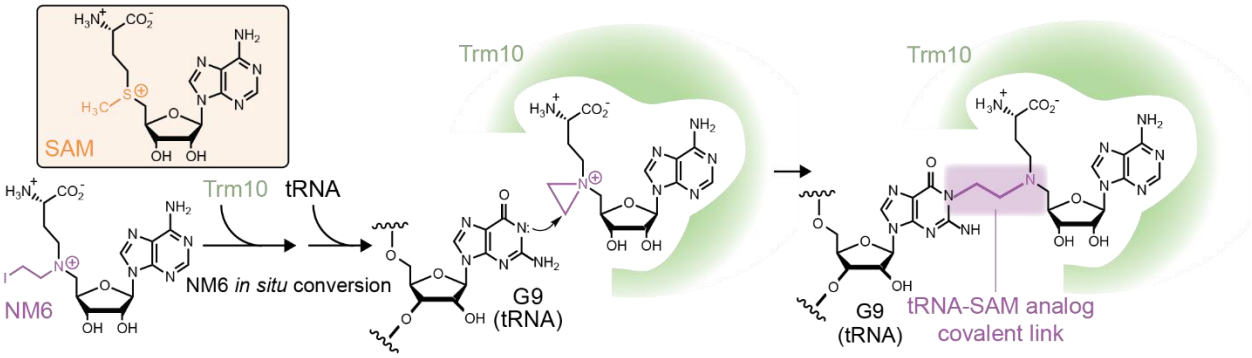


**Figure 4.1 Stabilization of the Trm10-tRNA complex using the SAM analog NM6**. N-mustard 6 (NM6; bottom left) is an analog of S-adenosyl-L-methionine (SAM; top left box) that Trm10 can use as a cosubstrate for modification of tRNA. In this enzymatic reaction, NM6 becomes covalently attached to the tRNA at the N1 base position of G9. The Trm10-tRNA complex is thus stabilized in a state immediately following catalysis by virtue of Trm10's affinity for both tRNA subunit and the cosubstrate analog covalently attached to G9.

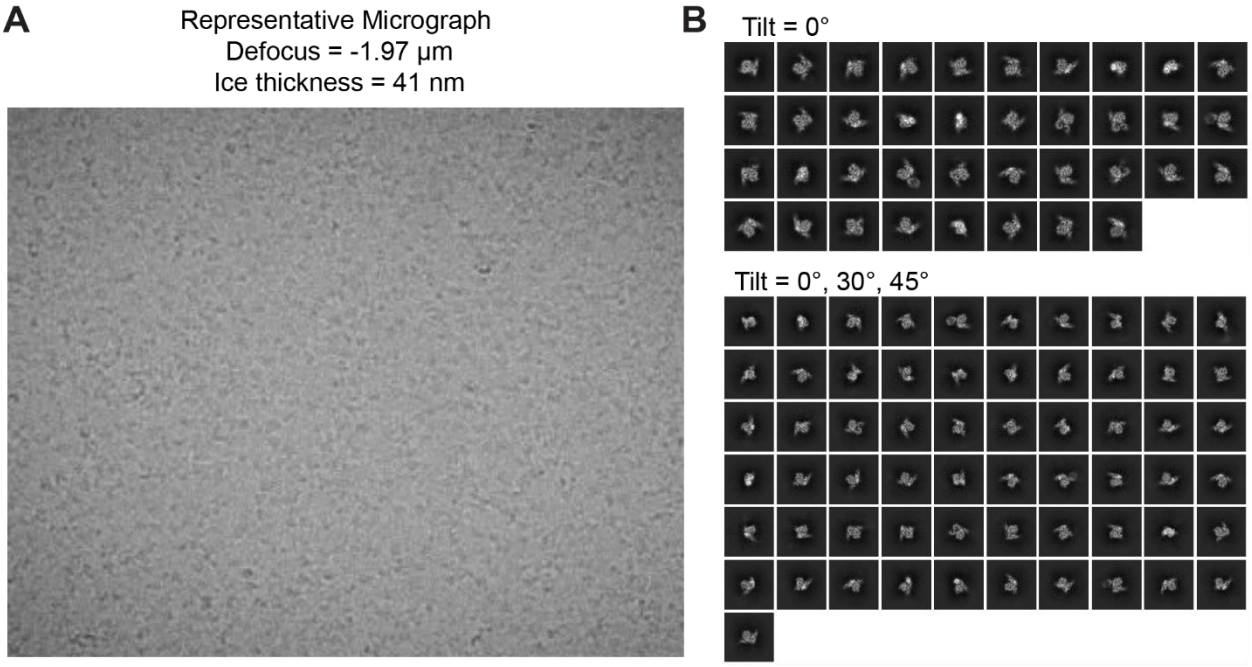


**Figure 4.2 Cryo-EM data collection and 2D classes.** ***A***, Representative micrograph from the cryo-EM dataset, at a defocus of -1.97 µm. ***B***, Two-dimensional class averages of UltrAuFoil grids without any tilt (*above*) and with tilting (*below*) which shows additional orientations of the Trm10-tRNA complex.

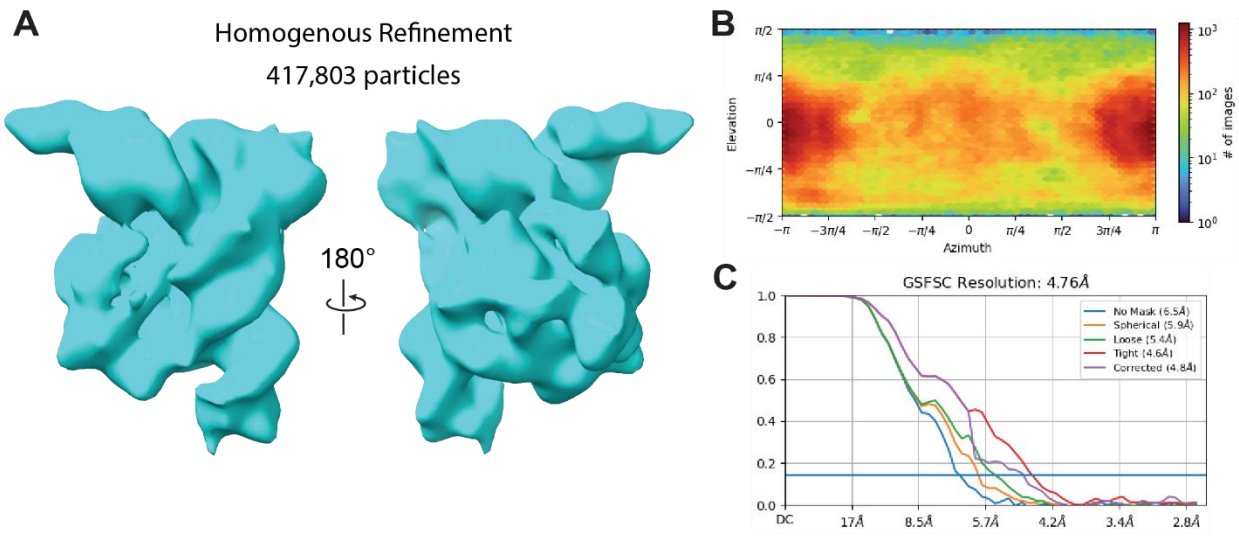


**Figure 4.3. Trm10-tRNA 3D reconstruction.** ***A,*** A 3D reconstruction using the homogenous refinement feature on cryoSPARC on a small 4x binned dataset containing 1,000 micrographs collected with 0˚, 30˚, and 45˚ tilt. ***B***, Angular distribution plots of particles contributing to the 3D reconstruction. Although the dataset still contains a preferred orientation, tilting the grids successfully captures Trm10-tRNA in a broader range of orientations. ***C***, The Gold Standard Fourier Shell Correlation from the homogenous refinement job, calculated using unfiltered half maps. Although the overall resolution is shown as 4.76 Å, the 3D reconstruction appears to be closer to 6-8 Å.

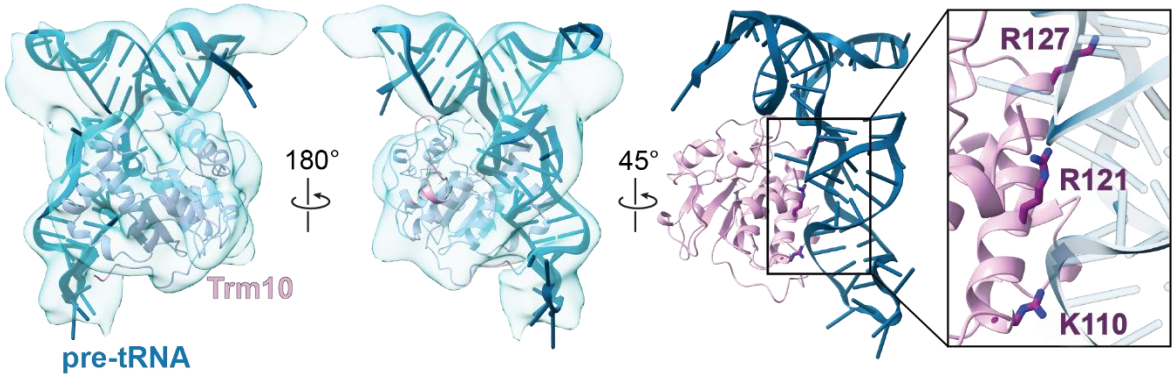


**Figure 4.4 Structure of Trm10 and tRNA modeled into 3D reconstruction.** The structures of *S. cerevisiae* Trm10 (PDB: 4JWJ) and pre-tRNA from the mitochondrial RNAse P structure (PDB: 7ONU) were modeled into the 3D reconstruction of the Trm10-tRNA complex using the fitmap feature in ChimeraX (*left*). The main alpha helices along the binding surface of Trm10 are clearly visible in the 3D reconstruction and align well with the solved structure. The α1 helix is positioned facing the site of modification with residues K110, K121, and R127 interacting directly with tRNA (*right*).

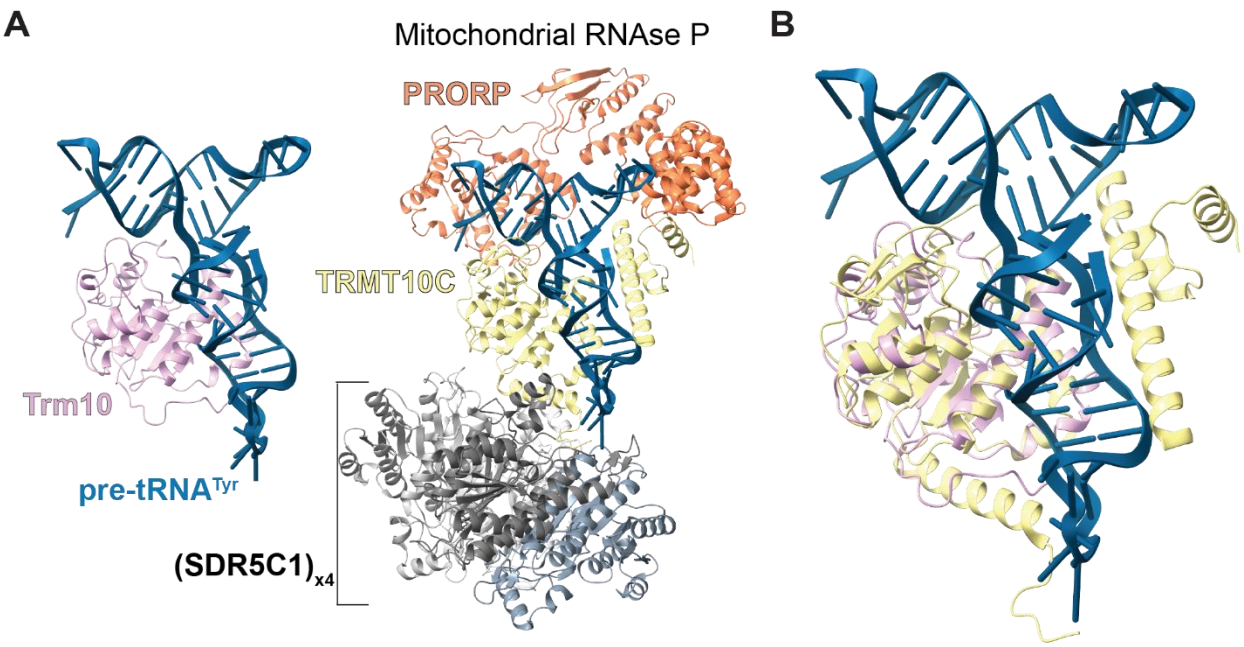


**Figure 4.5 Position of *S. cerevisiae* Trm10 and TRMT10C in relation to tRNA. *A***, The position of *S. cerevisiae* Trm10 (*pink*) bound to tRNA (*teal*) from the 3D reconstruction is shown next to the solved structure of TRMT10C (*yellow*) bound to pre-tRNA$^{Tyr}$ (*teal*) as part of the mitochondrial RNAse P complex. ***B***, The CTD of Trm10 and TRMT10C are aligned to show similarities in their positioning with respect to tRNA.

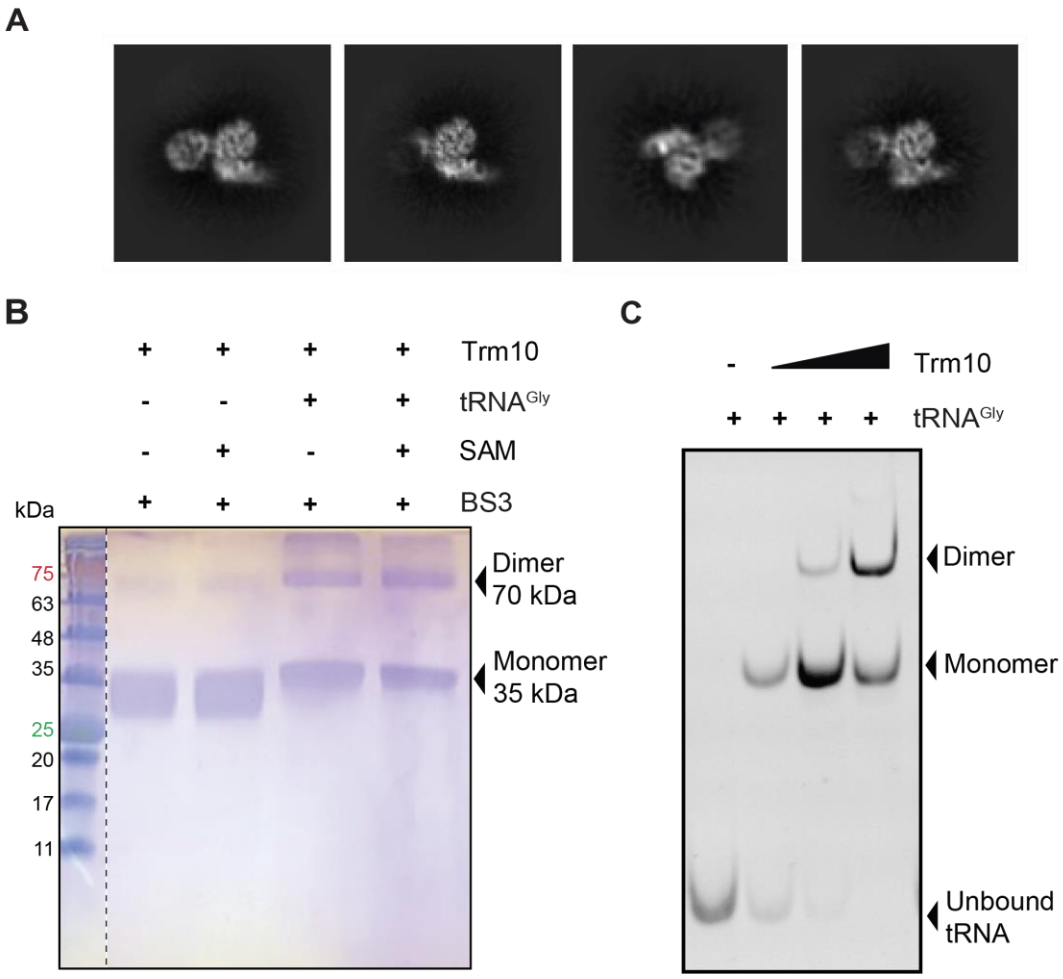


**Figure 4.6 Trm10 dimerization upon binding to substrate tRNA.** ***A***, Several 2D classes show a second Trm10 protomer binding to the Trm10-tRNA complex. ***B***, Trm10 dimerization upon binding to substrate tRNA was observed by adding a crosslinking reagent (BS3) to the reaction. Samples were run on a 9% sodium dodecyl-sulfate polyacrylamide gel electrophoresis gel and visualized by staining with Coomassie blue. ***C***, Multiple bands are observed on an EMSA using substrate tRNA and increasing amounts of Trm10. Samples were run on a 10% nondenaturing polyacrylamide gel and the gel was incubated with ethidium bromide for visualization by UV illumination. This second higher molecular weight band corresponding to a Trm10-tRNA species is consistent with a Trm10 dimer bound to tRNA.

## References


1. Motorin, Y., andHelm, M. (2022) RNA nucleotide methylation: 2021 update Wiley Interdiscip Rev RNA **13**, e1691 10.1002/wrna.1691

2. Hashimoto, H., Vertino, P. M., andCheng, X. (2010) Molecular coupling of DNA methylation and histone methylation Epigenomics **2**, 657-669 10.2217/epi.10.44

3. Phizicky, E. M., andHopper, A. K. (2015) tRNA processing, modification, and subcellular dynamics: past, present, and future RNA **21**, 483-485 10.1261/rna.049932.115

4. Zhang, X., Walker, R. C., Phizicky, E. M., andMathews, D. H. (2014) Influence of Sequence and Covalent Modifications on Yeast tRNA Dynamics J Chem Theory Comput **10**, 3473-3483 10.1021/ct500107y

5. Anantharaman, V., Koonin, E. V., andAravind, L. (2002) SPOUT: a class of methyltransferases that includes spoU and trmD RNA methylase superfamilies, and novel superfamilies of predicted prokaryotic RNA methylases J Mol Microbiol Biotechnol **4**, 71-75, https://www.ncbi.nlm.nih.gov/pubmed/11763972

6. Ito, T., Masuda, I., Yoshida, K., Goto-Ito, S., Sekine, S., Suh, S. W. *et al.* (2015) Structural basis for methyl-donor-dependent and sequence-specific binding to tRNA substrates by knotted methyltransferase TrmD Proc Natl Acad Sci U S A **112**, E4197-4205 10.1073/pnas.1422981112

7. Nureki, O., Shirouzu, M., Hashimoto, K., Ishitani, R., Terada, T., Tamakoshi, M. *et al.* (2002) An enzyme with a deep trefoil knot for the active-site architecture Acta Crystallogr D Biol Crystallogr **58**, 1129-1137 10.1107/s0907444902006601

8. Nureki, O., Watanabe, K., Fukai, S., Ishii, R., Endo, Y., Hori, H. *et al.* (2004) Deep knot structure for construction of active site and cofactor binding site of tRNA modification enzyme Structure **12**, 593-602 10.1016/j.str.2004.03.003

9. Tkaczuk, K. L., Dunin-Horkawicz, S., Purta, E., andBujnicki, J. M. (2007) Structural and evolutionary bioinformatics of the SPOUT superfamily of methyltransferases BMC Bioinformatics **8**, 73 10.1186/1471-2105-8-73

10. Elkins, P. A., Watts, J. M., Zalacain, M., van Thiel, A., Vitazka, P. R., Redlak, M. *et al.* (2003) Insights into catalysis by a knotted TrmD tRNA methyltransferase J Mol Biol **333**, 931-949 10.1016/j.jmb.2003.09.011

11. Michel, G., Sauve, V., Larocque, R., Li, Y., Matte, A., andCygler, M. (2002) The structure of the RlmB 23S rRNA methyltransferase reveals a new methyltransferase fold with a unique knot Structure **10**, 1303-1315 10.1016/s0969-2126(02)00852-3

12. Lim, K., Zhang, H., Tempczyk, A., Krajewski, W., Bonander, N., Toedt, J. *et al.* (2003) Structure of the YibK methyltransferase from Haemophilus influenzae (HI0766): a cofactor bound at a site formed by a knot Proteins **51**, 56-67 10.1002/prot.10323

13. Ahn, H. J., Kim, H. W., Yoon, H. J., Lee, B. I., Suh, S. W., andYang, J. K. (2003) Crystal structure of tRNA(m1G37)methyltransferase: insights into tRNA recognition EMBO J **22**, 2593-2603 10.1093/emboj/cdg269

14. Jackman, J. E., Montange, R. K., Malik, H. S., andPhizicky, E. M. (2003) Identification of the yeast gene encoding the tRNA m1G methyltransferase responsible for modification at position 9 RNA **9**, 574-585 10.1261/rna.5070303

15. Vilardo, E., Nachbagauer, C., Buzet, A., Taschner, A., Holzmann, J., andRossmanith, W. (2012) A subcomplex of human mitochondrial RNase P is a bifunctional methyltransferase--extensive moonlighting in mitochondrial tRNA biogenesis Nucleic Acids Res **40**, 11583-11593 10.1093/nar/gks910

16. Howell, N. W., Jora, M., Jepson, B. F., Limbach, P. A., andJackman, J. E. (2019) Distinct substrate specificities of the human tRNA methyltransferases TRMT10A and TRMT10B RNA **25**, 1366-1376 10.1261/rna.072090.119

17. Swinehart, W. E., Henderson, J. C., andJackman, J. E. (2013) Unexpected expansion of tRNA substrate recognition by the yeast m1G9 methyltransferase Trm10 RNA **19**, 1137-1146 10.1261/rna.039651.113

18. Vilardo, E., Amman, F., Toth, U., Kotter, A., Helm, M., andRossmanith, W. (2020) Functional characterization of the human tRNA methyltransferases TRMT10A and TRMT10B Nucleic Acids Res **48**, 6157-6169 10.1093/nar/gkaa353

19. Igoillo-Esteve, M., Genin, A., Lambert, N., Desir, J., Pirson, I., Abdulkarim, B. *et al.* (2013) tRNA methyltransferase homolog gene TRMT10A mutation in young onset diabetes and primary microcephaly in humans PLoS Genet **9**, e1003888 10.1371/journal.pgen.1003888

20. Gillis, D., Krishnamohan, A., Yaacov, B., Shaag, A., Jackman, J. E., andElpeleg, O. (2014) TRMT10A dysfunction is associated with abnormalities in glucose homeostasis, short stature and microcephaly J Med Genet **51**, 581-586 10.1136/jmedgenet-2014-102282

21. Yew, T. W., McCreight, L., Colclough, K., Ellard, S., andPearson, E. R. (2016) tRNA methyltransferase homologue gene TRMT10A mutation in young adult-onset diabetes with intellectual disability, microcephaly and epilepsy Diabet Med **33**, e21-25 10.1111/dme.13024

22. Zung, A., Kori, M., Burundukov, E., Ben-Yosef, T., Tatoor, Y., andGranot, E. (2015) Homozygous deletion of TRMT10A as part of a contiguous gene deletion in a syndrome of failure to thrive, delayed puberty, intellectual disability and diabetes mellitus Am J Med Genet A **167A**, 3167-3173 10.1002/ajmg.a.37341

23. Narayanan, M., Ramsey, K., Grebe, T., Schrauwen, I., Szelinger, S., Huentelman, M. *et al.* (2015) Case Report: Compound heterozygous nonsense mutations in TRMT10A are associated with microcephaly, delayed development, and periventricular white matter hyperintensities F1000Res **4**, 912 10.12688/f1000research.7106.1

24. Shao, Z., Yan, W., Peng, J., Zuo, X., Zou, Y., Li, F. *et al.* (2014) Crystal structure of tRNA m1G9 methyltransferase Trm10: insight into the catalytic mechanism and recognition of tRNA substrate Nucleic Acids Res **42**, 509-525 10.1093/nar/gkt869

25. Singh, R. K., Feller, A., Roovers, M., Van Elder, D., Wauters, L., Droogmans, L. *et al.* (2018) Structural and biochemical analysis of the dual-specificity Trm10 enzyme from Thermococcus kodakaraensis prompts reconsideration of its catalytic mechanism RNA **24**, 1080-1092 10.1261/rna.064345.117

26. Van Laer, B., Roovers, M., Wauters, L., Kasprzak, J. M., Dyzma, M., Deyaert, E. *et al.* (2016) Structural and functional insights into tRNA binding and adenosine N1-methylation by an archaeal Trm10 homologue Nucleic Acids Res **44**, 940-953 10.1093/nar/gkv1369

27. Lv, F., Zhang, T., Zhou, Z., Gao, S., Wong, C. C., Zhou, J. Q. *et al.* (2015) Structural basis for Sfm1 functioning as a protein arginine methyltransferase Cell Discov **1**, 15037 10.1038/celldisc.2015.37

28. Bhatta, A., Dienemann, C., Cramer, P., andHillen, H. S. (2021) Structural basis of RNA processing by human mitochondrial RNase P Nat Struct Mol Biol **28**, 713-723 10.1038/s41594-021-00637-y

29. Linpinsel, J. L., andConn, G. L. (2012) General protocols for preparation of plasmid DNA template, RNA in vitro transcription, and RNA purification by denaturing PAGE Methods Mol Biol **941**, 43-58 10.1007/978-1-62703-113-4_4

30. Weller, R. L., andRajski, S. R. (2006) Design, synthesis, and preliminary biological evaluation of a DNA methyltransferase-directed alkylating agent Chembiochem **7**, 243-245 10.1002/cbic.200500362

31. Stanevich, V., Jiang, L., Satyshur, K. A., Li, Y., Jeffrey, P. D., Li, Z. *et al.* (2011) The structural basis for tight control of PP2A methylation and function by LCMT-1 Mol Cell **41**, 331-342 10.1016/j.molcel.2010.12.030

32. Laughlin, Z. T., Nandi, S., Dey, D., Zelinskaya, N., Witek, M. A., Srinivas, P. *et al.* (2022) 50S subunit recognition and modification by the Mycobacterium tuberculosis ribosomal RNA methyltransferase TlyA Proc Natl Acad Sci U S A **119**, e2120352119 10.1073/pnas.2120352119

33. Punjani, A., Rubinstein, J. L., Fleet, D. J., andBrubaker, M. A. (2017) cryoSPARC: algorithms for rapid unsupervised cryo-EM structure determination Nat Methods **14**, 290-296 10.1038/nmeth.4169

34. Strassler, S. E., Bowles, I. E., Krishnamohan, A., Kim, H., Kuiper, E. G., Comstock, L. R. *et al.* (2023) tRNA m (1) G9 modification depends on substrate-specific RNA conformational changes induced by the methyltransferase Trm10 bioRxiv 10.1101/2023.02.01.526536

# CHAPTER FIVE:

Discussion

Trm10 is an evolutionarily conserved tRNA methyltransferase that modifies a subset of tRNA molecules on the 9$^{th}$ nucleotide in the core region (1). Although the substrates for Trm10 are well defined, prior to this work no common features had been identified for this pool of tRNAs that would explain how Trm10 is able to discriminate between substrate and nonsubstrate (2). Additionally, the molecular basis for substrate recognition by Trm10 had not been characterized. In this thesis, I used selective 2′-hydroxyl acylation analyzed by primer extension (SHAPE) and cryogenic electron microscopy (cryo-EM) to expand our understanding of tRNA substrate recognition and modification by Trm10.

In **Chapter 3**, I showed that Trm10 recognizes differences in tRNA structural plasticity which aid in substrate recognition. By using SHAPE RNA structure probing, I showed that there are inherent differences in the flexibility of substrate and nonsubstrate tRNAs. When Trm10 binds to a substrate, it must be able to induce a specific conformational change in the tRNA that would allow for methylation. These changes are not seen upon Trm10 binding to nonsubstrate tRNAs. Specifically, Trm10 induces a conformational change that results in increased flexibility in the core region and the D-loop around the site of modification to increase accessibility of the target nucleotide, as well as decreased flexibility in the anticodon loop, indicative of a more global conformational change to the tRNA or specific interactions with the NTD of Trm10. These conformational changes are also not observed for substrate tRNA in the presence of the tRNA-binding competent but catalytically inactive Trm10-KRR variant, confirming that they are important for methylation as opposed to binding. These studies highlight a novel mechanism of substrate recognition which may be employed by other tRNA-modifying enzymes which must discriminate between structurally similar tRNA species.

In **Chapter 4**, I used cryo-EM to solve the structure of Trm10 bound to substrate tRNA. This structure shows Trm10 binding to tRNA in a 1:1 ratio and is the first time a monomeric SPOUT methyltransferase has been observed bound to substrate in the absence of any additional proteins. Although the dataset needs to be processed and refined further to achieve the highest resolution possible and to see specific interactions between Trm10 and the tRNA, we can see Trm10 binding to the core region of the tRNA in the expected position with the helix containing residues involved in catalysis positioned near the target nucleotide. Additionally, a dimeric Trm10 protein can be seen in a small percentage of the 2D classes which may be an important intermediate for methylation by Trm10 (see below).

Collectively, these studies show that Trm10 binds to tRNA in a 1:1 ratio to induce specific conformational changes to the tRNA which are necessary for methylation. This research sheds light on a novel mechanism of tRNA substrate recognition and modification by a monomeric SPOUT methyltransferase. However, this research also raises several important new questions about specific interactions between Trm10 and tRNA, and between the Trm10-tRNA complex and a second Trm10 protomer, and the role these may play in Trm10's mechanism of action. There are also many unanswered questions about the molecular basis of substrate recognition by Trm10 and the role of the NTD which can only be answered by improving the resolution of the structure through further processing. Furthermore, Trm10 enzymes from different organisms and the three Trm10 paralogs in humans act on tRNA with differing substrate specificities despite similarities between the CTD and a common site of modification. Additional structures of

Trm10 enzymes in complex with substrate tRNAs are necessary to tease apart the molecular basis for these differences in substrate recognition.

**Validate the role of the NTD of Trm10**

The NTD of Trm10 is a highly flexible region which is enriched with positive residues that aid in tRNA binding (3). The importance of the NTD is highlighted by the drastic reduction in catalytic activity in a truncated Trm10 (Δ1-83) (3). However, no studies had been done to identify why the catalytic CTD of Trm10 was not fully functional on its own or how the NTD of Trm10 interacts with tRNA to aid in catalysis. Current assumptions about the role of the NTD come from the structure of the Trm10 paralog, TRMT10C, in complex with pre-tRNA as part of the mitochondrial RNase P complex (4). In this structure, the NTD of TRMT10C wraps around the anticodon loop of the tRNA to make contacts with distant regions of the T-loop of the tRNA. Although both the NTD of TRMT10C and the NTD of Trm10 are enriched with positive residues that may aid in tRNA binding, there is very little sequence conservation between the two NTDs. Additionally, these two paralogs do not act on the same substrates (2, 5).

Interestingly, our SHAPE RNA structure probing identified the anticodon loop as a region of the tRNA which changes conformation during substrate recognition. This region of the tRNA becomes less flexible when bound to Trm10 and this change in flexibility appears to be essential for catalysis. Paired with our knowledge of how the NTD interacts with the anticodon loop of tRNA in TRMT10C and the essential role of the NTD during substrate recognition, we speculated that the NTD of Trm10 may interact with the anticodon loop in a manner similar to the NTD of TRMT10C. This interaction between the

anticodon loop and the NTD which distorts the tRNA would help to explain why the NTD is essential for methylation. In the absence of the NTD, this distortion would not occur and the CTD of Trm10 would not recognize substrate tRNA for modification.

The most effective way to test this hypothesis regarding the interactions between the NTD and the anticodon loop will be to generate a high-resolution structure of Trm10 bound to substrate tRNA as the highly flexible NTD cannot be resolved in our current low-resolution structure. Through further processing of the larger dataset, we hope to be able to generate such a high-resolution structure that can then be used to guide mutagenesis studies to probe the role of specific interactions between the NTD and tRNA. We would be able to substitute residues that appear to be interacting with the anticodon loop and determine if this impacts distortions to this region of the tRNA and/ or catalytic activity. These studies would shed light on the role of both the NTD of Trm10 and the distortions to the anticodon loop of tRNA during substrate recognition, and if the two events are indeed related.

**Define the relevance of a Trm10 dimer interaction during substrate recognition**

Trm10 is a member of the SPOUT methyltransferase family of enzymes which are characterized by a trefoil knot in the catalytic domain adjacent to the SAM-binding pocket (6). Other than the Trm10 enzymes, all other RNA-modifying SPOUT methyltransferases are catalytically active as dimers with the active site located at the dimer interface (6). Although only one TRMT10C protomer binds to substrate tRNA, TRMT10C requires the presence of an additional binding partner, SDR5C1, in order to be catalytically active (4). Therefore, it is unclear how other Trm10 enzymes, including yeast Trm10 and human

TRMT10A and TRMT10B, are able to recognize and methylate their correct tRNA substrates in the absence of dimerization or any other known binding partner(s).

Our 3D reconstruction of Trm10 bound to tRNA generated through cryo-EM clearly shows one Trm10 protein bound to one tRNA. However, in some 2D classes, two Trm10 proteins can be seen binding to one tRNA molecule (**Figure 5.2A**). A Trm10 dimer was also seen in a crosslinking assay in which a higher molecular weight protein species appeared on a gel in the presence of tRNA and a crosslinking reagent (see **Chapter 4**). Furthermore, an additional band was seen on our EMSA when staining for tRNA with increasing amounts of Trm10, corresponding with a higher molecular weight Trm10-tRNA species. A mechanism which involves tRNA-dependent Trm10 dimerization would help to explain both of these observations.

Considering that two Trm10 proteins can only be seen in about 5% of cryo-EM particles and the second protein appears blurry in many of these classes, we can infer that binding of a second Trm10 protein is dynamic or that this protomer is not trapped as part of the complex by the SAM-analog NM6. NM6 becomes covalently bound to tRNA during methylation to stabilize the modified tRNA-enzyme complex but since only one bound cofactor (NM6) of a dimeric Trm10 would be active during methylation, only one Trm10 protein would be trapped by the SAM-analog during catalysis even if two Trm10 proteins are involved. The second Trm10 protein would remain free to dissociate following methyl transfer and only bind transiently. However, the fact that this interaction is only seen in a small percentage of particles does not mean that it does not play some role during catalysis. The presence of a second Trm10 protein in some classes presents the possibility that this second protomer plays an important role in substrate recognition and/

or methylation. This additional protomer may bind to the Trm10-tRNA complex transiently to initiate methylation which is performed by the first protomer (**Figure 5.2B**). This would mean that Trm10's mechanism of catalysis may be more similar to other dimeric SPOUT methyltransferases than we previously thought. However, Trm10 would be the first SPOUT methyltransferase to dimerize in a transient, substrate-dependent manner.

In order to probe the role of this second Trm10 protomer, it will be important to generate a 3D reconstruction of dimeric Trm10 bound to tRNA which may be possible once we process the full cryo-EM dataset, and therefore are able to see more particles in this dimeric state. A structure of dimeric Trm10 bound to tRNA would allow identification of the dimeric interface and residues that are involved in binding of the two proteins. We can then pinpoint which residue substitutions would allow us to disrupt the dimer interface without affecting interactions between Trm10 and tRNA. We would be able to confirm a disruption to the dimer interface using our crosslinking assay and EMSA in which higher molecular weight bands corresponding to tRNA-dependent dimerization of Trm10 should absent. Activity assays using this Trm10 mutant which is unable to dimerize would shed light on the role of Trm10 dimerization on methylation activity.

**Characterize the molecular basis for differences in substrate selectivity of *S. cerevisiae* Trm10 and other family members**

Many of our speculations about the structure of Trm10 from *S. cerevisiae* are based on the structure of TRMT10C as part of the mitochondrial RNAse P complex (4). Considering how well the CTD of Trm10 and TRMT10C align in relation to tRNA, it is reasonable to make assumptions about some common mechanisms of substrate recognition. However,

despite methylating the same position on tRNA and similarities between the structures of the CTDs, Trm10 and TRMT10C do not modify the same pool of substrates (2, 5). Additionally, Trm10 has a narrower substrate specificity than TRMT10C, modifying only tRNAs containing G9 whereas TRMT10C can modify tRNAs containing A9 or G9. Therefore, there must be subtle differences between the catalytic domains and how these domains interact with the target nucleotide that affect substrate selectivity.

Among other enzymes in the Trm10 family, substrate specificities analogous to those of Trm10 and TRMT10C have been identified. For example, TRMT10A in humans is the direct homolog of Trm10 from *S. cerevisiae* and can also only modify G9-containing tRNAs (7). Trm10 from *Thermococcus kodakarensis* is able to modify G9- and A9-containing tRNAs in a manner similar to TRMT10C (8). There is also a subset of Trm10 enzymes which can only modify tRNAs containing an A at position 9. This includes human TRMT10B and Trm10 from *Sulfolobus acidocaldarius* (7, 9). The molecular basis for these differences in target nucleotide specificity remains poorly understood despite extensive biochemical characterization and availability of multiple structures of different members of the Trm10 family.

Similar differences in substrate specificity have been seen among other SPOUT methyltransferases homologs. For example, the tRNA methyltransferase TrmJ modifies the 2’-OH of nucleotide 32 in the anticodon loop and, despite similar catalytic domains, homologs from different species have varying nucleotide specificity. TrmJ from *Escherichia coli* modifies the ribose of any base at position 32 whereas TrmJ from *S. acidocaldarius* is only able to modify a cytidine at the same position (10). The broad specificity of *E. coli* TrmJ has been attributed to slight differences in residues in the SAM-

binding pockets which force SAM into a “super-bent” position. This slight difference in the conformation of SAM allows for more space in the binding pocket to accommodate a larger variety of nucleotides. Therefore, it’s possible that taking a closer look at differences in the SAM-binding pocket of Trm10 enzymes may help us to understand the broad range of substrate specificities seen within the Trm10 family.

By solving a high-resolution structure of Trm10 bound to tRNA, we will be able to compare features of the CTDs of Trm10 with the structure of TRMT10C and other Trm10 enzymes. For example, we will be able to make conclusions about differences between the SAM-binding pockets, the orientation of catalytic residues, and how the target nucleotides fit into the active site. This information will help us to design Trm10 mutants to further understand which molecular interactions are responsible for the differences in substrate specificities. Unfortunately, the current structure of TRMT10C does not contain a SAM molecule in the SAM-binding pocket and the other structure of Trm10 enzymes do not include substrate tRNA. Therefore, additional structures are needed of Trm10 enzymes in complex with both substrate tRNA and SAM to assess differences in how SAM is bent or differences in positioning of target nucleotides.

**Final Remarks**

Prior to starting this work, there was very little known about which tRNA feature(s) are recognized by Trm10 or what the Trm10-tRNA complex looks like during substrate recognition. My work has thus contributed to our overall understanding of the role of tRNA flexibility in substrate recognition by Trm10. I also solved the first structure of Trm10 in complex with tRNA to gain critical insight into the conformation of Trm10 during

methylation and how it is oriented towards the tRNA. My thesis work has thus filled some critical gaps in our understanding of substrate recognition by Trm10 but also opens the door for future studies to further understand the molecular basis for this mechanism.

My findings on RNA conformational changes necessary for methylation by Trm10 shed light on a novel component to substrate recognition and can explain why no apparent trends in sequences have been identified to date among substrate or nonsubstrate tRNAs. Very different RNA sequences can result in similar inherent flexibilities in the tRNA structure and/ or capacity to be appropriately reconfigured upon Trm10 binding, as is observed for substrates $tRNA^{Gly\text{-}GCC}$ and $tRNA^{Trp\text{-}CCA}$. Therefore, consideration of RNA flexibility and deformability as potential recognition elements for a specific RNA-modifying enzyme may be critical in fully defining the recognition process. This may be especially true for other RNA-modifying enzymes which modify an inaccessible region or other tRNA-modifying enzymes which need to be able to discriminate between structurally similar tRNA species.

## Figures

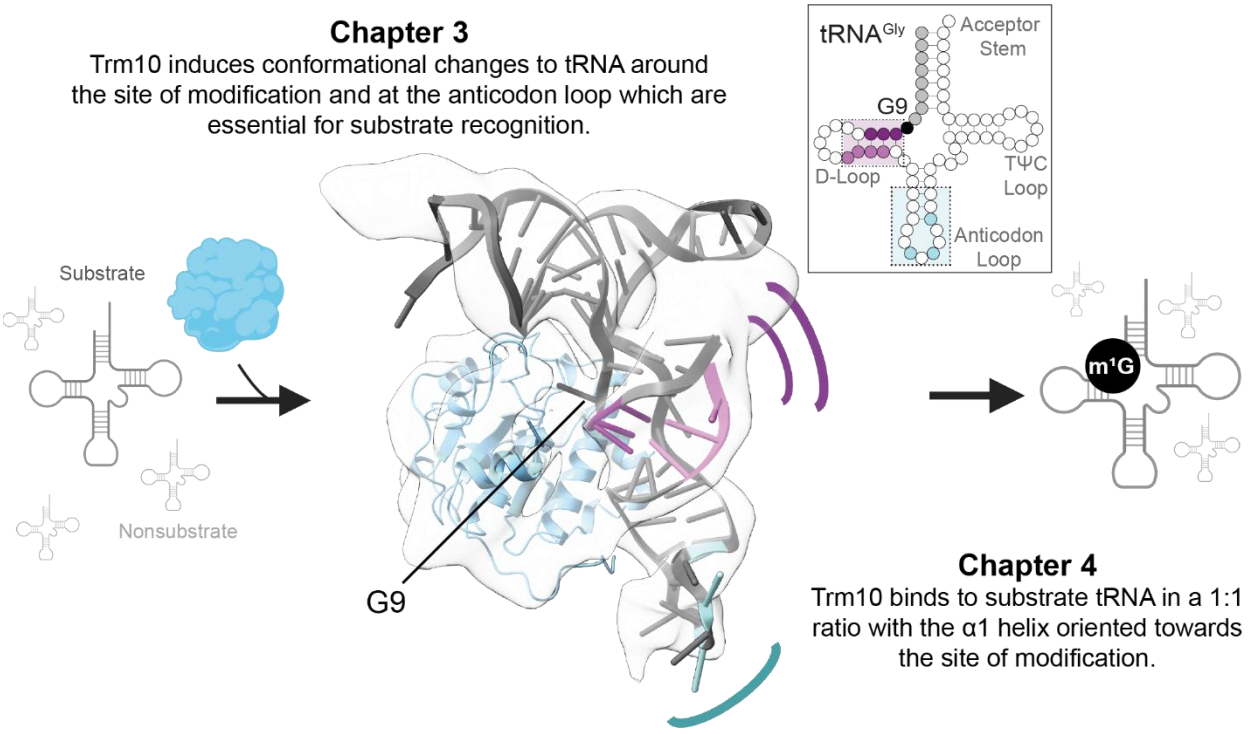


**Figure 5.1 Overview of main research findings.** As discussed in extensive detail in the preceding chapters, monomeric Trm10 (*blue*) binds to substrate tRNA (*dark gray*) to induce conformational changes that are necessary for substrate recognition. These conformational changes include increased flexibility (*purple*) near the site of modification and decreased flexibility (*cyan*) to the anticodon loop. These statements summarize the main takeaways from the two results chapters of this work (**Chapters 3-4**).

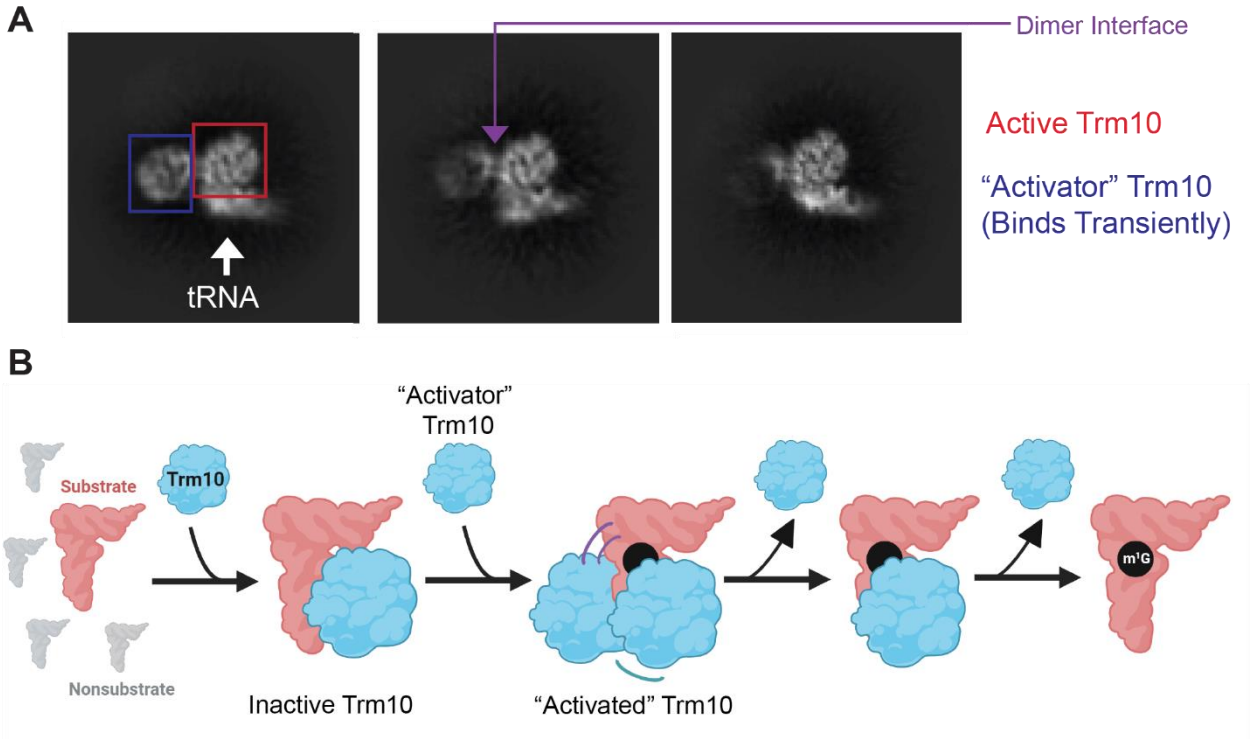


**Figure 5.2 Trm10 dimer has a possible role in initiating catalysis**. ***A***, A subset of 2D classes of cryo-EM particles show an additional Trm10 protomer which binds to the Trm10-tRNA complex transiently or dynamically, as evident from the blurry appearance and absence in most 2D classes. Considering that most SPOUT methyltransferases require dimerization in order to be catalytically active, it's possible the that second Trm10 protomer acts as an "activator" to activate the first Trm10 protomer which is responsible for methylating the tRNA. ***B***, A possible mechanism for Trm10 activation is shown in which dimerization of Trm10 with a Trm10 "activator" initiates catalysis.

## References


1. Jackman, J. E., Montange, R. K., Malik, H. S., andPhizicky, E. M. (2003) Identification of the yeast gene encoding the tRNA m1G methyltransferase responsible for modification at position 9 RNA **9**, 574-585 10.1261/rna.5070303
2. Swinehart, W. E., Henderson, J. C., andJackman, J. E. (2013) Unexpected expansion of tRNA substrate recognition by the yeast m1G9 methyltransferase Trm10 RNA **19**, 1137-1146 10.1261/rna.039651.113
3. Shao, Z., Yan, W., Peng, J., Zuo, X., Zou, Y., Li, F. *et al.* (2014) Crystal structure of tRNA m1G9 methyltransferase Trm10: insight into the catalytic mechanism and recognition of tRNA substrate Nucleic Acids Res **42**, 509-525 10.1093/nar/gkt869
4. Bhatta, A., Dienemann, C., Cramer, P., andHillen, H. S. (2021) Structural basis of RNA processing by human mitochondrial RNase P Nat Struct Mol Biol **28**, 713-723 10.1038/s41594-021-00637-y
5. Vilardo, E., Nachbagauer, C., Buzet, A., Taschner, A., Holzmann, J., andRossmanith, W. (2012) A subcomplex of human mitochondrial RNase P is a bifunctional methyltransferase--extensive moonlighting in mitochondrial tRNA biogenesis Nucleic Acids Res **40**, 11583-11593 10.1093/nar/gks910
6. Strassler, S. E., Bowles, I. E., Dey, D., Jackman, J. E., andConn, G. L. (2022) Tied up in knots: Untangling substrate recognition by the SPOUT methyltransferases J Biol Chem **298**, 102393 10.1016/j.jbc.2022.102393
7. Howell, N. W., Jora, M., Jepson, B. F., Limbach, P. A., andJackman, J. E. (2019) Distinct substrate specificities of the human tRNA methyltransferases TRMT10A and TRMT10B RNA **25**, 1366-1376 10.1261/rna.072090.119
8. Krishnamohan, A., Dodbele, S., andJackman, J. E. (2019) Insights into Catalytic and tRNA Recognition Mechanism of the Dual-Specific tRNA Methyltransferase from Thermococcus kodakarensis Genes (Basel) **10**, 10.3390/genes10020100
9. Kempenaers, M., Roovers, M., Oudjama, Y., Tkaczuk, K. L., Bujnicki, J. M., andDroogmans, L. (2010) New archaeal methyltransferases forming 1-methyladenosine or 1-methyladenosine and 1-methylguanosine at position 9 of tRNA Nucleic Acids Res **38**, 6533-6543 10.1093/nar/gkq451
10. Somme, J., Van Laer, B., Roovers, M., Steyaert, J., Versees, W., andDroogmans, L. (2014) Characterization of two homologous 2'-O-methyltransferases showing different specificities for their tRNA substrates RNA **20**, 1257-1271 10.1261/rna.044503.114